

Annexe 1.5. 1^{er} comptage en spectrométrie γ

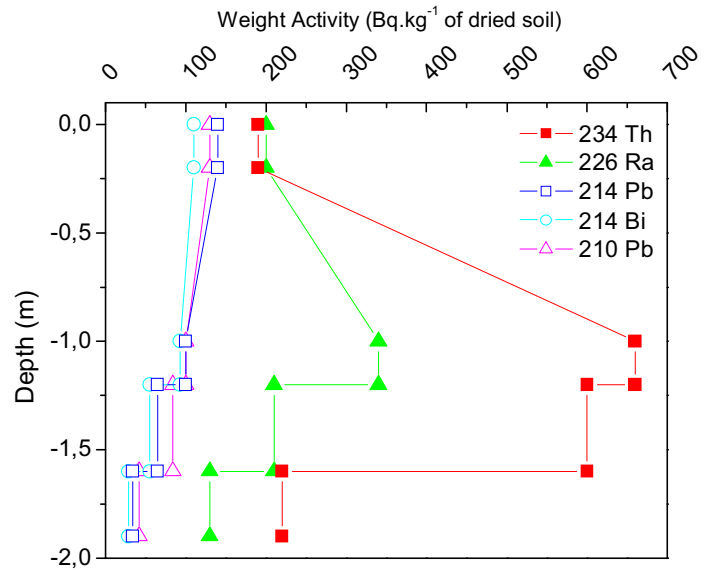


Figure 1 : Activité massique des descendants radioactifs de ^{238}U dans la tourbe totale, soit la fraction solide et l'eau interstitielle, mesurée par spectrométrie γ en novembre 2004.

Annexe 1.6. Cellules poreuses PRENART© PTFE/quartz : description et mode de prélèvement

Tableau 1 : Spécificités techniques des cellules de prélèvement en PTFE/Quartz.

Pore size	2 microns
Dimensions	OD 21 mm x L 95 mm
Weight	50 g
Porous area	33 cm ²
Hydraulic conductivity	3.31x10 ⁻⁷ cm/sec
Bubble pressure	> 500 mb
Efficiency in water	6 ml/cm ² /hr (600mb)

Tableau 2 : Limites de detection en mg.L⁻¹ des cellules de prélèvement en PTFE/Quartz.

Al	< 0.01	Mn	< 0.01
B	< 0.01	Na	< 0.05
C	< 5	NH ₄ -N	< 0.02
Ca	< 0.01	NO ₃ -N	< 0.02
Cl	< 0.05	Tot-N	< 0.02
Cu	< 0.01	P	< 0.05
F	< 0.05	PO ₄ -P	< 0.03
Fe	< 0.01	S	< 0.05
Org. C	< 0.05	SO ₄ -S	< 0.05
K	< 0.15	Si	< 0.05
Mg	< 0.01	Zn	< 0.01

Mesures du Eh et du pH sur site et prélèvements des eaux porales

Les mesures et prélèvements des eaux porales sont réalisés du point le moins concentré au plus concentré en uranium. La mesure du Eh se fait avant celle du pH car le système doit être en anoxie afin de perturber le moins possible les eaux porales. Le montage est représenté dans la photographie ci-dessous.



Photographie 1 : Mesure des paramètres des eaux interstitielles de tourbe.

Mesure du potentiel redox Eh

- Etalonnage de l'électrode de mesure ;
- Mise sous atmosphère d'azote (N_2 6.0) d'une cellule en verre flux à continu connectée à un flacon de prélèvement adapté (contenance 1L en polypropylène), nettoyé à l'acide nitrique dilué ;
 - Placer le tuyau de sortie de la bouteille d'azote au niveau des connexions de la cellule à flux continu puis au niveau du réservoir de la cellule, pendant quelques minutes. S'assurer du passage du flux d'azote par un souffle observé au niveau de la sortie du flacon de recueillement ;
 - Enlever l'arrivée d'azote puis fermer hermétiquement le système et vérifier son étanchéité, afin de rester sous atmosphère d'azote ;
- Connexion de l'entrée de la cellule à flux continu (partie inférieure) à la sortie de la cellule poreuse, et la sortie à un flacon de recueillement, lui-même connecté à la pompe à vide PAV 2000 ;
- Allumage de la pompe pour aspirer le contenu de la cellule poreuse. Un bullage de l'échantillon au niveau de la cellule à flux continu est observé ;
- Lecture des valeurs en attendant une stabilisation du paramètre.

Mesure du pH

- Arrêt de la pompe, sans toutefois la débrancher du flacon de recueillement (maintien du vide) ;
- Déconnexion entre l'entrée de la cellule à flux continu et le tuyau de sortie de la cellule poreuse (arrêt du prélèvement) ;
- Déconnexion entre la pompe et le flacon de recueillement afin de supprimer le vide à l'intérieur du système et récupération de 2 mL d'échantillon dans un tube Falcon ;
- Mise sous azote du tube et insertion de l'électrode pH pour la mesure.

Récupération des eaux porales

- Connexion de la sortie de la cellule poreuse au flacon de recueillement ;
- Connexion de la sortie de ce dernier à la pompe à vide ;
- Imposition d'une pression de 0,8 bar puis débranchement de la pompe tout en maintenant le vide à l'aide d'un clip ;
- Récupération d'environ 50 mL.

Remarques

- Entre chaque point de prélèvement, laver le système en connectant un flacon d'eau milliQ à l'entrée de la cellule à flux continu, et un flacon de recueillement, relié à la pompe à vide, à la sortie de la cellule ;
- A la fin des prélèvements, rincer la cellule à flux continu par de l'acide nitrique dilué ;
- Après utilisation, nettoyer les flacons de recueillement à l'acide nitrique dilué et laisser tremper 24 h.

Annexe 1.7. Mode opératoire du dosage de $[U]_{\text{tot.diss.}}$ par ICP-MS (Induced Coupled Plasma-Mass Spectrometry)

Principe

La spectrométrie de masse couplée à un plasma induit est une méthode d'analyse élémentaire qui consiste à séparer, identifier et quantifier les éléments d'un échantillon en fonction du rapport de leur masse sur leur charge m/z. Un spectromètre de masse quadripolaire est associé à une torche à plasma d'argon. L'échantillon est introduit dans une chambre de vaporisation où il est mis sous forme de micro-goutelettes par le nébuliseur. L'aérosol ainsi formé est ensuite dissocié à nouveau, atomisé et ionisé au contact du plasma d'argon. Un système de cônes permet d'envoyer les ions vers le quadripôle puis un multiplicateur d'électrons permettant d'amplifier le signal exprimé en nombre de coups.

Les appareillages ThermoVG X7 (Laboratoire d'Etudes des Transferts dans les Sols, IRSN de Fontenay-aux-Roses, DEI/SARG/LETS) et ICP 810-MS Varian ont été utilisés. Leur limite de détection est de l'ordre de quelques ppt pour l'uranium (Bouchoux et Sablier, 2005).

Préparation des étalons

Réactifs

- Solution standard U à $0,973 \text{ g.L}^{-1}$ ($4,197 \cdot 10^{-3} \text{ mol.L}^{-1}$) dans HNO_3 1,1 wt.% (U atomic absorption standard solution ALDRICH, n° art. 207624-100ML, n° lot. 10719KA,) ;
 - Solution standard Tl à 1 g.L^{-1} (étalon certifié SPEX Certiprep) ;
 - Solution HNO_3 à 2% préparé à partir de HNO_3 60% (NormatomII ultrapur, VWR).
- Préparation d'une solution de Tl à 50 mg.L^{-1} en prélevant 1 mL de solution standard Tl à diluer dans 20 mL ;
 - Selon le tableau suivant, préparer une solution mère U à 10 mg.L^{-1} (10 000 ppb), puis une solution intermédiaire à $0,1 \text{ mg.L}^{-1}$ (100 ppb) dans lesquelles on ne rajoutera pas de Tl.
 - Selon le tableau suivant, préparer les étalons U1 à U8 contenant au final 50 ppb de Tl :
 - Tarer le flacon ;
 - Prélever x mL de la solution à prélever (mère ou intermédiaire) ;
 - Peser ;
 - Compléter par HNO_3 2% jusqu'à obtenir 30 mL d'étalon ;
 - Peser ;
 - Tarer le flacon ;
 - Ajouter le plus précisément possible 30 μL de solution Tl à 50 mg.L^{-1} ;
 - Peser.
 - Préparer 4 blancs en suivant le même protocole mais sans rajouter U.

Tableau 3 : Récapitulatif des étalons pour analyses d'[U]_{tot.diss.} par ICP-MS.

Etalons	Sol. prélevée	V prélevé (mL)	V total (mL)	Dilution	C mol/L	C ppb
Solution mère	Standard	0,1001	10	99,90	4,20E-05	10000,0
Solution intermédiaire	Solution mère	0,0500	5	100,00	4,20E-07	100,0
U1-0,2ppb	Solution intermédiaire	0,0600	30	500,00	8,40E-10	0,2
U2-5ppb	Solution intermédiaire	1,5000	30	20,00	2,10E-08	5,0
U3-10ppb	Solution intermédiaire	3,0000	30	10,00	4,20E-08	10,0
U4-30ppb	Solution mère	0,0900	30	333,33	1,26E-07	30,0
U5-50ppb	Solution mère	0,1500	30	200,00	2,10E-07	50,0
U6-70ppb	Solution mère	0,2100	30	142,86	2,94E-07	70,0
U7-90ppb	Solution mère	0,2700	30	111,11	3,78E-07	90,0
U8-120ppb	Solution mère	0,3600	30	83,33	5,04E-07	120,0

Préparation des échantillons

- Tarer le flacon vide ;
- Ajouter x µL d'échantillon dans le flacon (selon la dilution nécessaire) ;
- Peser ;
- Compléter par HNO₃ 2% jusqu'à 10 mL ;
- Peser ;
- Tarer ;
- Ajouter le plus précisément possible 10 µL de solution Tl à 50 mg.L⁻¹ ;
- Peser ;

Analyses

Procéder à l'étalonnage puis insérer 1 blanc avant les échantillons.

Intercaler un étalon (ex : étalon U4) tous les 10 échantillons.

Penser à placer 1 blanc avant un échantillon *a priori* très dilué.

Annexe 1.8. Mode opératoire de la recherche automatique de particule par MEB

Principe

Le MEB consiste à appliquer un faisceau électronique d'énergie cinétique pouvant varier de 1 à 40 keV sur un échantillon dont la surface est rendue conductrice par métallisation (ici, au carbone). Les interactions faisceau/surface de l'échantillon produisent des électrons secondaires, rétrodiffusés et des rayons X notamment. L'analyse topographique, de grossissement compris entre 30 et 50 000, fait intervenir les électrons secondaires (énergie < 50 eV) qui donnent une information sur une profondeur d'environ 10 nm. L'analyse de la composition élémentaire met en jeu les rayons X, provenant de l'ionisation en couche interne des atomes, qui sont détectés par EDS (détecteur de rayons X à dispersion d'énergie). Un spectre du nombre de photons X en fonction de leur énergie est enregistré et permet d'identifier les éléments selon leurs pics caractéristiques. Un logiciel de recherche automatique de particules, Gun Shot Residue (GSR), est aussi utilisé afin de détecter des particules jusqu'à 1 µm de diamètre et de réaliser une analyse élémentaire par EDS.

Mode opératoire

Les appareils XL 30 PHILIPS ESEM (CEA de Bruyères-Le Châtel, DIF/DASE/SRCE/LMSG) et S-3500N HITACHI (IRSN de Fontenay-aux-Roses, DEI/SARG/LETS) ont été utilisés. Le premier est employé particulièrement pour la recherche automatique de particules d'U, quant au second, il est utilisé principalement pour observer la morphologie des particules majoritaires.

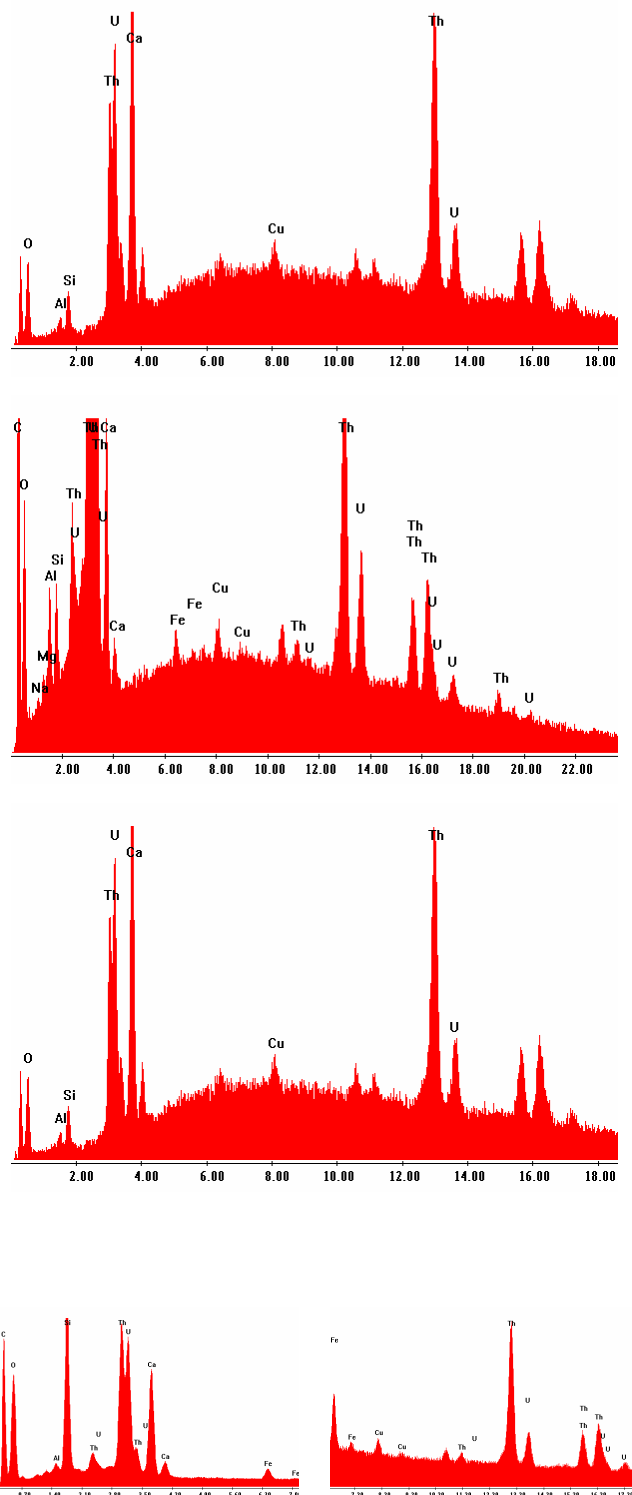
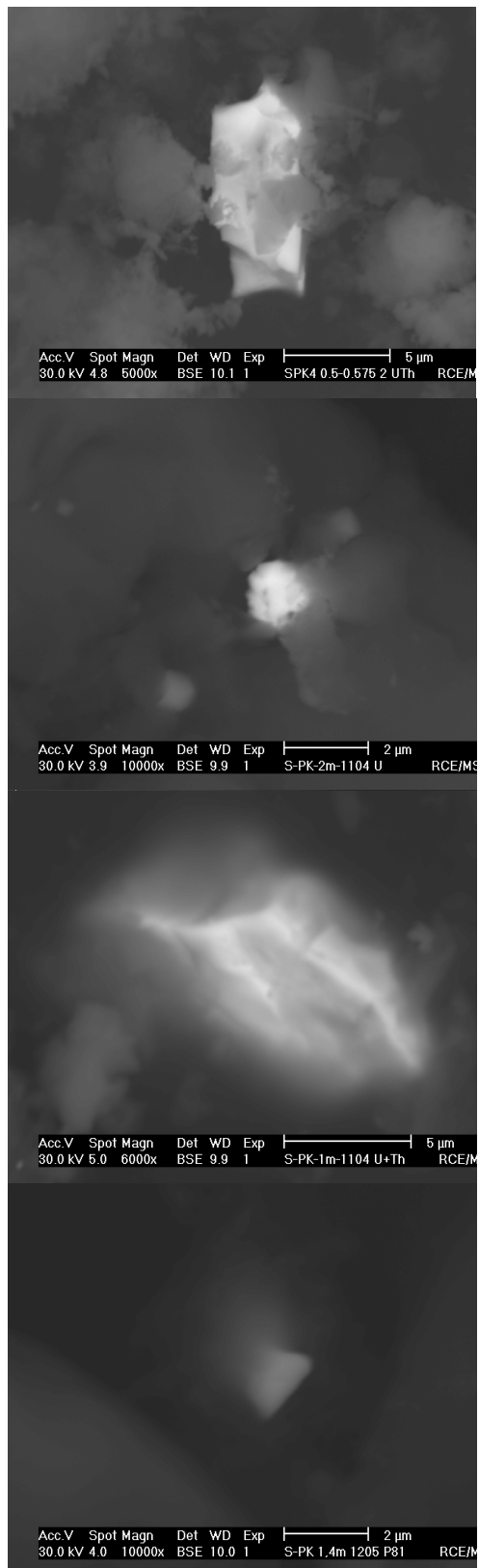
La première calibration consiste à régler le MEB :

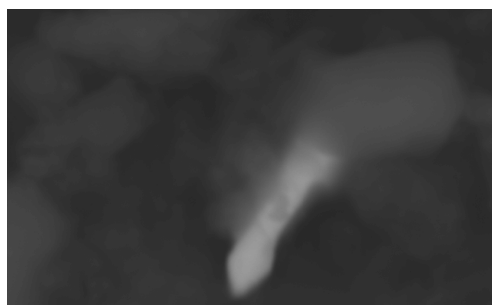
- Appliquer le vide à 3.10^{-4} mb, une tension de filament 30 kV et une intensité de 41 µA ;
- Aligner le filament en y et x ;
- Avec l'étalon Au, positionner manuellement à z = 10 mm au-dessus de la colle d'Ag ;
- Calibrer le détecteur d'électrons secondaires : i) régler le contraste sur l'étalon Au ; ii) régler la brillance au-dessus de la cage de Faraday
- Régler automatiquement la taille du spot de façon à obtenir 14 000 coups au-dessus de l'étalon Au avec une taille de spot de 4,8) ;
- Calibrer la masse Z par des mesures d'électrons secondaires sur les étalons Au, Nb, Ge, Si et C ;
- Calibrer le détecteur EDX avec l'étalon Cu.

La deuxième calibration concerne la recherche automatique de particules :

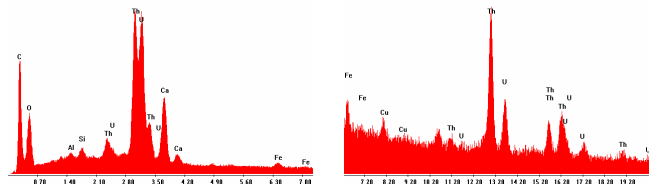
- Choisir un seuil de Z = 20 ou 25 ;
- Repérer chaque centre d'échantillon manuellement (un plot d'échantillon fait 12 mm de diamètre) ;
- Entrer les positions de chacun des centres repérés et imposer une recherche sur 11,5 mm ;
- Vérifier que 0,5 µm sont répartis sur 3 pixels et que le grossissement est de 190. Ceci permettra de quadriller l'échantillon en 266 champs (320 au total en comptant ceux qui sont sur le porte-échantillon) ;
- Régler manuellement la hauteur de chaque échantillon de façon à obtenir une image nette. Une différence de hauteur maximale de 600 µm entre le z des échantillons et celui de l'étalon Au ;
- Lors du dépouillement de la détection automatique, vérifier le spectre de chaque particule car si le rapport pic/bruit de fond est trop faible, le logiciel peut détecter des artefacts de pic.

Annexe 1.9. Photographies MEB et spectres EDX des particules d'U détectées

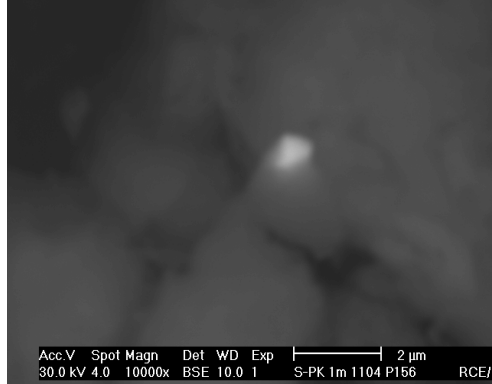
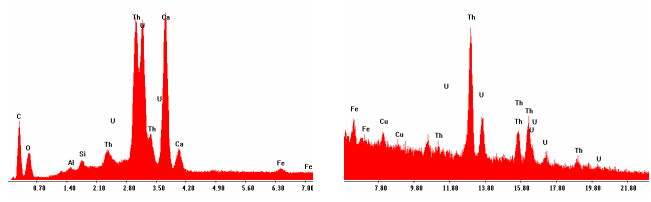




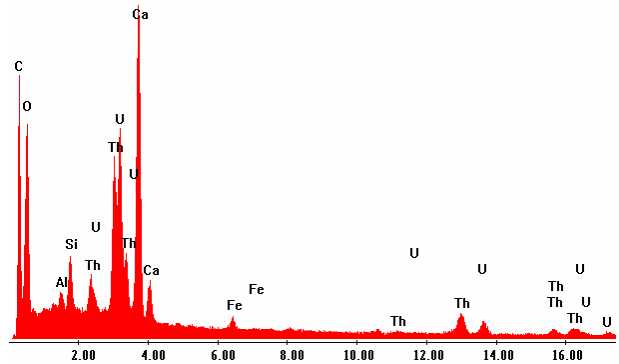
Acc.V Spot Magn Det WD Exp | 2 µm
30.0 kV 4.0 10000x BSE 9.9 1 S-PK 1.4m 1205 P168 RCE/M



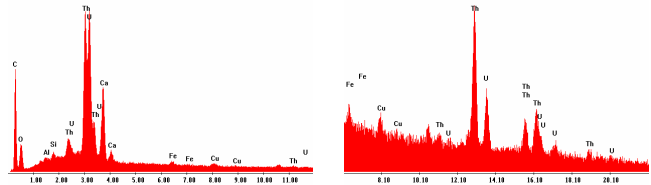
Acc.V Spot Magn Det WD Exp | 2 µm
30.0 kV 4.0 10000x BSE 10.0 1 S-PK 1m 1104 P141 RCE/M

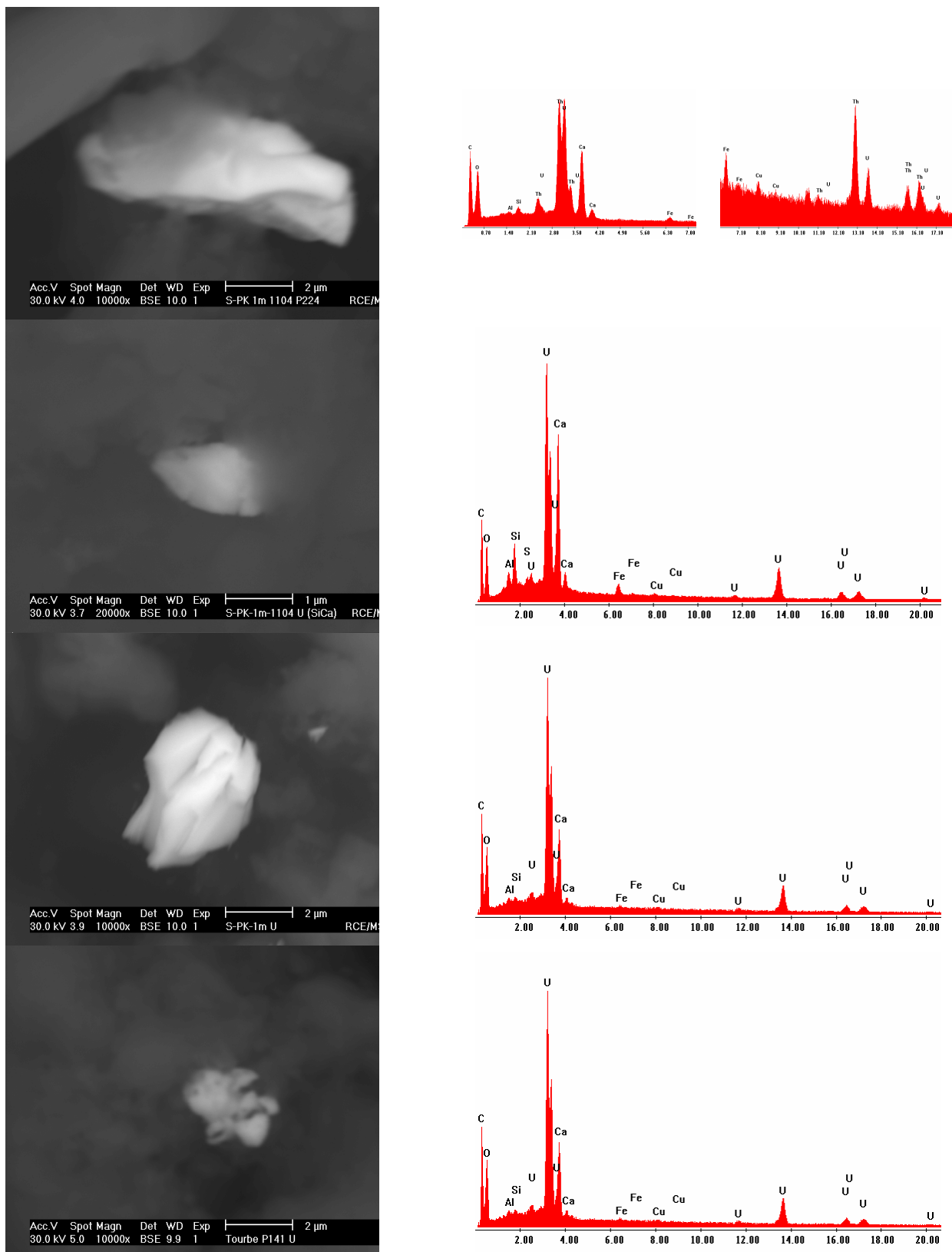


Acc.V Spot Magn Det WD Exp | 2 µm
30.0 kV 4.0 10000x BSE 10.0 1 S-PK 1m 1104 P156 RCE/M



Acc.V Spot Magn Det WD Exp | 2 µm
30.0 kV 4.0 10000x BSE 10.0 1 S-PK 1m 1104 P195 RCE/M





Photographie 2 : Photographies de particules d'U et mixtes d'U-Th, par MEB avec une tension de 30 kV réalisées en mode « électrons rétrodiffusés » (CEA DIF/DASE/SRCE/LMSG).

Annexe 1.10. Mode opératoire et résultats complémentaires d'EXAFS (Extended X-ray Absorption Fine Structure)

Principe

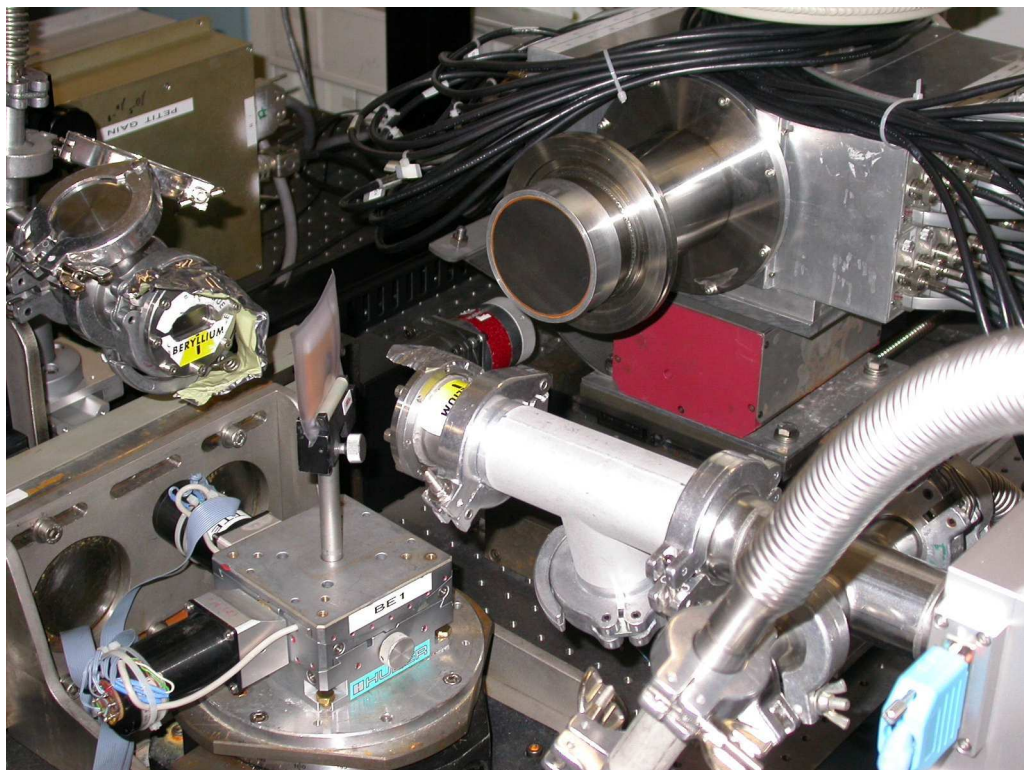
L'EXAFS est une méthode d'analyse spectroscopique qui apporte des informations sur un atome étudié et les distances de liaison et les nombres de coordination de ses proches voisins. L'échantillon est soumis à un faisceau de rayons X nécessitant une installation synchrotron pour pouvoir faire varier son énergie.

L'absorption est mesurée au fur et à mesure que l'énergie des rayons X incidents est augmentée. D'abord, un saut d'absorption correspondant au seuil d'ionisation de l'élément étudié, est mesuré. La région de l'EXAFS correspond aux oscillations observées environ 150 eV après ce seuil. Ces oscillations sont liées à la dualité onde-particule, c'est-à-dire que le photo-électron émis par l'atome excité peut être considéré comme une onde sphérique qui se réfléchit sur les atomes environnants. Ces ondes réfléchies peuvent interférer de façon constructive ou destructrice vis-à-vis de l'onde incidente et induire des variations de la quantité de photo-électrons globale. Au final, des variations d'absorption sont mesurées selon les longueurs d'onde des photo-électrons qui sont caractéristiques de la nature, la distance et le nombre des atomes voisins. Le signal mesuré ne peut être interprété tel quel, il subit une transformée de Fourier et une transformée de Fourier inverse.

Cette méthode est couplée avec la technique XANES (X-Ray Absorption Near Edge Structure) qui renseigne sur l'état d'oxydation de l'élément étudié.

Mode opératoire

Les analyses EXAFS de la raie L_{III^-} de l'uranium ont été réalisées sur la ligne FAME à l'ESRF (Grenoble), à l'aide d'un monochromateur à double cristal de Si (220). Les spectres ont été collectés en mode rendement de fluorescence grâce à un détecteur Canberra 30 éléments. Jusqu'à 27 spectres par échantillon sont collectés, comparé entre eux pour validation, et moyennés. Les échantillons sont translatés périodiquement après quelques spectres afin de changer la surface d'impact du faisceau de rayons X, ceci évitant une altération due au rayonnement. Les spectres d'absorption X sont normalisés selon l'algorithme Autoback de Ifeffit. Ensuite, les spectres XXAFS sont extraits à l'aide de techniques standard (Teo, 1986). Comme plusieurs espèces distinctes peuvent contribuer à un spectre donné, il n'est pas réalisé de filtre Fourier sur les données EXAFS. Au lieu de cela, les spectres XANES et EXAFS sont modélisés par une combinaison linéaire des spectres de référence (Catalano et Brown, 2004; Catalano *et al.*, 2004). L'ajustement est réalisé comme suit. Premièrement, les spectres expérimentaux sont ajustés en utilisant un seul spectre de référence. Le spectre montrant le meilleur ajustement est gardé, et ensuite un ajustement à deux composantes est effectué par un spectre systématiquement testé pour la seconde composante. Ce processus est répété jusqu'à ce que le paramètre mesurant la différence de compatibilité entre l'échantillon et la combinaison modélisée ne diminue pas de plus de 10%. Jusqu'à 4 composantes peuvent être ajoutées pour obtenir un ajustement acceptable des spectres EXAFS. Au contraire, les spectres XANES d'uranium pour l'espèce uranyle sont la plupart du temps dominé par la contribution des atomes d'oxygène liés par liaison covalente. Donc, le XANES peut difficilement discriminer entre les différentes espèces uranyle, et seulement un ou deux spectres étaient nécessaires pour faire un bon ajustement.



A



B

Photographie 3 : Montage EXAFS de la ligne BM30 (Fame) à l'ESRF de Grenoble (A) et échantillon de tourbe présentant des traces d'impacts du faisceau de rayons X sur l'enveloppe plastique (B).

Annexe 1.11. Mode opératoire des extractions à l'eau régale et à l'acide fluorhydrique

Extraction à l'eau régale

L'extraction des métaux traces (en l'occurrence l'uranium) par l'eau régale est réalisée selon la norme ISO 11466:1995 sur des échantillons de tourbe séchés à 105°C, broyés manuellement dans un mortier en agate et tamisés à 100 µm.

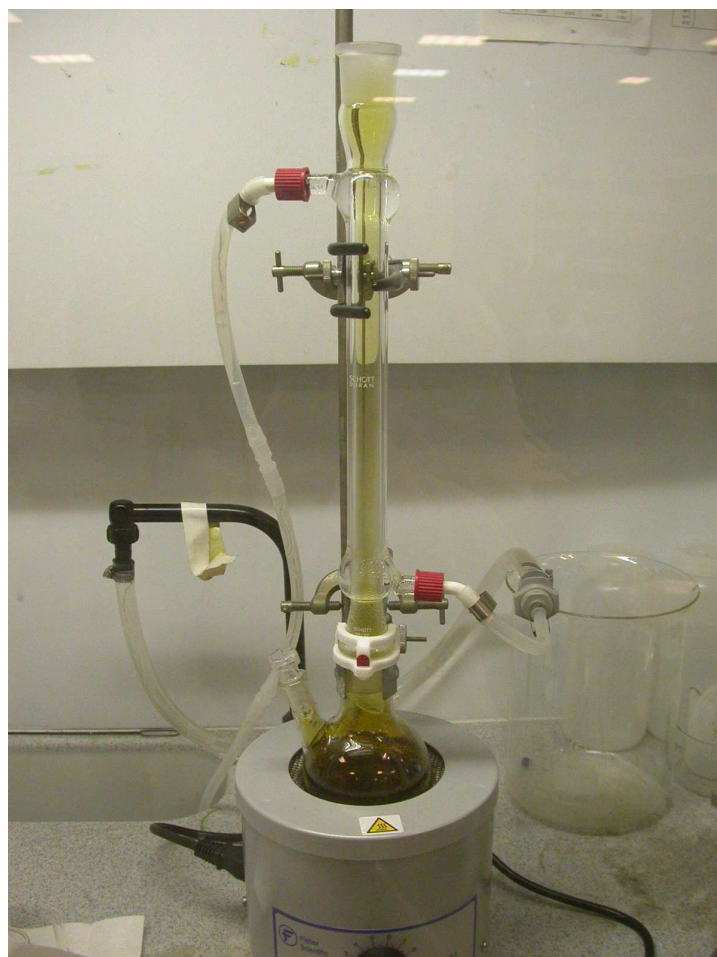
Réactifs

- HNO₃ à 70% trace analysis grade Fisher Scientific, M=63,01 g.mol⁻¹, d=1,42, code : N/2271/PB15, batch : 0565206 ;
- HCl à 37% normapur VWR Prolabo, M=36,46 g.mol⁻¹, d=1,18, prod. : 20.252.290, batch : 0601883.

Solution à préparer

- Solution de lavage HNO₃ à environ 0,5 mol.L⁻¹

Photo du montage



Photographie 4 : Montage de l'extraction d'uranium de la tourbe par attaque à l'eau régale.

Mode opératoire

- Nettoyer toute la verrerie par trempage dans HNO_3 0,5 mol.L⁻¹ pendant au moins 6 heures, puis rincer à l'eau milliQ ;
- Opérer sous hotte aspirante avec gants et lunettes de protection pour toutes les manipulations suivantes ;
- Peser environ 3 g de tourbe (noter la masse exacte) et ajouter quelques billes de verre dans le ballon ;
- Humecter avec 2 mL d'eau milliQ ;
- Ajouter 21 mL de HCl à 37% goutte à goutte car il y a formation de mousse par dissolution de la calcite et la réaction est légèrement exothermique ;
- Ajouter 7 mL de HNO_3 70% en procédant de la même manière ;
- Laisser « digérer » à température ambiante sous hotte aspirante pendant 16 heures ;
- Ajouter 10 mL de HNO_3 70% goutte à goutte car il y a encore formation de mousse ;
- Installer le ballon dans le montage et procéder au chauffage à faible thermostat avec ventilation maximale de la hotte car il y a formation de vapeurs nitreuses brun orangé ;
- Monter le thermostat à 2-3 progressivement ;
- Une fois le reflux en place, laisser pendant 3 heures ;
- Laisser refroidir ;
- Noter la masse des filtres à 5 et 0,2 μm en acétate de cellulose qui vont être utilisés ;
- Filtrer à 5 μm ;
- Filtrer à 0,2 μm ;
- Rincer le solide avec 10 mL de HNO_3 70% ;
- Transvaser le filtrat dans une fiole de 100 mL ;
- Conserver les filtres que l'on laissera sécher à température ambiante sous hotte afin de les peser une fois secs.

Résultat

$$C_m(U)_{tourbe} = 10^6 \times \frac{M(U) \times [U]_{extrait} \times V_{extrait}}{m_{tourbe}}$$

avec

$C_m(U)_{tourbe}$: concentration massique de U dans la tourbe ($\mu\text{g.g}^{-1}$ soit ppm) ;

$M(U)$: masse molaire de U (238,03 g.mol⁻¹) ;

$[U]_{extrait}$: concentration en solution de U dans l'extrait (mol.L⁻¹) ;

$V_{extrait}$: volume de l'extrait (L) ;

m_{tourbe} : masse initiale de tourbe (g).

***Extraction à l'acide fluorhydrique (réalisée par M. Tabarant,
CEA/DEN/DANS/DPC/SECR/LRSI)***

Réactifs

- HNO₃ à 70% trace analysis grade Fisher Scientific, M=63,01 g.mol⁻¹, d=1,42 ;
- HCl à 37% normapur VWR Prolabo, M=36,46 g.mol⁻¹, d=1,18 ;
- HF à 40%

Mode opératoire

- Nettoyer toute la verrerie par trempage dans HNO₃ 0,5 mol.L⁻¹ pendant au moins 6 heures, puis rincer à l'eau milliQ ;
- Opérer sous hotte aspirante avec gants et lunettes de protection pour toutes les manipulations suivantes ;
- Peser environ 1 g de tourbe (noter la masse exacte) et ajouter quelques billes de verre dans le ballon ;
- Ajouter 15 mL d'eau milliQ, 15 mL de HNO₃ à 70% et 15 mL de HCl à 37% goutte à goutte car il y a formation de mousse par dissolution de la calcite et la réaction est légèrement exothermique ;
- Chauffer à reflux pendant 8 heures ;
- Remettre à sec par évaporation ;
- Au résidu sec, ajouter 15 mL de HNO₃ à 70%, 5 mL de HF concentré et 15 mL de HCl à 37% goutte à goutte ;
- Chauffer à reflux pendant 8 heures ;
- Remettre à sec par évaporation ;
- Répéter les 3 étapes précédentes ;
- Remettre en solution dans HNO₃ dilué ;
- Filtrer à 0,2 µm et rincer le résidu avec HNO₃ dilué.

Annexe 2

Annexe 2.1. Constantes thermodynamiques des réactions ajoutées ou modifiées à la base de données Minteq (sur PhreeqC)

Tableau 4 : Constantes thermodynamiques des reactions ajoutées ou modifiées à la base de données Minteq.

Réaction	Log K	Source
$\text{UO}_2 + 2 + 2\text{e}^- + 4\text{H}^+ = \text{U}^{+4} + 2\text{H}_2\text{O}$	9,05	(a)
$\text{U}^{+4} + \text{H}_2\text{O} = \text{UOH}^{+3} + \text{H}^+$	-0,5400	(a)
$\text{UO}_2 + 2 + \text{H}_2\text{O} = \text{UO}_2\text{OH}^+ + \text{H}^+$	-5,2500	(a)
$\text{UO}_2 + 2 + 2\text{H}_2\text{O} = \text{UO}_2(\text{OH})_2 + 2\text{H}^+$	-12,1641	(a)
$\text{UO}_2 + 2 + 3\text{H}_2\text{O} = \text{UO}_2(\text{OH})_3^- + 3\text{H}^+$	-20,2500	(a)
$\text{U}^{+4} + 4\text{H}_2\text{O} = \text{U}(\text{OH})_4 + 4\text{H}^+$	-4,541	(a)
$\text{UO}_2 + 2 + 4\text{H}_2\text{O} = \text{UO}_2(\text{OH})_4^- + 4\text{H}^+$	-32,4000	(a)
$2\text{UO}_2 + 2 + \text{H}_2\text{O} = (\text{UO}_2)_2\text{OH}^{+3} + \text{H}^+$	-2,7000	(a)
$2\text{UO}_2 + 2 + 2\text{H}_2\text{O} = (\text{UO}_2)_2(\text{OH})_2 + 2\text{H}^+$	-5,6200	(a)
$3\text{UO}_2 + 2 + 4\text{H}_2\text{O} = (\text{UO}_2)_3(\text{OH})_4 + 2 + 4\text{H}^+$	-11,9000	(a)
$3\text{UO}_2 + 2 + 5\text{H}_2\text{O} = (\text{UO}_2)_3(\text{OH})_5^+ + 5\text{H}^+$	-15,5500	(a)
$3\text{UO}_2 + 2 + 7\text{H}_2\text{O} = (\text{UO}_2)_3(\text{OH})_7^- + 7\text{H}^+$	-32,2000	(a)
$4\text{UO}_2 + 2 + 7\text{H}_2\text{O} = (\text{UO}_2)_4(\text{OH})_7 + 7\text{H}^+$	-21,9000	(a)
$\text{UO}_2 + 2 + \text{CO}_3 - 2 = \text{UO}_2\text{CO}_3$	9,9570	(a)
$\text{UO}_2 + 2 + 2\text{CO}_3 - 2 = \text{UO}_2(\text{CO}_3)_2 - 2$	16,6394	(a)
$\text{UO}_2 + 2 + 3\text{CO}_3 - 2 = \text{UO}_2(\text{CO}_3)_3 - 4$	21,8801	(a)
$\text{U}^{+4} + 4\text{CO}_3 - 2 = \text{U}(\text{CO}_3)_4 - 4$	35,1823	(a)
$\text{U}^{+4} + 5\text{CO}_3 - 2 = \text{U}(\text{CO}_3)_5 - 6$	34,0647	(a)
$3\text{UO}_2 + 2 + 6\text{CO}_3 - 2 = (\text{UO}_2)_3(\text{CO}_3)_6 - 6$	54,0000	(a)
$2\text{UO}_2 + 2 + \text{CO}_3 - 2 + 3\text{H}_2\text{O} = (\text{UO}_2)_2(\text{OH})_3\text{CO}_3^- + 3\text{H}^+$	-0,8531	(a)
$3\text{UO}_2 + 2 + \text{CO}_3 - 2 + 3\text{H}_2\text{O} = (\text{UO}_2)_3(\text{OH})_3\text{CO}_3^+ + 3\text{H}^+$	0,6490	(a)
$11\text{UO}_2 + 2 + 6\text{CO}_3 - 2 + 12\text{H}_2\text{O} = (\text{UO}_2)_{11}(\text{OH})_{12}(\text{CO}_3)_6 - 2 + 12\text{H}^+$	36,4883	(a)
$\text{UO}_2 + 2 + 3\text{CO}_3 - 2 + \text{Ca}^{+2} = \text{Ca}\text{UO}_2(\text{CO}_3)_3 - 2$	25,4	(b)
$\text{UO}_2 + 2 + 3\text{CO}_3 - 2 + 2\text{Ca}^{+2} = \text{Ca}_2\text{UO}_2(\text{CO}_3)_3$	29,8	(c)
$\text{U}^{+4} + \text{F}^- = \text{UF}^{+3}$	9,4312	(a)
$\text{UO}_2 + 2 + \text{F}^- = \text{UO}_2\text{F}^+$	5,1666	(a)
$\text{U}^{+4} + 2\text{F}^- = \text{UF}_2^{+2}$	16,5494	(a)
$\text{UO}_2 + 2 + 2\text{F}^- = \text{UO}_2\text{F}_2$	8,8406	(a)
$\text{U}^{+4} + 3\text{F}^- = \text{UF}_3^+$	21,9163	(a)
$\text{UO}_2 + 2 + 3\text{F}^- = \text{UO}_2\text{F}_3^-$	10,9133	(a)
$\text{U}^{+4} + 4\text{F}^- = \text{UF}_4$	26,3709	(a)
$\text{UO}_2 + 2 + 4\text{F}^- = \text{UO}_2\text{F}_4 - 2$	11,8547	(a)
$\text{U}^{+4} + 5\text{F}^- = \text{UF}_5^-$	27,7630	(a)
$\text{U}^{+4} + 6\text{F}^- = \text{UF}_6 - 2$	29,8357	(a)
$\text{UO}_2 + 2 + \text{Oxalate} - 2 = \text{UO}_2\text{Oxalate}$	6,23	(d)
$\text{UO}_2 + 2 + 2\text{Oxalate} - 2 = \text{UO}_2(\text{Oxalate})_2 - 2$	10,42	(d)
$\text{UO}_2 + 2 + 3\text{Oxalate} - 2 = \text{UO}_2(\text{Oxalate})_3 - 4$	11	(d)

U+4 + PO4-3 + H+ = UHPO4+2	24,3006	(e)
UO2+2 + PO4-3 + H+ = UO2HPO4	19,55724	(a)
U+4 + 2PO4-3 + 2H+ = U(HPO4)2	46,6222	(e)
U+4 + 3PO4-3 + 3H+ = U(HPO4)3-2	67,5511	(e)
U+4 + 4PO4-3 + 4H+ = U(HPO4)4-4	87,8936	(e)
UO2+2 + PO4-3 + 2H+ = UO2H2PO4+	22,7933	(a)
UO2+2 + H4SiO4 = UO2H3SiO4+ + H+	-1,8400	(a)
U+4 + SO4-2 = USO4+2	6,5873	(a)
UO2+2 + SO4-2 = UO2SO4	3,1546	(a)
U+4 + 2SO4-2 = U(SO4)2	10,5225	(a)
<hr/>		
Uraninite	-4,8516	(a)
UO2 + 4H+ = U+4 + 2H2O		
UO2(am)	0,9324	(a)
UO2 + 4H+ = U+4 + 2H2O		
(UO2)3(PO4)2(s)	-49,4000	(a)
(UO2)3(PO4)2 = 3UO2+2 + 2PO4-3		
Rutherfordine	-14,4621	(a)
UO2CO3 = UO2+2 + CO3-2		
Schoepite	4,8116	(a)
UO2(OH)2:H2O + 2H+ = UO2+2 + 3H2O		
U(Oxalate)2:6H2O(C)	21,3665	(f)
U(Oxalate)2:6H2O = U+4 + 2Oxalate-2 + 6H2O		
UO2(Oxalate):3H2O(C)	9,1517	(g) avec correction par constante acidité de l'oxalate
UO2(Oxalate):3H2O = UO2+2 + Oxalate-2 + 3H2O		
<hr/>		
Ba+2 + Oxalate-2 = BaOxalate	2,33	(b)
Ca+2 + Oxalate-2 = CaOxalate	3,19	(b)
CO3-2 + H+ = HCO3-	10,3439	(e)
Fe+2 + H2O = FeOH+ + H+	-9,5149	(h)
Fe+3 + H2O = FeOH+2 + H+	-2,1638	(h)
Fe+2 + 2H2O = Fe(OH)2 + 2H+	-20,6338	(i)
Fe+3 + 2H2O = Fe(OH)2+ + 2H+	-5,6804	(i)
Fe+2 + 3H2O = Fe(OH)3- + 3H+	-31,8527	(i)
Fe+3 + 3H2O = Fe(OH)3 + 3H+	-12,5795	(i)
Fe+2 + 4H2O = Fe(OH)4-2 + 4H+	-45,9093	(h)
Fe+3 + 4H2O = Fe(OH)4- + 4H+	-21,6383	(i)
2Fe+3 + 2H2O = Fe2(OH)2+4 + 2H+	-2,9535	(h)
3Fe+3 + 4H2O = Fe3(OH)4+5 + 4H+	-6,3088	(h)
Fe+2 + CO3-2 = FeCO3	5,6987	(i)
Fe+3 + CO3-2 = FeCO3+	9,7350	(i)
Fe+2 + 2CO3-2 = Fe(CO3)2-2	7,4613	(i)
Fe+3 + 2CO3-2 = Fe(CO3)2-	19,6314	(i)
Fe+2 + HCO3- = FeHCO3+	1,4425	(i)
Fe+2 + HCO3- + H2O = FeOHCO3- + 2H+	-14,3829	(i)
Fe+3 + HCO3- + H2O = FeOHCO3 + 2H+	-14,1776	(h)

Fe+2 + Oxalate-2 = FeOxalate	3,97	(b)
Fe+3 + Oxalate-2 = FeOxalate+	9,15	(b)
Fe+2 + 2Oxalate-2 = Fe(Oxalate)2-2	5,9	(b)
Fe+3 + 2Oxalate-2 = Fe(Oxalate)2-	15,45	(b)
Fe+3 + 3Oxalate-2 = Fe(Oxalate)3-3	19,83	(b)
Fe+2 + PO4-3 + 2H+ = FeH2PO4+	20,7017	(h)
Fe+3 + PO4-3 + 2H+ = FeH2PO4+2	21,5984	(h)
Fe+2 + PO4-3 + H+ = FeHPO4	14,3912	(h)
Fe+3 + PO4-3 + H+ = FeHPO4+	20,8614	(h)
Fe+2 + SO4-2 = FeSO4	2,2164	(h)
Fe+3 + SO4-2 = FeSO4+	4,1573	(i)
Fe+3 + 2SO4-2 = Fe(SO4)2-	5,3927	(h)
Fe+2 + SO4-2 + H+ = FeHSO4+	1,0319	(h)
Fe+3 + SO4-2 + H+ = FeHSO4+2	1,4214	(j)
Fe+3 + 2SO4-2 + H+ = FeSO4HSO4	1,7759	(j)
2Fe+3 + 3SO4-2 = Fe2(SO4)3	4,2600	(k)
K+ + Oxalate-2 = KOxalate-	0,8	(b)
Li+ + Oxalate-2 = LiOxalate-	1,2	(b)
Mg+2 + Oxalate-2 = MgOxalate	3,62	(b)
Mn+2 + Oxalate-2 = MnOxalate	3,95	(b)
Mn+2 + 2Oxalate-2 = Mn(Oxalate)2-2	5,25	(b)
Na+ + Oxalate-2 = NaOxalate-	0,9	(b)
Oxalate-2 + H+ = HOxalate-	4,25	(a)
Oxalate-2 + 2H+ = H2Oxalate	5,65	(a)
PO4-3 + H+ = HPO4-2	12,3090	(e)
PO4-3 + 2H+ = H2PO4-	19,5143	(a)
PO4-3 + 3H+ = H3PO4	21,6619	(a)
Sr+2 + Oxalate-2 = SrOxalate	2,54	(b)
Fe(OH)2(ppd)		
Fe(OH)2 + 2H+ = Fe+2 + 2H2O	12,7843	(i)
Ferrihydrite		
Fe(OH)3 + 3H+ = Fe+3 + 3H2O	3,9011	(i)

Goethite		
FeOOH + 3H+ = Fe+3 + 2H2O	-0,2703	(i)
Hematite		
Fe2O3 + 6H+ = 2Fe+3 + 3H2O	-0,0472	(i)
Lepidocrocite	0,7651	(i)
FeOOH + 3H+ = Fe+3 + 2H2O		
Pyrite		
FeS2 + 2H+ + 2e- = Fe+2 + 2HS-	-15,8812	(i)
Siderite		
FeCO3 = Fe+2 + CO3-2	-10,8170	(i)

Caoxite		
CaOxalate:3H2O = Ca+2 + Oxalate-2 + 3H2O	-8,24	(l)
Weddellite		
CaOxalate:2H2O = Ca+2 + Oxalate-2 + 2H2O	-8,34	(l)
Whewellite		
CaOxalate:H2O = Ca+2 + Oxalate-2 + H2O	-8,77	(l)

- (a) : Guillaumont *et al.*, 2003.
- (b) : KTH Sweden, TDB thermo_minteq_gwb4 Geochemist workbench.
- (c) : Kalmykov and Choppin, 2000.
- (d) : Alliot, 2003.
- (e) : TDB thermo Geochemist workbench.
- (f) : Zakharova and Moskvin, 1960.
- (g) : Moskvin and Zakharova, 1959.
- (h) : Chivot, 1998.
- (i) : Chivot, 2004.
- (j) : Liu and Papangelakis, 1995.
- (k) : Gissenger-Bonnissel, 1997.
- (l) : Streit *et al.*, 1998.

Annexe 2.2. Variations de quelques paramètres avec la profondeur au PZPK

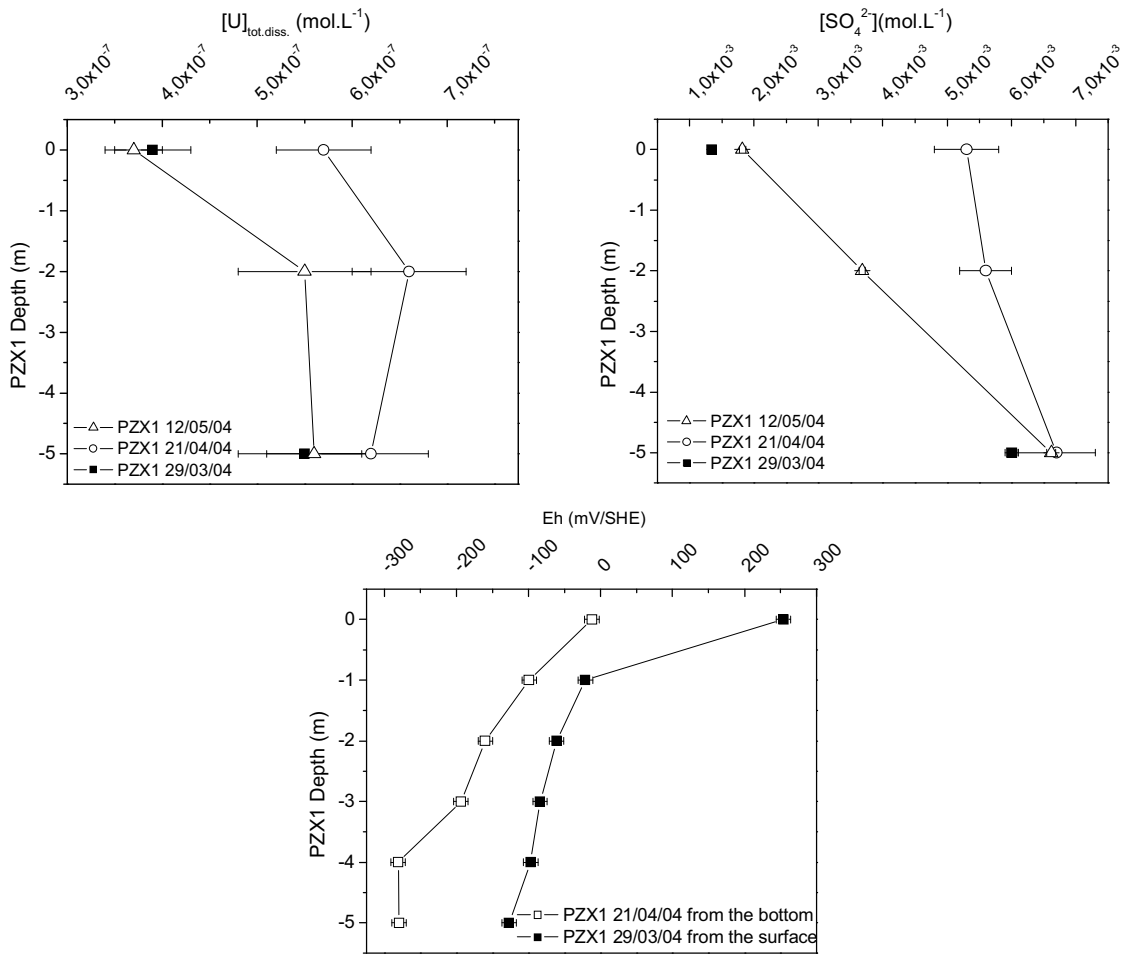


Figure 2 : $[U]_{\text{tot.diss.}}$, $[SO_4^{2-}]$ et Eh en fonction de la profondeur au PZPK.

Annexe 2.3. Pose des cellules poreuses PRENART© en PTFE/Quartz



Photographie 5 : Canules en polypropylène permettant la mise en place des cellules poreuses en PTFE/Quartz à 5 m du piézomètre PZPK.

Annexe 2.4. Mode opératoire des analyses de cations par ICP-OES (Induced coupling plasma-Optical Emission Spectroscopy)

Principe

L'ICP-OES est une méthode d'analyse élémentaire. Comme dans le cas de l'ICP-MS (Induced Coupled Plasma-Mass Spectrometry), l'échantillon est entraîné par un plasma d'argon. Les éléments constitutifs de l'échantillon sont alors atomisés et ionisés à forte température et émettent des photons à des longueurs qui leur sont spécifiques. La lumière émise est séparée par un réseau dispersif et son intensité est mesurée à l'aide d'un détecteur CID.

Appareillage et mode opératoire

Les analyses sont effectuées à l'aide d'un appareil Perkin-Elmer Optima 2000 DV. Les échantillons à analyser sont filtrés à 0,2 µm et acidifiés à pH 2 par ajout de HNO₃ concentré suprapur au moment du prélèvement. Ils sont ensuite dilués dans HNO₃ 0,5 mol.L⁻¹. Des étalons SPEX sont utilisés.

Plusieurs longueurs d'onde sont sélectionnées pour chaque élément afin de se prémunir d'éventuelles interférences (Cf. Tableau ci-dessous) et 6 réplicats de mesure sont effectués pour chaque échantillon.

Tableau 5 : Longueurs d'onde sélectionnées pour le dosage de Ca, K, Mg et Na.

Element	λ1 (nm)	λ2 (nm)
Ca	317,933	396,847
K	766,490	769,896
Mg	279,077	285,213
Na	588,995	589,592

Annexe 2.5. Récapitulatif des résultats du suivi de la chimie de l'eau

Uranium

Tableau 6 : [U]_{tot.diss.} au PZPK.

Date	PZPK		09/02/2006*	8,93.10-7	6.10-9
	[U] _{tot.diss}	σ			
25/04/2002	3,4.10-7	4.10-8	09/02/2006*	9,38.10-7	6.10-9
30/07/2002	7.10-8	2.10-8	09/02/2006*	8,59.10-7	5.10-9
28/01/2003	1,8.10-6	2.10-7	09/02/2006*	8,37.10-7	6.10-9
14/05/2003	6,5.10-7	7.10-8	10/02/2006	7,24.10-7	5.10-9
23/07/2003	1,4.10-7	2.10-8	10/02/2006	7,16.10-7	5.10-9
15/10/2003	6,9.10-7	6.10-8	10/02/2006	6,99.10-7	5.10-9
10/02/2004	1,4.10-6	3.10-7	12/03/2006*	8,05.10-7	6.10-9
29/03/2004	3,9.10-7	4.10-8	13/03/2006	9,29.10-7	7.10-9
07/04/2004	8.10-7	1.10-7	11/04/2006*	1,270.10-6	5.10-9
15/04/2004	8.10-7	1.10-7	12/04/2006	1,190.10-6	6.10-9
09/05/2004	4,880.10-7		09/05/2006		
21/04/2004	6,6.10-7	6.10-8	07/07/2006	7,41.10-7	4.10-9
28/04/2004	6,6.10-7	9.10-8	31/08/2006	1,02.10-7	1.10-9
05/05/2004	5,4.10-7	5.10-8	12/09/2006	1,70.10-7	1.10-9
12/05/2004	5,5.10-7	7.10-8	11/10/2006	7,38.10-8	9.10-10
25/05/2004	2,51.10-7	1.10-9	07/12/2006*	2,690.10-6	2.10-9
26/08/2004	3,4.10-7	5.10-10	07/12/2006	1,780.10-6	4.10-9
24/11/2004	5,1.10-7	6.10-10	07/12/2006* ^{x2}	1,730.10-6	2.10-9
16/02/2005	1,1.10-6	1.10-9	07/12/2006* ^{x3}	1,640.10-6	1.10-9
18/05/2005	4,20.10-7	2.10-9	16/01/2007	3,460.10-6	4.10-9
30/06/2005*	9,622.10-7	6.10-10	13/02/2007	2,54.10-6	1.10-8
01/07/2005	5,64.10-7	1.10-9	12/03/2007	1,580.10-6	5.10-9
01/07/2005^a	6,021.10-7	6.10-10	05/06/2007	1,417.10-6	2.10-11
01/07/2005^b	5,622.10-7	8.10-10	03/07/2007	5,640.10-7	9.10-12
01/07/2005^c	5,65.10-7	1.10-9	13/07/2007	7,108.10-7	2.10-11
04/07/2005	1,5.10-7	8.10-8			
30/08/2005*	5,39.10-8	9.10-10			
31/08/2005	1,15.10-7	1.10-9			
14/11/2005	1,5.10-8	1.10-9			
24/11/2005	5,27.10-8	8.10-10			
27/01/2006	9,77.10-7	6.10-9			

Les valeurs en italique sont estimées et utilisées pour les calculs de spéciation

* Avant vidange

^a Filtration à 3 µm

^b Filtration à 0,1 µm

^c Filtration à 0,01 µm

^{x2} Après 2 vidanges

^{x3} Après 3 vidanges

Tableau 7 : $[U]_{\text{tot.diss.}}$ dans les eaux porales et PZVP.

Date	EPX1-0.5m		EPX1-0.8m		EPX1-1.1m		EPX1-1.4m		PZVP	
	$[U]_{\text{tot.diss}}$	σ								
	(mol.L ⁻¹)		(mol.L ⁻¹)		(mol.L ⁻¹)		(mol.L ⁻¹)		(mol.L ⁻¹)	
14/11/2005	5,11.10-6	2.10-8	7,09.10-6	3.10-8						
27/01/2006	2,32.10-6	1.10-8					6,57.10-9	4.10-11		
13/03/2006	1,46.10-6	1.10-8	1,63.10-6	1.10-8	6,32.10-9	5.10-11	1,19.10-9	4.10-11		
12/04/2006	2,070.10-6	4.10-9	2,470.10-6	5.10-9	6,65.10-9	5.10-11	1,13.10-9	4.10-11		
08/05/2006			1,760.10-6	6.10-9						
09/05/2006	1,820.10-6	8.10-9			3,4.10-9	2.10-10	7.10-10	2.10-10		
07/07/2006					1,8.10-8	1.10-9	4.10-9	1.10-9		
31/08/2006	4,26.10-6	2.10-8	5,36.10-6	2.10-8	5,5.10-9	7.10-10	1,3.10-9	3.10-10		
12/09/2006					4,6.10-9	1.10-10	<i>1,0.10-9</i>			
11/10/2006	3,320.10-6	9.10-9	4,580.10-6	4.10-9	4,4.10-9	4.10-10	8.10-10	1.10-10	9,2.10-10	8.10-11
07/12/2006	2,580.10-6	7.10-9	2,990.10-6	1.10-9	4,1.10-9	2.10-10	8,3.10-10	8.10-11	9,0.10-10	8.10-11
16/01/2007	2,200.10-6	2.10-9	2,700.10-6	4.10-9	3,5.10-9	3.10-10	7,38.10-10	7.10-12	4,7.10-10	4.10-11
13/02/2007	1,670.10-6	6.10-9	2,07.10-6	2.10-8	2,31.10-9	1.10-11	5,36.10-10	3.10-12	4,2.10-10	4.10-12
12/03/2007	1,190.10-6	5.10-9	1,65.10-6	1.10-8						
03/04/2007	<i>1,19.10-6</i>		<i>1,10.10-6</i>		<i>1,9.10-9</i>					
05/06/2007	2,800.10-7	1.10-11	5,838.10-7	2.10-11	<i>1,5.10-9</i>		1,00.10-9	3.10-12		
13/07/2007	1,320.10-7	1.10-11	4,188.10-7	2.10-11	1,00.10-9	1.10-11	1,00.10-9	4.10-12	1,00.10-9	4.10-12

Les valeurs en italique sont estimées et utilisées pour les calculs de spéciation

Eh**Tableau 8 : Eh au PZPK.**

Date	PZPK Eh mV/ENH	27/04/2006*	-18
25/04/2002	<i>-50</i>	28/04/2006	-49
30/07/2002	-143	08/05/2006*	44,0
28/01/2003	88,5	09/05/2006	22,0
14/05/2003	<i>0</i>	07/07/2006	144
23/07/2003	<i>-50</i>	31/08/2006	-128
15/10/2003	-175	12/09/2006	29
10/02/2004	<i>100</i>	11/10/2006	-105
29/03/2004	-61	07/12/2006*	11
07/04/2004	-355	07/12/2006	9
15/04/2004	-16	07/12/2006 ^{x2}	33
21/04/2004	-160	07/12/2006 ^{x3}	35
28/04/2004	-286	16/01/2007	8
25/05/2004	<i>0</i>	13/02/2007	0
26/08/2004	<i>-50</i>	12/03/2007	8
24/11/2004	48	03/04/2007	-21
16/02/2005	<i>103</i>	05/06/2007	47
18/05/2005	-74	03/07/2007	31
30/06/2005*	-104	13/07/2007	-75
01/07/2005	-27	<i>Les valeurs en italique sont estimées et utilisées pour les calculs de spéciation</i>	
30/08/2005*	-195	* Avant vidange	
31/08/2005	-118	^a Filtration à 3 µm	
24/11/2005	-158	^b Filtration à 0,1 µm	
27/01/2006	104	^c Filtration à 0,01 µm	
15/02/2006	110	^{x2} Après 2 vidanges	
12/03/2006*	143	^{x3} Après 3 vidanges	
13/03/2006	153	Incertitude : 10 mV/ENH	
12/04/2006	-10		

Tableau 9 : Eh dans les eaux porales et PZVP.

Date	EPX1-0.5m Eh mV/ENH	EPX1-0.8m Eh mV/ENH	EPX1-1.1m Eh mV/ENH	EPX1-1.4m Eh mV/ENH	PZVP Eh mV/ENH
14/11/2005	200	200			
27/01/2006	200			200	
13/03/2006	100	100	100	100	
12/04/2006	25	20	100	100	
09/05/2006	25	20	-7	33	
07/07/2006	-53		-37	-24	
31/08/2006	-53	-43	-40	-30	
12/09/2006	0		0	10	
11/10/2006	100	100	100	100	-125
07/12/2006	205	224	189	167	-25
16/01/2007	117	139	114	168	-65
13/02/2007	258	220	248	201	-76
12/03/2007	23	21			
03/04/2007	25	20	100	100	
05/06/2007	29	39	-7	33	-135
13/07/2007	-53	-43	-37	-24	-142

Les valeurs en italique sont estimées et utilisées pour les calculs de spéciation

Incertitude : 10 mV/ENH

pH**Tableau 10 : pH au PZPK.**

Date	PZPK pH	12/04/2006	6,9
25/04/2002	6,7	27/04/2006*	6,9
30/07/2002	6,7	28/04/2006	6,9
28/01/2003	6,7	08/05/2006*	6,9
14/05/2003	6,7	09/05/2006	7,0
23/07/2003	6,6	07/07/2006	6,9
15/10/2003	6,9	31/08/2006	6,6
10/02/2004	6,4	12/09/2006	6,6
29/03/2004	7,0	11/10/2006	8,7
07/04/2004	7,0	07/12/2006*	7,4
15/04/2004	7,0	07/12/2006	7,4
21/04/2004	7,0	07/12/2006 ^{x2}	7,2
28/04/2004	6,8	07/12/2006 ^{x3}	7,1
25/05/2004	6,8	16/01/2007	6,7
26/08/2004	6,9	13/02/2007	7,1
24/11/2004	6,9	12/03/2007	6,9
16/02/2005	7,1	03/04/2007	6,9
18/05/2005	7,0	05/06/2007	6,8
30/06/2005*	6,8	03/07/2007	7,0
01/07/2005	6,9	13/07/2007	7,7
30/08/2005*	6,7		
31/08/2005	6,7		
24/11/2005	6,6	* Avant vidange	
27/01/2006	6,8	^a Filtration à 3	
15/02/2006	6,7	µm	
12/03/2006*	6,8	^b Filtration à 0,1	
13/03/2006	7,0	µm	

^c Filtration à 0,01 µm
^{x2} Après 2
vidanges
^{x3} Après 3
vidanges
Incertitude : 0,1

Tableau 11 : pH dans les eaux porales et PZVP.

Date	EPX1-0.5m pH	EPX1-0.8m pH	EPX1-1.1m pH	EPX1-1.4m pH	PZVP pH
14/11/2005	8,0	8,0			
27/01/2006	8,0				7,5
13/03/2006	7,8	7,5	7,3	7,3	
12/04/2006	8,0	8,0	7,5	7,5	
09/05/2006	7,9	7,9	7,6	7,4	
07/07/2006	8,0		7,6	7,9	
31/08/2006	8,0	8,0	7,5	8,0	
12/09/2006	7,6	7,5	7,5	7,6	
11/10/2006	7,4	7,5	7,1	7,1	8,7
07/12/2006	8,0	8,1	7,9	8,0	6,9
16/01/2007	7,3	7,4	7,6	7,3	6,1
13/02/2007	7,9	8,0	7,7	8,0	6,7
12/03/2007	7,7	7,9			
03/04/2007	8,0	8,0	8,0	8,0	
05/06/2007	8,3	8,3	8,1	8,3	7,2
13/07/2007	8,3	8,3	8,3	8,3	8,0

Les valeurs en italique sont estimées et utilisées pour les calculs de spéciation

Incertitude : 0,1

*Autres paramètres***Tableau 12 : Conductivité, Solides Dissous Totaux, Oxygène dissous, Température et Turbidité au PZPK.**

Date	Conductivité mS.m ⁻¹	Solides Dissous Totaux g.L ⁻¹	Oxygène dissous mg.L ⁻¹	Température °C	Turbidité NTU
σ	1	0,01	0,01	0,1	1
30/07/2002	126		1,55	14,9	0
28/01/2003	148	0,90	0,63	9,9	36
14/05/2003	105	0,43	1,80	12,9	
23/07/2003	122	0,80	0,70	14,3	
15/10/2003	121	0,80	0,60	14,6	2
10/02/2004	267	1,70		9,9	32
29/03/2004	187	1,20	0,00	11,9	0
07/04/2004	204	1,30	0,00	12,1	26
15/04/2004	200	1,30	0,00	11,0	-6
21/04/2004	174	1,10	0,00	11,2	3
28/04/2004	226		0,00	12,1	
25/05/2004	174	1,10		13,8	41
24/11/2004	167	1,10	6,75	15,1	24
16/02/2005	64	0,40	0,00	11,2	11
18/05/2005	62	0,38	0,00	15,3	55
30/06/2005*	31	0,43	0,34	15,9	66
01/07/2005	56	0,36	0,33	15,4	62
30/08/2005*	64	0,41	1,22	15,0	83
31/08/2005	63	0,41	3,90	15,4	75
24/11/2005	62	0,40	7,46	15,4	10
27/01/2006	123	0,80	7,92	9,7	17
15/02/2006	92	0,60	10,86	8,9	48
12/03/2006*	89	0,57	6,94	8,7	63
13/03/2006	89	0,57	6,55	8,6	14
12/04/2006	88	0,56	5,24	10,6	58
27/04/2006*	96	0,62	5,85	12,2	58
28/04/2006	103	0,70	6,46	12,8	103
08/05/2006*	60	0,39	7,12	14,1	52
09/05/2006	63	0,41	9,1	14,9	50
07/07/2006	68	0,43	5,32	14,2	163
31/08/2006	123	0,80	3,95	14,2	56
12/09/2006	123	0,80	1,73	14,9	9
11/10/2006	76	0,48	1,30	15,4	0
07/12/2006*	141	0,90	1,52	15,9	
07/12/2006	121	0,80	2,09	15,4	
07/12/2006 ^{x2}	113	0,70	1,92	15,1	
07/12/2006 ^{x3}	106	0,70	2,04	15,2	
16/01/2007	122	0,80	1,87	13,3	2
13/02/2007	155	1,00	11,00	12,4	36
12/03/2007	78	0,50	1,14	12,2	16

Date	Conductivité mS.m ⁻¹	Solides Dissous Totaux g.L ⁻¹	Oxygène dissous mg.L ⁻¹	Température °C	Turbidité NTU
σ	1	0,01	0,01	0,1	1
03/04/2007	77	0,49	1,38	12,6	0
05/06/2007	80	0,51	1,72	18,3	3
03/07/2007	71	0,46	3,27	19,8	110
13/07/2007	99	0,63	2,43	18,4	240

* Avant vidange

^a Filtration à 3

μm

^b Filtration à

0,1 μm

^c Filtration à 0,01 μm

^{x2} Après 2

vidanges

^{x3} Après 3

vidanges

Alcalinité

Tableau 13 : Alcalinité au PZPK.

Date	PZPK Alcalinité (éq.L ⁻¹)	σ	10/02/2006	9,4.10-3	1.10-4
25/04/2002	<i>9,8.10-3</i>		<i>12/03/2006*</i>	9,16.10-3	7.10-5
30/07/2002	1,16.10-2	2.10-4	<i>13/03/2006</i>	1,03.10-2	2.10-4
28/01/2003	8,04.10-3	8.10-5	<i>11/04/2006*</i>	1,33.10-2	2.10-4
14/05/2003	6,43.10-3	8.10-5	<i>12/04/2006</i>	1,308.10-2	9.10-5
23/07/2003	9,85.10-3	5.10-4	<i>09/05/2006</i>	8,9.10-3	2.10-4
15/10/2003	8,20.10-3	2.10-4	<i>07/07/2006</i>	4,59.10-3	8.10-5
10/02/2004	<i>5,0.10-3</i>		<i>31/08/2006</i>	1,00.10-2	8.10-5
07/04/2004	8,80.10-3	6.10-4	<i>11/10/2006</i>	9,9.10-3	2.10-4
15/04/2004	9,40.10-3	6.10-4	<i>07/12/2006*</i>	9,8.10-3	2.10-4
21/04/2004	8,90.10-3	6.10-4	<i>07/12/2006^{x2}</i>	9,2.10-3	2.10-4
28/04/2004	9,80.10-3	6.10-4	<i>07/12/2006^{x3}</i>	9,2.10-3	2.10-4
05/05/2004	6,80.10-3	5.10-4	<i>16/01/2007</i>	1,25.10-2	2.10-4
12/05/2004	8,60.10-3	6.10-4	<i>13/02/2007</i>	1,05.10-2	2.10-4
25/05/2004	1,10.10-2	1.10-3	<i>12/03/2007</i>	1,08.10-2	1.10-4
26/08/2004	1,85.10-2	4.10-4	<i>03/04/2007</i>	1,42.10-2	2.10-4
24/11/2004	8,40.10-3	1.10-4	<i>05/06/2007</i>	1,73.10-2	2.10-4
16/02/2005	7,90.10-3	7.10-5	<i>03/07/2007</i>	2,45.10-2	3.10-4
18/05/2005	9,27.10-3	6.10-5	<i>13/07/2007</i>	1,66.10-2	2.10-4
30/06/2005*	7,20.10-3	1.10-4			
01/07/2005	6,50.10-3	1.10-4			
04/07/2005	5,20.10-3	1.10-4			
30/08/2005*	1,2.10-2	6.10-3			
31/08/2005	1,1.10-2	7.10-3			
14/11/2005	8,67.10-3	3.10-6			
24/11/2005	1,02.10-2	5.10-5			
27/01/2006	8,00.10-3	7.10-5			
09/02/2006*	9,93.10-3	9.10-5			

Les valeurs en italique sont estimées et utilisées pour les calculs de spéciation

* Avant vidange

^a Filtration à 3

µm

^b Filtration à 0,1

µm

^c Filtration à 0,01 µm

^{x2} Après 2

vidanges

^{x3} Après 3

vidanges

Tableau 14 : Alcalinité dans les eaux porales et PZVP.

Date	EPX1-0.5m		EPX1-0.8m		EPX1-1.1m		EPX1-1.4m		PZVP	
	Alcalinité (éq.L ⁻¹)	σ								
14/11/2005	1,080.10-2	5.10-6	1,01.10-2	8.10-6						
27/01/2006	1,10.10-2	1.10-4					1,00.10-2	1.10-4		
13/03/2006	1,38.10-2	2.10-4	1,41.10-2	1.10-4	1,23.10-2	2.10-4	1,11.10-2	1.10-4		
12/04/2006	1,68.10-2	4.10-4	1,72.10-2	1.10-4	1,45.10-2	1.10-4	1,32.10-2	2.10-4		
09/05/2006	1,45.10-2	2.10-4	1,49.10-2	2.10-4	1,09.10-2	2.10-4	1,09.10-2	1.10-4		
07/07/2006					6,56.10-3	5.10-5	9,53.10-3	3.10-5		
31/08/2006							9,68.10-3	3.10-5		
11/10/2006	1,07.10-2	2.10-4	1,10.10-2	2.10-4	1,07.10-2	2.10-4	1,06.10-2	2.10-4	1,02.10-2	2.10-4
07/12/2006	1,23.10-2	2.10-4	1,36.10-2	2.10-4	1,06.10-2	2.10-4			1,02.10-2	2.10-4
16/01/2007	1,42.10-2	2.10-4	1,50.10-2	2.10-4	1,02.10-2	2.10-4	8,52.10-3	1.10-4	8,91.10-3	2.10-4
13/02/2007	1,52.10-2	2.10-4	1,52.10-2	2.10-4	1,04.10-2	2.10-4	1,06.10-2	2.10-4	1,20.10-2	2.10-4
03/04/2007	1,72.10-2	2.10-4	1,91.10-2	2.10-4	1,13.10-2	1.10-4	1,06.10-2	1.10-4	1,18.10-2	1.10-4
05/06/2007	3,01.10-2	4.10-4	1,79.10-2	2.10-4	1,52.10-2	2.10-4	1,73.10-2	2.10-4	2,71.10-2	3.10-4
13/07/2007	2,46.10-2	3.10-4	2,26.10-2	3.10-4	1,73.10-2	2.10-3	1,54.10-2	2.10-4	1,51.10-2	2.10-4

Les valeurs en italique sont estimées et utilisées pour les calculs de spéciation

Sulfate**Tableau 15 : $[\text{SO}_4^{2-}]$ au PZPK.**

Date	$[\text{SO}_4^{2-}]$ (mol.L ⁻¹)	PZPK σ	10/02/2006	7,2.10-3	3.10-4	
25/04/2002	3,75.10-3	4.10-5	12/03/2006*	2,94.10-3	5.10-5	
30/07/2002	7,97.10-4	9.10-6	13/03/2006	3,28.10-3	6.10-5	
28/01/2003	7,26.10-4	7.10-6	11/04/2006*	2,81.10-3	7.10-5	
14/05/2003	1,550.10-3	9.10-6	12/04/2006	3,02.10-3	8.10-5	
23/07/2003	1,170.10-3	8.10-6	09/05/2006	1,290.10-3	4.10-6	
10/02/2004	1,57.10-3	8.10-5	07/07/2006	2,050.10-3	3.10-6	
07/04/2004	6,2.10-3	4.10-4	31/08/2006	6,9.10-4	1.10-5	
15/04/2004	7,2.10-3	4.10-4	12/09/2006	7,6.10-4	1.10-5	
21/04/2004	5,6.10-3	4.10-4	11/10/2006	7,0.10-4	4.10-6	
28/04/2004	6,96.10-3	8.10-5	07/12/2006*	6,0.10-3	5.10-4	
05/05/2004	2,10.10-3	9.10-5	07/12/2006 ^{x2}	4,3.10-3	5.10-5	
12/05/2004	3,68.10-3	5.10-5	07/12/2006 ^{x3}	4,1.10-3	1.10-4	
25/05/2004	4,24.10-3	5.10-5	16/01/2007	3,36.10-3	5.10-5	
26/08/2004	9,5.10-4	3.10-5	13/02/2007	2,07.10-3	5.10-5	
24/11/2004	3,24.10-3	2.10-5	12/03/2007	1,331.10-3	7.10-6	
16/02/2005	2,20.10-3	3.10-5	05/06/2007	1,330.10-3	1.10-6	
18/05/2005	3,2.10-4	5.10-5	03/07/2007	9,0.10-4	1.10-5	
30/06/2005*	2,30.10-3	7.10-5	13/07/2007	1,30.10-3	1.10-5	
01/07/2005	1,35.10-3	3.10-5	<i>Les valeurs en italique sont estimées et utilisées pour les calculs de spéciation</i>			
04/07/2005	7,0.10-4	2.10-5				
30/08/2005*	7,5.10-4	1.10-5				
31/08/2005	8,0.10-4	1.10-5				
14/11/2005	8,24.10-4	5.10-6				
24/11/2005	8,39.10-4	7.10-6				
27/01/2006	6,8.10-3	1.10-4				
09/02/2006*	7,4.10-3	1.10-4				

** Avant vidange**^a Filtration à 3**µm**^b Filtration à 0,1**µm**^c Filtration à 0,01 µm**^{x2} Après 2**vidanges**^{x3} Après 3**vidanges*

Tableau 16 : $[SO_4^{2-}]$ dans les eaux porales et PZVP.

Date	EPX1-0.5m		EPX1-0.8m		EPX1-1.1m		EPX1-1.4m		PZVP	
	$[SO_4^{2-}]$ (mol.L ⁻¹)	σ								
14/11/2005	5,3.10-3	3.10-4	7,60.10-3	6.10-5					2,30.10-3	4.10-5
27/01/2006	5,41.10-3	2.10-5							2,36.10-3	
13/03/2006	4,26.10-3	4.10-5	4,3.10-3	3.10-4	2,48.10-3	3.10-5			2,92.10-3	6.10-6
12/04/2006	4,24.10-3	6.10-5	4,55.10-3	6.10-5	3,08.10-3	7.10-5			2,55.10-3	7.10-5
09/05/2006	3,3.10-3	2.10-4	3,60.10-3	6.10-5	2,52.10-3	7.10-5			2,48.10-3	3.10-6
07/07/2006					2,49.10-3	2.10-5			2,92.10-3	3.10-6
31/08/2006					3,00.10-3				3,26.10-3	5.10-5
12/09/2006					3,09.10-3	5.10-5			2,93.10-3	6.10-5
02/10/2006	5,13.10-3	3.10-5			2,98.10-3	2.10-5			2,92.10-3	2.10-5
11/10/2006	4,17.10-3	3.10-5	5,72.10-3	4.10-5	3,01.10-3	2.10-5			2,10-5	5,18.10-4 2.10-6
12/12/2006	5,60.10-3	1.10-4	4,53.10-3	5.10-5	3,16.10-3	6.10-5				5,01.10-4 7.10-6
16/01/2007	4,84.10-3	1.10-4	4,48.10-3	1.10-4	3,30.10-3	7.10-5			2,80.10-3	6.10-5 5,70.10-4 1.10-5
13/02/2007	4,05.10-3	9.10-5	3,70.10-3	6.10-5	3,10.10-3	2.10-4			3,13.10-3	5.10-5 5,63.10-4 7.10-6
14/03/2007	2,99.10-3	3.10-5	2,94.10-3	2.10-5					2,75.10-3	
04/04/2007	<i>2,99.10-3</i>		<i>2,00.10-3</i>		<i>3,00.10-3</i>				<i>2,60.10-3</i>	
05/06/2007	1,50.10-3	8.10-6	1,30.10-3	2.10-6	2,59.10-3	2.10-6			3,57.10-3	4.10-6 4,89.10-4 2.10-6
13/07/2007	1,27.10-3	3.10-6	8,89.10-4	2.10-5	3,08.10-3	2.10-4			5.10-4	<i>5,00.10-5</i>

Les valeurs en italique sont estimées et utilisées pour les calculs de spéciation

Chlorure**Tableau 17 : [Cl⁻] au PZPK.**

PZPK					
Date	[Cl ⁻] (mol.L ⁻¹)	σ			
25/04/2002	2,39.10-4	3.10-6	12/03/2006*	1,54.10-3	6.10-5
30/07/2002	8,7.10-4	1.10-5	13/03/2006	1,88.10-3	7.10-5
28/01/2003	3,2.10-4	3.10-5	11/04/2006*	1,55.10-3	7.10-5
14/05/2003	3,1.10-4	3.10-5	12/04/2006	1,56.10-3	7.10-5
23/07/2003	1,17.10-4	8.10-6	09/05/2006	7,77.10-4	4.10-6
10/02/2004	5,3.10-4	3.10-5	07/07/2006	1,43.10-3	5.10-7
07/04/2004	5,6.10-4	2.10-5	31/08/2006	1.10-3	1.10-4
15/04/2004	6,2.10-4	2.10-5	12/09/2006	1.10-3	1.10-4
21/04/2004	4,9.10-4	2.10-5	11/10/2006	9,7.10-4	3.10-5
28/04/2004	6,4.10-4	2.10-5	07/12/2006*	1,6.10-3	1.10-4
05/05/2004	2,5.10-4	2.10-5	07/12/2006 ^{x2}	1,21.10-3	4.10-5
12/05/2004	4,1.10-4	2.10-5	07/12/2006 ^{x3}	1,19.10-3	5.10-5
25/05/2004	8,3.10-4	2.10-5	16/01/2007	1,99.10-3	8.10-5
26/08/2004	9,7.10-4	2.10-5	13/02/2007	1,56.10-3	8.10-5
24/11/2004	4,7.10-4	2.10-5	12/03/2007	1,14.10-3	3.10-5
16/02/2005	8,3.10-4	2.10-5	05/06/2007	8,9.10-4	9.10-7
18/05/2005	6,0.10-4	2.10-5	03/07/2007	6,5.10-4	1.10-6
30/06/2005*	9,5.10-4	3.10-5	13/07/2007	1,2.10-3	1.10-5
01/07/2005	6,5.10-4	2.10-5	<i>Les valeurs en italique sont estimées et utilisées pour les calculs de spéciation</i>		
04/07/2005	2,5.10-4	2.10-5	* Avant vidange		
30/08/2005*	8,3.10-4	2.10-5	^a Filtration à		
31/08/2005	9,6.10-4	2.10-5	3 μm		
14/11/2005	1,02.10-3	4.10-5	^b Filtration à		
24/11/2005	1,05.10-3	4.10-5	0,1 μm		
27/01/2006	1,26.10-3	6.10-5	^c Filtration à 0,01 μm		
09/02/2006*	1,35.10-3	6.10-5	^{x2} Après 2		
10/02/2006	1,33.10-3	8.10-5	vidanges		
			^{x3} Après 3		
			vidanges		

Tableau 18 : $[Cl^-]$ dans les eaux porales et PZVP.

Date	EPX1-0.5m		EPX1-0.8m		EPX1-1.1m		EPX1-1.4m		PZVP	
	$[Cl^-]$ (mol.L ⁻¹)	σ								
14/11/2005	1,17.10-3	6.10-5	1,50.10-3	5.10-5						
27/01/2006	1,73.10-3	8.10-6					1,27.10-3	2.10-5		
13/03/2006	2,84.10-3	3.10-5	2,7.10-3	2.10-4	8,87.10-4	1.10-5	1,24.10-3	3.10-6		
12/04/2006	2,26.10-3	7.10-5	2,10.10-3	7.10-5	9.10-4	1.10-4	7,5.10-4	6.10-5		
09/05/2006	2,6.10-3	1.10-4	2,50.10-3	4.10-5	8,9.10-4	2.10-5	9,65.10-4	1.10-6		
					1,010.10-					
					3	6.10-6	8,86.10-4	1.10-6		
31/08/2006					1,00.10-3		8,4.10-4	9.10-5		
12/09/2006					1.10-3	1.10-4	9.10-4	1.10-4		
02/10/2006	1,24.10-3	3.10-5			9.10-4	3.10-5	8,09.10-4	3.10-5		
11/10/2006	1,04.10-3	3.10-5	1,35.10-3	3.10-5	8,95.10-4	3.10-5	8,09.10-4	3.10-5	1,02.10-3	3.10-5
12/12/2006	3,75.10-3	1.10-4	3,44.10-3	5.10-5	6,34.10-3	1.10-4			1,04.10-3	4.10-5
16/01/2007	2,28.10-3	9.10-5	2,22.10-3	9.10-5	2,71.10-3	1.10-4	1,06.10-3	8.10-5	1,07.10-3	8.10-5
13/02/2007	2,49.10-3	9.10-5	4,61.10-3	1.10-4	2,45.10-3	2.10-4	1,13.10-3	8.10-5	1,04.10-3	8.10-5
14/03/2007	1,94.10-3	3.10-5	6,62.10-3	5.10-5						
04/04/2007	1,94.10-3		6,62.10-3		3,00.10-3		9,50.10-4			
05/06/2007	2,28.10-3	1.10-5	2,33.10-3	6.10-6	3,36.10-3	4.10-6	8,90.10-4	2.10-6	8,76.10-4	3.10-6
13/07/2007	1,99.10-3	1.10-5	1,69.10-3	4.10-5	1,43.10-3	3.10-5	1,85.10-3	3.10-4	1,04.10-3	2.10-5

Les valeurs en italique sont estimées et utilisées pour les calculs de spéciation

Nitrate**Tableau 19 : $[NO_3^-]$ au PZPK.**

PZPK			09/02/2006*	7,6.10-5	9.10-6
Date	$[NO_3^-]$	σ	10/02/2006	2,8.10-4	2.10-5
	(mol.L ⁻¹)		12/03/2006*	5,8.10-5	9.10-6
25/04/2002	1,0.10-6	1.10-7	13/03/2006	7,6.10-5	9.10-6
30/07/2002	1,19.10-7	6.10-9	11/04/2006*	4,3.10-5	9.10-6
28/01/2003	5,42.10-5	4.10-7	12/04/2006	4,4.10-5	9.10-6
14/05/2003	1,38.10-5	2.10-7	09/05/2006	1,5.10-4	1.10-5
23/07/2003	6,3.10-7	2.10-8	07/07/2006	7,60.10-4	8.10-6
10/02/2004	1,3.10-5	3.10-6	31/08/2006	8,1.10-5	9.10-6
07/04/2004	1,9.10-5	3.10-6	12/09/2006	6,1.10-5	9.10-6
15/04/2004	6,6.10-5	4.10-6	11/10/2006	4,7.10-5	7.10-6
21/04/2004	4,3.10-5	5.10-6	16/01/2007	2,5.10-5	9.10-6
28/04/2004	1,1.10-5	3.10-6	13/02/2007	2,5.10-5	9.10-6
05/05/2004	4,0.10-5	4.10-6	12/03/2007	3,5.10-5	9.10-6
12/05/2004	3,5.10-5	3.10-6	05/06/2007	3,24.10-5	1.10-7
25/05/2004	5,5.10-5	9.10-6	03/07/2007	7,1.10-6	1.10-7
26/08/2004	3,9.10-5	9.10-6	13/07/2007	2,8.10-6	9.10-7
24/11/2004	4,3.10-5	6.10-6	<i>Les valeurs en italique sont estimées et utilisées pour les calculs de spéciation</i>		
16/02/2005	5,5.10-5	8.10-6	^a Avant vidange		
18/05/2005	1,1.10-5	2.10-6	^a Filtration à 3		
30/06/2005*	2,3.10-5	7.10-6	^b μm		
01/07/2005	7,7.10-5	4.10-6	^b Filtration à 0,1 μm		
04/07/2005	1,15.10-4	4.10-6	^c Filtration à 0,01 μm		
30/08/2005*	3,2.10-5	9.10-6	^{x2} Après 2		
31/08/2005	2,2.10-5	4.10-6	^{x3} Vidanges		
14/11/2005	3,6.10-5	3.10-6	^{x3} Après 3		
24/11/2005	2,6.10-5	3.10-6	^{x3} Vidanges		
27/01/2006	2,4.10-4	1.10-5			

Tableau 20 : $[NO_3^-]$ dans les eaux porales et PZVP.

Date	EPX1-0.5m		EPX1-0.8m		EPX1-1.1m		EPX1-1.4m		PZVP	
	$[NO_3^-]$ (mol.L ⁻¹)	σ								
14/11/2005	3,3.10-4	2.10-5	3,5.10-4	2.10-5						
27/01/2006	2,50.10-4	3.10-6					7,8.10-5	4.10-6		
13/03/2006	1,7.10-4	1.10-5	1,48.10-4	7.10-6	8,05.10-5	8.10-6	8,7.10-5	2.10-6		
12/04/2006	1,2.10-4	1.10-5	1,2.10-4	1.10-5	1,3.10-4	1.10-5	1,1.10-4	1.10-5		
09/05/2006	1,2.10-4	2.10-5	1,01.10-4	8.10-6	1,36.10-4	9.10-6	9.10-5	3.10-5		
07/07/2006					1,29.10-4	1.10-6	1,39.10-4	3.10-6		
31/08/2006					8,50.10-5		6.10-5	2.10-5		
12/09/2006					6,82.10-5	7.10-6	7,1.10-5	7.10-6		
02/10/2006	4,88.10-5	7.10-6			6,95.10-5	7.10-6	1,83.10-4	7.10-6		
11/10/2006	5,10.10-5	7.10-6	6,88.10-5	7.10-6	6,86.10-5	7.10-6	7,3.10-5	8.10-6	5,2.10-5	7.10-6
12/12/2006	5,00.10-5		4,00.10-5		4,50.10-5					
16/01/2007	4,98.10-5	2.10-5	2,83.10-5	2.10-5	2,65.10-5	2.10-5	5.10-5	2.10-5		
13/02/2007	3,07.10-4	2.10-5	1,40.10-4	2.10-5	3,28.10-4	2.10-5	1,8.10-4	2.10-5	2,4.10-5	7.10-6
14/03/2007	1,1.10-4	1.10-5	6,081.10-5	1.10-5						
04/04/2007	1,10.10-4		6,00.10-5		2,00.10-4		1,00.10-4			
05/06/2007	1,43.10-4	1.10-6	7,19.10-5	2.10-6	1,78.10-4	5.10-7	7,20.10-5	8.10-8	3,19.10-5	2.10-7
13/07/2007	7,545.10-5	2.10-6	3,433.10-5	1.10-6	3,39.10-5	5.10-7	4,6.10-5	6.10-6	4,0.10-6	9.10-7

Les valeurs en italique sont estimées et utilisées pour les calculs de spéciation

Carbone total**Tableau 21 : C total au PZPK.**

Date	C total (mol de C.L ⁻¹)	PZPK σ	10/02/2006	1,112.10-2	2.10-5	
10/02/2004	5.10-3	8.10-5	10/02/2006	8.97.10-3	2.10-5	
07/04/2004	3,08.10-3	6.10-4	12/03/2006*	9,35.10-3	2.10-5	
15/04/2004	3,14.10-3	6.10-5	13/03/2006	9,85.10-3	2.10-5	
21/04/2004	3,61.10-3	9.10-5	11/04/2006*	1,124.10-2	6.10-5	
28/04/2004	3,90.10-3	3.10-5	12/04/2006	1,118.10-2	6.10-5	
05/05/2004	5,48.10-3	7.10-5	09/05/2006	9,88.10-3	1.10-5	
12/05/2004	4,51.10-3	9.10-5	07/07/2006	7,46.10-3	4.10-6	
25/05/2004	9,38.10-3	3.10-5	31/08/2006	1,07.10-2	2.10-5	
26/08/2004	9,86.10-3	4.10-5	12/09/2006	1,08.10-2	2.10-5	
24/11/2004	1,03.10-2	4.10-5	11/10/2006	9,251.10-3	9.10-6	
16/02/2005	9,99.10-3	4.10-5	07/12/2006*	1,139.10-2	2.10-5	
18/05/2005	1,10.10-2	5.10-5	07/12/2006	1,02.10-2	2.10-5	
30/06/2005*	9,72.10-3	6.10-5	07/12/2006^{x2}	1,02.10-2	2.10-5	
01/07/2005	8,49.10-3	6.10-5	07/12/2006^{x3}	1,03.10-2	2.10-5	
01/07/2005^b	8,49.10-3	8.10-5	16/01/2007	1,41.10-2	3.10-5	
01/07/2005^c	8,60.10-3	5.10-5	13/02/2007	1,11.10-2	2.10-5	
04/07/2005	6,50.10-3	4.10-4	03/04/2007	9,95.10-3	1.10-5	
30/08/2005*	9,22.10-3	5.10-5	05/06/2007	1,07.10-2	5.10-5	
31/08/2005	1,01.10-2	6.10-5	<i>Les valeurs en italique sont estimées et utilisées pour les calculs de spéciation</i>			
14/11/2005	1,03.10-2	3.10-5	<i>* Avant vidange</i>			
24/11/2005	1,08.10-2	3.10-5	<i>^a Filtration à 3</i>			
27/01/2006	1,01.10-2	3.10-5	<i>^b Filtration à</i>			
09/02/2006*	1,148.10-2	2.10-5	<i>0,1 µm</i>			
09/02/2006*	1,164.10-2	2.10-5	<i>^c Filtration à 0,01 µm</i>			
09/02/2006*	1,032.10-2	2.10-5	<i>^{x2} Après 2</i>			
10/02/2006	1,113.10-2	2.10-5	<i>vidanges</i>			
			<i>^{x3} Après 3</i>			
			<i>vidanges</i>			

Tableau 22 : C total dans les eaux porales et PZVP.

Date	EPX1-0.5m		EPX1-0.8m		EPX1-1.1m		EPX1-1.4m		PZVP	
	C total (mol de C.L ⁻¹)	σ	C total (mol de C.L ⁻¹)	σ	C total (mol de C.L ⁻¹)	σ	C total (mol de C.L ⁻¹)	σ	C total (mol de C.L ⁻¹)	σ
14/11/2005	1,173.10-2	3.10-5	7,16.10-3	2.10-5						
27/01/2006	1,370.10-2	3.10-5					1,18.10-2	3.10-5		
13/03/2006	1,408.10-2	3.10-5	1,394.10-2	3.10-5	1,188.10-2	2.10-5	1,16.10-2	3.10-5		
12/04/2006	1,366.10-2	8.10-5	1,337.10-2	6.10-5	1,036.10-2	5.10-5	7,38.10-3	5.10-5		
09/05/2006	1,4580.10-2	7.10-6	1,380.10-2	2.10-5	1,130.10-2	4.10-6	1,096.10-2	5.10-5		
07/07/2006					1,126.10-2	1.10-5	1,051.10-2	3.10-5		
31/08/2006							8,96.10-3	2.10-5		
12/09/2006					1,02.10-2	2.10-5	1,140.10-2	2.10-5		
02/10/2006	1,28.10-2	3.10-5	1,26.10-2	3.10-5	1,13.10-2	3.10-5	1,114.10-2	2.10-5		
11/10/2006	1,274.10-2	3.10-5	1,120.10-2	3.10-6	1,11.10-2	3.10-5	1,038.10-2	2.10-5	1,088.10-2	2.10-5
12/12/2006	1,442.10-2	2.10-5	1,213.10-2	2.10-5	1,12.10-2	3.10-5			1,027.10-2	2.10-5
16/01/2007	1,61.10-2	3.10-5	1,67.10-2	3.10-5	9,73.10-3	2.10-5	9,42.10-3	2.10-5	9,00.10-3	2.10-5
13/02/2007	1,75.10-2	3.10-5	1,73.10-2	2.10-5	1,14.10-2	2.10-5	1,11.10-2	3.10-5	1,06.10-2	3.10-5
14/03/2007										
04/04/2007	1,48.10-2	1.10-5	1,43.10-2	1.10-5	9,94.10-3	1.10-5	9,98.10-3	5.10-6	9,00.10-3	2.10-5
05/06/2007	1,89.10-2	7.10-5	1,85.10-2	3.10-5	1,195.10-2	2.10-5	1,19.10-2	2.10-5	1,10.10-2	3.10-5
13/07/2007										

Les valeurs en italique sont estimées et utilisées pour les calculs de spéciation

C inorganique total (CIT)**Tableau 23 : CIT au PZPK.**

Date	PZPK	<i>CIT</i>	σ	10/02/2006	8,60.10-3	3.10-5	
		(mol de C.L ⁻¹)		10/02/2006	8,66.10-3	6.10-5	
25/04/2002	<i>7,50.10-3</i>			10/02/2006*	6,50.10-3	4.10-5	
28/01/2003	<i>5,70.10-3</i>			12/03/2006*	7,20.10-3	3.10-5	
14/05/2003	<i>6,43.10-3</i>			13/03/2006	7,31.10-3	3.10-5	
23/07/2003	<i>9,85.10-3</i>			11/04/2006*	7,5.10-3	1.10-4	
10/02/2004	2,85.10-3	6.10-5		12/04/2006	7,64.10-3	7.10-5	
07/04/2004	1,80.10-3	3.10-5		09/05/2006	5,87.10-3	1.10-5	
15/04/2004	1,46.10-3	3.10-5		07/07/2006	<i>4,59.10-3</i>	4.10-6	
21/04/2004	1,88.10-3	3.10-5		31/08/2006	9,07.10-3	3.10-5	
28/04/2004	1,75.10-3	3.10-5		12/09/2006	9,09.10-3	3.10-5	
05/05/2004	2,82.10-3	4.10-5		11/10/2006	7,34.10-3	1.10-5	
12/05/2004	2,29.10-3	3.10-5		07/12/2006*	6,57.10-3	2.10-5	
25/05/2004	5,67.10-3	3.10-5		07/12/2006	6,29.10-3	1.10-5	
26/08/2004	5,85.10-3	3.10-5		07/12/2006 ^{x2}	6,59.10-3	1.10-5	
24/11/2004	6,14.10-3	3.10-5		07/12/2006 ^{x3}	6,28.10-3	1.10-5	
16/02/2005	6,09.10-3	3.10-5		16/01/2007	8,43.10-3	1.10-5	
18/05/2005	6,61.10-3	2.10-4		13/02/2007	7,35.10-3	1.10-5	
30/06/2005*	8,13.10-3	2.10-5		12/03/2007	<i>7,35.10-3</i>		
01/07/2005	7,29.10-3	3.10-5		03/04/2007	8,91.10-3	9.10-6	
01/07/2005 ^b	7,14.10-3	3.10-5		05/06/2007	1,07.10-2	2.10-5	
01/07/2005 ^c	7,02.10-3	2.10-5		13/07/2007	<i>1,70.10-2</i>		
04/07/2005	1,21.10-3	2.10-4		<i>Les valeurs en italique sont estimées et utilisées pour les calculs de spéciation</i>			
30/08/2005*	8,37.10-3	4.10-5		* Avant vidange			
31/08/2005	9,35.10-3	4.10-5		^a Filtration à			
14/11/2005	6,58.10-3	5.10-5		3 μm			
24/11/2005	6,83.10-3	5.10-5		^b Filtration à			
27/01/2006	5,94.10-3	5.10-5		0,1 μm			
09/02/2006*	9,35.10-3	3.10-5		^c Filtration à 0,01 μm			
09/02/2006*	8,97.10-3	7.10-5		^{x2} Après 2			
09/02/2006*	7,54.10-3	3.10-5		vidanges			
				^{x3} Après 3			
				vidanges			

Tableau 24 : CIT dans les eaux porales et PZVP.

Date	EPX1-0.5m		EPX1-0.8m		EPX1-1.1m		EPX1-1.4m		PZVP	
	CIT (mol de C.L. ⁻¹)	σ								
14/11/2005	7,909.10-3	3.10-5	<i>7,50.10-3</i>	3.10-5						
27/01/2006	8,07.10-3	5.10-5					7,28.10-3	5.10-5		
13/03/2006	1,10.10-2	3.10-5	1,10.10-2	3.10-5	9,82.10-3	4.10-5	8,3.10-3	4.10-4		
12/04/2006	9,230.10-3	7.10-5	8,90.10-3	7.10-5	8,4.10-3	7.10-5	4,86.10-3	6.10-5		
09/05/2006	7,94.10-3	1.10-5	7,35.10-3	8.10-6	6,72.10-3	8.10-6	6,57.10-3	4.10-6		
07/07/2006					7,32.10-3	3.10-6	6,37.10-3	4.10-7		
31/08/2006					<i>9,00.10-3</i>		7,13.10-3	3.10-5		
12/09/2006					8,23.10-3	3.10-5	9,44.10-3	3.10-5		
02/10/2006	7,41.10-3	7.10-5	7,29.10-3	7.10-5	7,39.10-3	7.10-5	7,39.10-3	7.10-5		
11/10/2006	7,20.10-3	1.10-5	7,48.10-3	2.10-5	7,32.10-3	7.10-5	7,22.10-3	1.10-5	7,06.10-3	1.10-5
12/12/2006	8,52.10-3	1.10-5	8,09.10-3	1.10-5	7,30.10-3	2.10-5			7,03.10-3	1.10-5
16/01/2007	1,17.10-2	2.10-5	1,25.10-2	3.10-5	5,76.10-3	2.10-5	5,47.10-3	1.10-5	6,08.10-3	1.10-5
13/02/2007	1,35.10-2	2.10-5	1,31.10-2	3.10-5	7,17.10-3	1.10-5	7,23.10-3	1.10-5	7,08.10-3	1.10-5
14/03/2007			<i>1,25.10-2</i>							
04/04/2007	1,30.10-2	1.10-4	1,22.10-2	5.10-6	9,50.10-3	5.10-6	9,43.10-3	6.10-6	9,11.10-3	7.10-6
05/06/2007	1,60.10-2	1.10-6	1,64.10-2	7.10-6	1,08.10-2	1.10-5	1,11.10-2	9.10-6	1,09.10-2	1.10-5
13/07/2007	<i>1,60.10-2</i>		<i>1,80.10-2</i>		<i>1,00.10-2</i>		<i>1,11.10-2</i>		<i>1,09.10-2</i>	

Les valeurs en italique sont estimées et utilisées pour les calculs de spéciation

C organique total (COT)**Tableau 25 : COT au PZPK.**

Date	PZPK		10/02/2006	2,47.10-3	6.10-5	
	COT	σ	10/02/2006	2,47.10-3	4.10-5	
	(mol de C.L ⁻¹)		12/03/2006*	2,15.10-3	4.10-5	
10/02/2004	2,60.10-3	1.10-4	13/03/2006	2,54.10-3	4.10-5	
07/04/2004	1,28.10-3	6.10-4	11/04/2006*	3,7.10-3	1.10-4	
15/04/2004	1,68.10-3	7.10-5	12/04/2006	3,55.10-3	9.10-5	
21/04/2004	1,73.10-3	9.10-5	09/05/2006	4,01.10-3	1.10-5	
28/04/2004	2,15.10-3	4.10-5	07/07/2006	<i>2,87.10-3</i>	6.10-6	
05/05/2004	2,66.10-3	8.10-5	31/08/2006	1,64.10-3	4.10-5	
12/05/2004	2,22.10-3	9.10-5	12/09/2006	1,72.10-3	4.10-5	
25/05/2004	3,71.10-3	5.10-5	11/10/2006	1,91.10-3	1.10-5	
26/08/2004	4,01.10-3	5.10-5	07/12/2006*	4,82.10-3	3.10-5	
24/11/2004	4,16.10-3	5.10-5	07/12/2006	<i>3,87.10-3</i>	2.10-5	
16/02/2005	3,90.10-3	5.10-5	07/12/2006	<i>3,56.10-3</i>	2.10-5	
18/05/2005	4,39.10-3	2.10-4	07/12/2006	<i>4,01.10-3</i>	2.10-5	
30/06/2005*	1,59.10-3	6.10-5	16/01/2007	5,70.10-3	3.10-5	
01/07/2005	1,20.10-3	7.10-5	13/02/2007	3,72.10-3	2.10-5	
01/07/2005 ^b	1,35.10-3	9.10-5	03/04/2007	1,04.10-3	2.10-5	
01/07/2005 ^c	1,58.10-3	5.10-5	05/06/2007	0	5.10-5	
04/07/2005	5,29.10-3	4.10-4	<i>Les valeurs en italique sont estimées et utilisées pour les calculs de spéciation</i>			
30/08/2005*	8,50.10-4	6.10-5	<i>* Avant vidange</i>			
31/08/2005	7,50.10-4	7.10-5	<i>^a Filtration à</i>			
14/11/2005	3,72.10-3	6.10-5	<i>3 µm</i>			
24/11/2005	3,92.10-3	6.10-5	<i>^b Filtration à</i>			
27/01/2006	4,13.10-3	6.10-5	<i>0,1 µm</i>			
09/02/2006*	2,13.10-3	4.10-5	<i>^c Filtration à 0,01 µm</i>			
09/02/2006*	2,67.10-3	7.10-5	<i>^{x2} Après 2</i>			
09/02/2006*	2,78.10-3	4.10-5	<i>vidanges</i>			
10/02/2006	2,53.10-3	4.10-5	<i>^{x3} Après 3</i>			
			<i>vidanges</i>			

Tableau 26 : COT dans les eaux porales et PZVP.

Date	EPX1-0.5m		EPX1-0.8m		EPX1-1.1m		EPX1-1.4m		PZVP	
	COT	σ								
	(mol de C.L ⁻¹)		(mol de C.L ⁻¹)		(mol de C.L ⁻¹)		(mol de C.L ⁻¹)		(mol de C.L ⁻¹)	
14/11/2005	3,82.10-3	4.10-5	0	4.10-5						
27/01/2006	5,63.10-3	6.10-5					4,52.10-3	6.10-5		
13/03/2006	3,11.10-3	4.10-5	2,97.10-3	4.10-5	2,06.10-3	4.10-5	3,36.10-3	4.10-4		
12/04/2006	4,4.10-3	1.10-4	4,48.10-3	9.10-5	1,99.10-3	9.10-5	2,52.10-3	8.10-5		
09/05/2006	6,64.10-3	1.10-5	6,46.10-3	2.10-5	4,58.10-3	9.10-6	4,39.10-3	5.10-5		
07/07/2006					3,94.10-3	1.10-5	4,14.10-3	3.10-5		
31/08/2006							1,84.10-3	4.10-5		
12/09/2006					1,99.10-3	4.10-5	1,96.10-3	4.10-5		
02/10/2006	5,39.10-3	8.10-5	5,35.10-3	8.10-5	3,86.10-3	8.10-5	3,75.10-3	7.10-5		
11/10/2006	5,54.10-3	3.10-5	3,72.10-3	2.10-5	3,80.10-3	8.10-5	3,16.10-3	2.10-5	3,82.10-3	2.10-5
12/12/2006	5,90.10-3	2.10-5	4,04.10-3	2.10-5	3,91.10-3	4.10-5			3,24.10-3	2.10-5
16/01/2007	4,35.10-3	4.10-5	4,23.10-3	4.10-5	3,97.10-3	3.10-5	3,95.10-3	2.10-5	2,92.10-3	2.10-5
13/02/2007	4,01.10-3	4.10-5	4,23.10-3	4.10-5	4,24.10-3	2.10-5	3,83.10-3	3.10-5	3,47.10-3	3.10-5
14/03/2007										
04/04/2007	1,9.10-3	1.10-4	2,01.10-3	1.10-5	4,47.10-4	2.10-5	5,51.10-4	7.10-6	0,00E+00	2.10-5
05/06/2007	2,91.10-3	7.10-5	2,07.10-3	3.10-5	1,13.10-3	2.10-5	7,88.10-4	2.10-5	8.10-5	4.10-5
13/07/2007										

Les valeurs en italique sont estimées et utilisées pour les calculs de spéciation

Calcium**Tableau 27 : [Ca²⁺] au PZPK.**

PZPK					
Date	[Ca ²⁺] (mol.L ⁻¹)	σ			
25/04/2002	8,27.10-3	2.10-5	12/03/2006*	1,30.10-2	1.10-4
30/07/2002	5,39.10-3	6.10-6	13/03/2006	1,18.10-2	2.10-4
23/10/2002	1,53.10-2	2.10-3	11/04/2006*	7,58.10-3	6.10-5
28/01/2003	<i>4,32.10-3</i>	4.10-5	12/04/2006	7,77.10-3	8.10-5
14/05/2003	<i>5,04.10-3</i>	5.10-5	09/05/2006	5,60.10-3	3.10-5
23/07/2003	4,60.10-3	4.10-5	07/07/2006	5,43.10-3	3.10-5
15/10/2003	5,76.10-3	1.10-5	31/08/2006	4,92.10-3	3.10-5
10/02/2004	<i>6,9.10-3</i>	1.10-4	12/09/2006	4,95.10-3	6.10-5
07/04/2004	<i>4,59.10-3</i>	2.10-4	11/10/2006	5,1.10-3	1.10-4
15/04/2004	1,10.10-2	2.10-4	07/12/2006*	1,02.10-2	2.10-4
21/04/2004	9,3.10-3	2.10-4	07/12/2006	8,7.10-3	2.10-4
28/04/2004	1,20.10-2	2.10-4	07/12/2006 ^{x2}	8,4.10-3	2.10-4
05/05/2004	5,4.10-3	1.10-4	07/12/2006 ^{x3}	8,4.10-3	1.10-4
12/05/2004	7,9.10-3	2.10-4	16/01/2007	9,92.10-3	1.10-4
25/05/2004	9,0.10-3	2.10-4	13/02/2007	6,85.10-3	1.10-4
26/08/2004	5,0.10-3	1.10-4	12/03/2007	5,95.10-3	1.10-4
24/11/2004	7,8.10-3	2.10-4	03/04/2007	6,00.10-3	1.10-4
16/02/2005	6,3.10-3	1.10-4	05/06/2007	<i>5,58.10-3</i>	1.10-4
18/05/2005	3,7.10-3	1.10-4	03/07/2007	1,12.10-2	1.10-4
30/06/2005*	6,4.10-3	1.10-4	13/07/2007	7,81.10-3	1.10-4
01/07/2005	4,9.10-3	1.10-4			
04/07/2005	3,80.10-3	6.10-5			
30/08/2005*	4,4.10-3	1.10-4			
31/08/2005	4,9.10-3	1.10-4			
14/11/2005	4,9.10-3	1.10-4			
24/11/2005	4,9.10-3	1.10-4			
27/01/2006	1,13.10-2	2.10-4			
10/02/2006	1,19.10-2	1.10-4			

Les valeurs en italique sont estimées et utilisées pour les calculs de spéciation

* Avant vidange

^a Filtration

à 3 µm

^b Filtration

à 0,1 µm

^c Filtration à 0,01 µm

^{x2} Après 2

vidanges

^{x3} Après 3

vidanges

Tableau 28 : [Ca²⁺] dans les eaux porales et PZVP.

Date	EPX1-0.5m		EPX1-0.8m		EPX1-1.1m		EPX1-1.4m		PZVP	
	[Ca ²⁺] (mol.L ⁻¹)	σ								
14/11/2005	1,03.10-2	2.10-4	1,26.10-2	2.10-4						
27/01/2006	1,18.10-2	2.10-4					6,9.10-3	1.10-4		
13/03/2006	1,07.10-2	1.10-4	1,06.10-2	1.10-4	7,36.10-3	8.10-5	6,98.10-3	7.10-5		
12/04/2006	1,06.10-2	1.10-4	1,10.10-2	1.10-4	7,38.10-3	8.10-5	6,92.10-3	1.10-4		
09/05/2006			<i>7,65.10-3</i>	1.10-4	7,62.10-3	7.10-5	6,95.10-3	5.10-5		
07/07/2006					<i>4,01.10-3</i>		7,03.10-3	8.10-5		
31/08/2006					<i>6,00.10-3</i>		<i>7,00.10-3</i>			
12/09/2006					7,07.10-3	4.10-5	<i>7,00.10-3</i>			
02/10/2006	9,29.10-3	1.10-4	9,86.10-3	1.10-4	6,76.10-3	8.10-5	6,48.10-3	8.10-5		
11/10/2006	8,9.10-3	2.10-4	1,03.10-2	1.10-4	7,2.10-3	1.10-4	6,79.10-3	9.10-5	4,70.10-3	7.10-5
12/12/2006	1,13.10-2	2.10-4	1,05.10-2	2.10-4	7,5.10-3	2.10-4	6,7.10-3	1.10-4	4,65.10-3	9.10-5
16/01/2007	1,13.10-2	2.10-4	1,12.10-2	2.10-4	<i>7,45.10-3</i>		7,04.10-3	1.10-4	4,58.10-3	9.10-5
13/02/2007	1,05.10-2	2.10-4	1,09.10-2	2.10-4	7,36.10-3	2.10-4	7,09.10-3	1.10-4	4,58.10-3	9.10-5
14/03/2007	1,03.10-2	2.10-4	1,02.10-2	2.10-4						
04/04/2007	7,66.10-3	2.10-4	<i>1,07.10-2</i>	2.10-4	<i>8,00.10-3</i>	2.10-4	7,60.10-3	1.10-4	4,61.10-3	9.10-5
05/06/2007	8,01.10-3	2.10-4	8,33.10-3	2.10-4	7,67.10-3	2.10-4	7,32.10-3	1.10-4	1,17.10-2	9.10-5
13/07/2007	<i>8,01.10-3</i>	2.10-4	<i>8,87.10-3</i>	2.10-4	<i>8,00.10-3</i>	2.10-4	<i>8,01.10-3</i>	1.10-4	4,53.10-3	9.10-5

Les valeurs en italique sont estimées et utilisées pour les calculs de spéciation

Sodium**Tableau 29 : $[Na^+]$ au PZPK.**

PZPK			12/03/2006*	2,85.10-3	2.10-5
Date	$[Na^+]$	σ	13/03/2006	2,74.10-3	4.10-5
	(mol.L ⁻¹)		11/04/2006*	1,47.10-3	1.10-5
25/04/2002	<i>6,00.10-4</i>	<i>3.10-5</i>	12/04/2006	1,44.10-3	1.10-5
30/07/2002	<i>1,60.10-3</i>	<i>2.10-5</i>	09/05/2006	7,54.10-4	7.10-6
28/01/2003	<i>6,30.10-4</i>	<i>3.10-5</i>	07/07/2006	1,11.10-3	4.10-6
14/05/2003	<i>4,20.10-4</i>	<i>3.10-5</i>	31/08/2006	1,09.10-3	5.10-6
23/07/2003	<i>1,20.10-3</i>	<i>4.10-5</i>	12/09/2006	1,08.10-3	7.10-6
15/10/2003	<i>1,30.10-3</i>	<i>2.10-5</i>	11/10/2006	1,15.10-3	1.10-5
10/02/2004	<i>8,70.10-4</i>	<i>2.10-5</i>	07/12/2006*	2,08.10-3	2.10-5
07/04/2004	<i>6,80.10-4</i>	<i>3.10-5</i>	07/12/2006	1,61.10-3	2.10-5
15/04/2004	<i>7,30.10-4</i>	<i>3.10-5</i>	07/12/2006^{x2}	1,55.10-3	1.10-5
21/04/2004	<i>6,30.10-4</i>	<i>2.10-5</i>	07/12/2006^{x3}	1,52.10-3	1.10-5
28/04/2004	<i>7,70.10-4</i>	<i>3.10-5</i>	16/01/2007	3,96.10-3	7.10-6
05/05/2004	<i>3,60.10-4</i>	<i>2.10-5</i>	13/02/2007	2,78.10-3	7.10-6
12/05/2004	<i>4,90.10-4</i>	<i>2.10-5</i>	12/03/2007	2,04.10-3	7.10-6
25/05/2004	<i>9,4.10-4</i>	<i>2.10-5</i>	03/04/2007	2,22.10-3	7.10-6
26/08/2004	<i>1,09.10-3</i>	<i>2.10-5</i>	05/06/2007	2,22.10-3	7.10-6
24/11/2004	<i>4,9.10-4</i>	<i>2.10-5</i>	03/07/2007	1,22.10-3	7.10-6
16/02/2005	<i>9,29.10-4</i>	<i>2.10-5</i>			
18/05/2005	<i>4</i>	<i>2.10-5</i>	13/07/2007	2,09.10-3	7.10-6
30/06/2005*	<i>5,6.10-4</i>	<i>1.10-5</i>			
01/07/2005	<i>8,8.10-4</i>	<i>2.10-5</i>			
04/07/2005	<i>6,9.10-4</i>	<i>1.10-5</i>			
30/08/2005*	<i>3,01.10-4</i>	<i>6.10-6</i>			
31/08/2005	<i>1,14.10-4</i>	<i>2.10-5</i>			
14/11/2005	<i>3</i>	<i>2.10-5</i>			
24/11/2005	<i>1,1.10-3</i>	<i>2.10-4</i>			
27/01/2006	<i>1,2.10-3</i>	<i>1.10-4</i>			
10/02/2006	<i>1,4.10-3</i>	<i>1.10-4</i>			
	<i>1,39.10-3</i>				
	<i>3</i>	<i>1.10-5</i>			

Les valeurs en italique sont estimées et utilisées pour les calculs de spéciation

* Avant vidange

^a Filtration à

3 µm

^b Filtration à 0,1 µm

^c Filtration à 0,01 µm

^{x2} Après 2

vidanges

^{x3} Après 3

vidanges

Tableau 30 : $[Na^+]$ dans les eaux porales et PZVP.

Date	EPX1-0.5m		EPX1-0.8m		EPX1-1.1m		EPX1-1.4m		PZVP	
	$[Na^+]$ (mol.L ⁻¹)	σ								
14/11/2005	2,75.10-3	3.10-5	3,90.10-3	2.10-5						
27/01/2006	2,3.10-3	2.10-4					1,9.10-3	2.10-4		
13/03/2006	2,69.10-3	3.10-5	2,60.10-3	1.10-5	1,99.10-3	1.10-5	2,04.10-3	2.10-5		
12/04/2006	2,72.10-3	1.10-5	2,67.10-3	2.10-5	1,95.10-3	2.10-5	2,04.10-3	9.10-6		
09/05/2006			2,72.10-3	1.10-5	1,94.10-3	2.10-5	2,04.10-3	8.10-6		
07/07/2006					7,33.10-3	6.10-5	2,04.10-3	2.10-5		
31/08/2006					4,60.10-3		2,50.10-3			
12/09/2006					2,00.10-3	1.10-5	3,07.10-3	3.10-5		
02/10/2006	2,24.10-3	9.10-6	2,86.10-3	2.10-5	2,02.10-3	2.10-5	2,05.10-3	1.10-5		
11/10/2006	2,02.10-3	3.10-5	2,72.10-3	3.10-5	1,91.10-3	1.10-5	2,09.10-3	2.10-5	1,84.10-3	3.10-5
12/12/2006	2,54.10-3	2.10-5	2,40.10-3	3.10-5	2,08.10-3	3.10-5	2,34.10-3	3.10-5	1,80.10-3	2.10-5
16/01/2007	3,52.10-3	2.10-5	3,22.10-3	3.10-5	2,00.10-3		2,13.10-3	3.10-5	2,00.10-3	3.10-5
13/02/2007	3,74.10-3	2.10-5	3,48.10-3	3.10-5	2,13.10-3	3.10-5	2,13.10-3	3.10-5	2,00.10-3	3.10-5
14/03/2007	4,00.10-3	2.10-5	3,78.10-3	3.10-5						
04/04/2007	3,22.10-3	2.10-5	2,96.10-3	3.10-5	2,17.10-3	3.10-5	2,22.10-3	3.10-5	2,09.10-3	3.10-5
05/06/2007	2,74.10-3	2.10-5	2,65.10-3	3.10-5	2,39.10-3	3.10-5	2,17.10-3	3.10-5	1,83.10-3	3.10-5
13/07/2007	1,26.10-3	2.10-5	1,22.10-3	3.10-5	1,09.10-3	3.10-5	1,09.10-3	3.10-5	2,13.10-3	3.10-5

Les valeurs en italique sont estimées et utilisées pour les calculs de spéciation

Magnésium**Tableau 31 : [Mg²⁺] au PZPK.**

Date	[Mg ²⁺] (mol.L ⁻¹)	σ	PZPK	11/04/2006*	4,75.10- 4	4.10-6
25/04/2002	4,48.10- 4	8.10-6		12/04/2006	4,81.10- 4	2.10-6
30/07/2002	7,90.10- 4	1.10-5		09/05/2006	3,05.10- 4	2.10-6
28/01/2003	2,80.10- 4	1.10-5		07/07/2006	3,59.10- 4	2.10-6
14/05/2003	2,77.10- 4	8.10-6		31/08/2006	5,82.10- 4	2.10-6
23/07/2003	6,59.10- 4	8.10-6		12/09/2006	5,81.10- 4	1.10-5
15/10/2003	6,00.10- 4	1.10-5		11/10/2006	5,68.10- 4	3.10-6
10/02/2004	3,32.10- 4	9.10-6		07/12/2006*	6,42.10- 4	6.10-6
07/04/2004	5,00.10- 4	8.10-6		07/12/2006 ^{x2}	5,04.10- 4	1.10-6
15/04/2004	5,31.10- 4	9.10-6		07/12/2006 ^{x3}	4,83.10- 4	4.10-6
21/04/2004	4,53.10- 4	9.10-6		16/01/2007	7,36.10- 4	1.10-5
28/04/2004	5,50.10- 4	1.10-5		13/02/2007	5,64.10- 4	1.10-5
05/05/2004	2,57.10- 4	9.10-6		12/03/2007	4,32.10- 4	1.10-5
12/05/2004	3,70.10- 4	8.10-6		03/04/2007	4,81.10- 4	1.10-5
25/05/2004	5,6.10-4	3.10-5		05/06/2007	6,13.10- 4	1.10-5
26/08/2004	5,7.10-4	6.10-5		03/07/2007	3,95.10- 4	1.10-5
24/11/2004	4,20.10- 4	8.10-6		13/07/2007	5,64.10- 4	1.10-5
16/02/2005	3,4.10-4	2.10-5				
18/05/2005	5,6.10-4					
01/07/2005	3,7.10-4					
30/08/2005*	4,7.10-4	2.10-5				
31/08/2005	5,6.10-4	2.10-5				
14/11/2005	6,0.10-4	1.10-5				
24/11/2005	6,0.10-4	1.10-5				
27/01/2006	6,7.10-4	3.10-5				
10/02/2006	6,98.10- 4	5.10-6				
12/03/2006*	8,09.10- 4	5.10-6				
13/03/2006	7,58.10- 4	3.10-6				

Les valeurs en italique sont estimées et utilisées pour les calculs de spéciation

* Avant vidange

^a Filtration à

3 µm

^b Filtration à
0,1 µm

^c Filtration à 0,01 µm

^{x2} Après 2
vidanges

^{x3} Après 3
vidanges

Tableau 32 : $[Mg^{2+}]$ dans les eaux porales et PZVP.

Date	EPX1-0.5m		EPX1-0.8m		EPX1-1.1m		EPX1-1.4m		PZVP	
	$[Mg^{2+}]$ (mol.L ⁻¹)	σ								
14/11/2005	8,90.10-4	2.10-5	9,60.10-4	2.10-5						
27/01/2006	1,04.10-3	4.10-5					8,4.10-4	4.10-5		
13/03/2006	9,55.10-4	3.10-6	8,96.10-4	4.10-6	7,69.10-4	5.10-6	8,04.10-4	4.10-6		
12/04/2006	9,30.10-4	4.10-6	9,09.10-4	7.10-6	7,73.10-4	4.10-6	8,10.10-4	3.10-6		
09/05/2006			9,06.10-4	5.10-6	7,76.10-4	3.10-6	8,18.10-4	8.10-6		
07/07/2006					1,00.10-3		8,17.10-4	6.10-6		
31/08/2006					1,00.10-3		9,50.10-4			
12/09/2006					7,33.10-4	3.10-6	1,18.10-3	4.10-6		
02/10/2006	8,33.10-4	4.10-6	8,68.10-4	4.10-6	7,27.10-4	2.10-6	7,69.10-4	5.10-6		
11/10/2006	7,12.10-4	4.10-6	8,18.10-4	5.10-6	6,96.10-4	4.10-6	7,36.10-4	4.10-6	5,43.10-4	3.10-6
12/12/2006	9,14.10-4	5.10-6	8,47.10-4	4.10-6	7,2.10-4	1.10-5	7,28.10-4	6.10-6	5,16.10-4	1.10-6
16/01/2007	1,07.10-3	5.10-6	1,00.10-3	5.10-6	7,60.10-4		8,02.10-4	6.10-6	5,64.10-4	3.10-6
13/02/2007	1,01.10-3	5.10-6	9,79.10-4	5.10-6	8,06.10-4	1.10-5	8,02.10-4	6.10-6	5,60.10-4	3.10-6
14/03/2007	9,83.10-4	5.10-6	9,09.10-4	5.10-6						
04/04/2007	7,36.10-4	5.10-6	6,99.10-4	5.10-6	8,02.10-4	1.10-5	8,56.10-4	6.10-6	5,64.10-4	3.10-6
05/06/2007	7,45.10-4	5.10-6	7,24.10-4	5.10-6	8,27.10-4	1.10-5	8,23.10-4	6.10-6	4,81.10-4	3.10-6
13/07/2007	4,28.10-4	5.10-6	4,03.10-4	5.10-6	3,66.10-4	1.10-5	4,20.10-4	6.10-6	5,35.10-4	3.10-6

Les valeurs en italique sont estimées et utilisées pour les calculs de spéciation

Potassium**Tableau 33 : $[K^+]$ au PZPK.**

PZPK			12/03/2006*	2,27.10-4	6.10-6
Date	$[K^+]$	σ	13/03/2006	2,14.10-4	4.10-6
		(mol.L ⁻¹)	11/04/2006*	1,26.10-4	7.10-6
25/04/2002	7,37.10-4	2.10-6	12/04/2006	1,36.10-4	5.10-6
30/07/2002	1,17.10-4	3.10-7	09/05/2006	1,34.10-4	6.10-6
28/01/2003	1,40.10-4	1.10-5	07/07/2006	7,45.10-5	3.10-6
14/05/2003	2,22.10-4	8.10-6	31/08/2006	9,87.10-5	4.10-6
23/07/2003	1,54.10-4	9.10-6	12/09/2006	9,41.10-5	5.10-6
15/10/2003	1,30.10-4	8.10-6	11/10/2006	6,4.10-5	4.10-6
10/02/2004	1,36.10-4	9.10-6	07/12/2006*	1,40.10-4	4.10-6
07/04/2004	2,10.10-4	1.10-5	07/12/2006	5,9.10-5	5.10-6
15/04/2004	2,22.10-4	9.10-6	07/12/2006^{x2}	5,8.10-5	5.10-6
21/04/2004	2,10.10-4	9.10-6	07/12/2006^{x3}	5,7.10-5	2.10-6
28/04/2004	2,40.10-4	9.10-6	16/01/2007	1,25.10-4	5.10-6
05/05/2004	1,60.10-4	8.10-6	13/02/2007	1,41.10-4	5.10-6
12/05/2004	2,00.10-4	8.10-6	12/03/2007	1,38.10-4	5.10-6
25/05/2004	1,76.10-4	8.10-6	03/04/2007	1,61.10-4	5.10-6
26/08/2004	1,2.10-4	4.10-5	05/06/2007	1,23.10-4	5.10-6
24/11/2004	1,61.10-4	6.10-6	03/07/2007	1,05.10-4	5.10-6
16/02/2005	1,29.10-4	7.10-6	13/07/2007	1,64.10-4	5.10-6
18/05/2005	1,68.10-4	5.10-6	<i>Les valeurs en italique sont estimées et utilisées pour les calculs de spéciation</i>		
30/06/2005*	1,33.10-4	5.10-6	* Avant vidange		
01/07/2005	1,16.10-4	4.10-6	^a Filtration à 3 µm		
04/07/2005	9,7.10-5	4.10-6	^b Filtration à 0,1 µm		
30/08/2005*	1,55.10-4	5.10-6	^c Filtration à 0,01 µm		
31/08/2005	1,02.10-4	6.10-6	^{x2} Après 2 vidanges		
14/11/2005	9,4.10-5	5.10-6	^{x3} Après 3 vidanges		
24/11/2005	9,79.10-5	3.10-6			
27/01/2006	1,9.10-4	2.10-5			
10/02/2006	2,19.10-4	4.10-6			

Tableau 34 : $[K^+]$ dans les eaux porales et PZVP.

Date	EPX1-0.5m		EPX1-0.8m		EPX1-1.1m		EPX1-1.4m		PZVP	
	$[K^+]$ (mol.L ⁻¹)	σ								
14/11/2005	2,05.10-5	5.10-6	1,38.10-5							
27/01/2006	6.10-5	2.10-5					1,6.10-4	2.10-5		
13/03/2006	1,30.10-4	5.10-6	9,01.10-5	4.10-6	1,88.10-4	5.10-6	1,63.10-4	5.10-6		
12/04/2006	1,12.10-4	8.10-6	1,07.10-4	4.10-6	1,61.10-4	6.10-6	1,69.10-4	4.10-6		
09/05/2006			1,59.10-4	6.10-6	1,67.10-4	3.10-6	1,73.10-4	5.10-6		
07/07/2006					6,18.10-4	1.10-5	1,61.10-4	4.10-6		
31/08/2006					3,80.10-4		2,00.10-4			
12/09/2006					1,66.10-4	3.10-6	2,50.10-4	6.10-6		
02/10/2006	1,89.10-5	6.10-6	1,02.10-5	4.10-6	1,71.10-4	5.10-6	1,78.10-4	6.10-6		
11/10/2006	1,535.10-5	6.10-6	3,5.10-5	3.10-6	9,0.10-5	7.10-6	9,8.10-5	6.10-6	9,6.10-5	4.10-6
12/12/2006	1,07.10-4	1.10-6	1,04.10-4	1.10-6	4,5.10-3	6.10-5	2,47.10-3	3.10-5	6,4.10-5	4.10-6
16/01/2007	1,59.10-4	6.10-6	2,07.10-4	4.10-6	3,00.10-3		4,78.10-4	1.10-4	4	4.10-6
13/02/2007	4,86.10-4	6.10-6	2,89.10-3	4.10-6	1,60.10-3	6.10-5	3,99.10-4	1.10-4	1,20.10-4	4.10-6
14/03/2007	1,56.10-4	6.10-6	4,96.10-3	4.10-6					1,15.10-4	
04/04/2007	1,10.10-4	6.10-6	1,02.10-4	4.10-6	2,33.10-4	6.10-5	1,84.10-4	1.10-4	1,38.10-4	4.10-6
05/06/2007	1,68.10-3	6.10-6	1,76.10-3	4.10-6	3,17.10-3	6.10-5	7,60.10-3	1.10-4	4	4.10-6
13/07/2007	3,17.10-4	6.10-6	2,30.10-4	4.10-6	1,71.10-4	6.10-5	2,81.10-4	1.10-4	1,82.10-4	4.10-6

Les valeurs en italique sont estimées et utilisées pour les calculs de spéciation

Strontium**Tableau 35 : [Sr²⁺] au PZPK.**

Date	[Sr ²⁺] (mol.L ⁻¹)	σ	PZPK	10/02/2006	7,76.10-5	4.10-6
25/04/2002	4,59.10-5	9.10-7		10/02/2006		
30/07/2002	2,50.10-5	7.10-7		10/02/2006		
23/10/2002				10/02/2006		
28/01/2003				15/02/2006		
14/05/2003				12/03/2006*	4,63.10-5	2.10-6
23/07/2003				13/03/2006	5,07.10-5	3.10-6
15/10/2003				11/04/2006*	4,96.10-5	2.10-6
10/02/2004	3,42.10-5	2.10-6		12/04/2006	5,24.10-5	3.10-6
29/03/2004				27/04/2006*		
07/04/2004	6,81.10-5	3.10-6		28/04/2006		
15/04/2004	7,43.10-5	4.10-6		08/05/2006*		
21/04/2004	6,17.10-5	3.10-6		09/05/2006	3,72.10-5	2.10-6
28/04/2004	7,48.10-5	4.10-6		07/07/2006	4,18.10-5	2.10-6
05/05/2004	3,29.10-5	2.10-6		31/08/2006	5,07.10-5	3.10-6
12/05/2004	5,25.10-5	3.10-6		12/09/2006	4,87.10-5	2.10-6
25/05/2004	6,44.10-5	3.10-6		11/10/2006		
26/08/2004	4,90.10-5	2.10-6		07/12/2006*	5,8.10-5	3.10-6
24/11/2004	5,36.10-5	3.10-6		07/12/2006	4,7.10-5	2.10-6
16/02/2005	3,99.10-5	2.10-6		07/12/2006 ^{x2}	4,6.10-5	2.10-6
18/05/2005	3,88.10-5	2.10-6		07/12/2006 ^{x3}	4,6.10-5	2.10-6
30/06/2005*	4,68.10-5	2.10-6		16/01/2007	4,7.10-5	2.10-6
01/07/2005	3,50.10-5	2.10-6		13/02/2007	3,7.10-5	2.10-6
01/07/2005 ^a				12/03/2007	3,2.10-5	2.10-6
01/07/2005 ^b				03/04/2007	3,0.10-5	2.10-6
01/07/2005 ^c				05/06/2007	4,0.10-5	2.10-6
04/07/2005	2,24.10-5	1.10-6		03/07/2007	2,3.10-5	1.10-6
30/08/2005*	4,41.10-5	2.10-6		13/07/2007	3,2.10-5	2.10-6
31/08/2005	5,34.10-5	3.10-6				
14/11/2005	5,60.10-5	3.10-6				
24/11/2005	5,47.10-5	3.10-6				
27/01/2006	7,53.10-5	4.10-6				
09/02/2006*	1,10.10-4	5.10-6				
09/02/2006*						
09/02/2006*						
09/02/2006*						

Les valeurs en italique sont estimées et utilisées pour les calculs de spéciation

* Avant vidange

^a Filtration à

3 µm

^b Filtration à

0,1 µm

^c Filtration à 0,01 µm

^{x2} Après 2

vidanges

^{x3} Après 3

vidanges

Tableau 36 : [Sr²⁺] dans les eaux porales et PZVP.

Date	EPX1-0.5m		EPX1-0.8m		EPX1-1.1m		EPX1-1.4m		PZVP	
	[Sr ²⁺] (mol.L ⁻¹)	σ								
14/11/2005	9,2.10-5	5.10-6	9,2.10-5							
27/01/2006	9,6.10-5	5.10-6					9,4.10-5	5.10-6		
13/03/2006	9,6.10-5	5.10-6	9,2.10-5	5.10-6	8,9.10-5	4.10-6	9,4.10-5	5.10-6		
12/04/2006	9,6.10-5	5.10-6	7,7.10-5	4.10-6	9,0.10-5	5.10-6	9,2.10-5	5.10-6		
09/05/2006	8,8.10-5	4.10-6	9,5.10-5	5.10-6	8,4.10-5	4.10-6	8,7.10-5	4.10-6		
07/07/2006					8,8.10-5	4.10-6	7,1.10-5	4.10-6		
31/08/2006	9,2.10-5	5.10-6	8,6.10-5	4.10-6	8,9.10-5	4.10-6	9,5.10-5	5.10-6		
12/09/2006					8,5.10-5		8,4.10-5	4.10-6		
02/10/2006	<i>6,4.10-5</i>				<i>7,7.10-5</i>		<i>8,0.10-5</i>			
11/10/2006	6,4.10-5	3.10-6	6,8.10-5	3.10-6	7,7.10-5	4.10-6	7,4.10-5	4.10-6	4,2.10-5	2.10-6
12/12/2006	7,9.10-5	4.10-6	7,0.10-5	4.10-6	7,5.10-5	4.10-6	7,8.10-5	4.10-6	4,4.10-5	2.10-6
16/01/2007	7,8.10-5	4.10-6	7,6.10-5	4.10-6	<i>7,6.10-5</i>		8,0.10-5	4.10-6	4,2.10-5	2.10-6
13/02/2007	7,2.10-5	4.10-6	7,1.10-5	4.10-6	7,7.10-5	4.10-6	7,4.10-5	4.10-6	4,1.10-5	2.10-6
14/03/2007	6,5.10-5	3.10-6	6,7.10-5	3.10-6						
04/04/2007	6,0.10-5	3.10-6	5,8.10-5	3.10-6	7,2.10-5	4.10-6	7,5.10-5	4.10-6	4,3.10-5	2.10-6
05/06/2007	5,9.10-5	3.10-6	6,1.10-5	3.10-6	8,8.10-5	4.10-6	8,1.10-5	4.10-6	3,5.10-5	2.10-6
13/07/2007	2,4.10-5	1.10-6	2,3.10-5	1.10-6	2,6.10-5	1.10-6	2,9.10-5	1.10-6	3,0.10-5	1.10-6

Les valeurs en italique sont estimées et utilisées pour les calculs de spéciation

Baryum**Tableau 37 : [Ba²⁺] au PZPK.**

Date	PZPK [Ba ²⁺] (mol.L ⁻¹)	σ	10/02/2006	1,15.10-6	1.10-7	
25/04/2002	2,80.10-6	8.10-8	10/02/2006			
30/07/2002	1,63.10-6	7.10-8	10/02/2006			
23/10/2002			10/02/2006			
28/01/2003			15/02/2006			
14/05/2003			12/03/2006*	1,28.10-6	1.10-7	
23/07/2003			13/03/2006	1,33.10-6	1.10-7	
15/10/2003			11/04/2006*	1,45.10-6	1.10-7	
10/02/2004	1,72.10-6	1.10-7	12/04/2006	1,49.10-6	1.10-7	
29/03/2004			27/04/2006*			
07/04/2004	4,37.10-7	1.10-7	28/04/2006			
15/04/2004	3,79.10-7	1.10-7	08/05/2006*			
21/04/2004	4,22.10-7	1.10-7	09/05/2006	1,35.10-6	1.10-7	
28/04/2004	4,15.10-7	1.10-7	07/07/2006	1,41.10-6	1.10-7	
05/05/2004	1,65.10-6	1.10-7	31/08/2006	1,38.10-6	1.10-7	
12/05/2004	1,08.10-6	1.10-7	12/09/2006	1,32.10-6	1.10-7	
25/05/2004	1,42.10-6	1.10-7	11/10/2006			
26/08/2004	1,70.10-6	1.10-7	07/12/2006*	1,97.10-6	1.10-7	
24/11/2004	1,91.10-6	1.10-7	07/12/2006	1,75.10-6	1.10-7	
16/02/2005	1,59.10-6	1.10-7	07/12/2006 ^{x2}	1,75.10-6	1.10-7	
18/05/2005	1,75.10-6	1.10-7	07/12/2006 ^{x3}	1,67.10-6	1.10-7	
30/06/2005*	1,88.10-6	1.10-7	16/01/2007	1,67.10-6	1.10-7	
01/07/2005	1,57.10-6	1.10-7	13/02/2007	1,38.10-6	1.10-7	
01/07/2005 ^a			12/03/2007	1,31.10-6	1.10-7	
01/07/2005 ^b			03/04/2007	1,38.10-6	1.10-7	
01/07/2005 ^c			05/06/2007	2,91.10-6	1.10-7	
04/07/2005	1,25.10-6	1.10-7	03/07/2007	1,53.10-6	1.10-7	
30/08/2005*	1,52.10-6	1.10-7	13/07/2007	2,18.10-6	1.10-7	
31/08/2005	1,72.10-6	1.10-7	<i>Les valeurs en italique sont estimées et utilisées pour les calculs de spéciation</i>			
14/11/2005	1,66.10-6	1.10-7	<i>* Avant vidange</i>			
24/11/2005	1,62.10-6	1.10-7	<i>^a Filtration à 3 µm</i>			
27/01/2006	1,12.10-6	1.10-7	<i>^b Filtration à 0,1 µm</i>			
09/02/2006*	1,31.10-6	1.10-7	<i>^c Filtration à 0,01 µm</i>			
09/02/2006*			<i>^{x2} Après 2 vidanges</i>			
09/02/2006*			<i>^{x3} Après 3 vidanges</i>			
09/02/2006*						

Tableau 38 : [Ba²⁺] dans les eaux porales et PZVP.

Date	EPX1-0.5m		EPX1-0.8m		EPX1-1.1m		EPX1-1.4m		PZVP	
	[Ba ²⁺] (mol.L ⁻¹)	σ								
14/11/2005	1,2.10-6	5.10-8	<i>1,2.10-6</i>							
27/01/2006	1,4.10-6	5.10-8					8,4.10-7	5.10-8		
13/03/2006	1,4.10-6	5.10-8	1,2.10-6	5.10-8	6,9.10-7	5.10-8	7,9.10-7	5.10-8		
12/04/2006	1,4.10-6	5.10-8	1,3.10-6	5.10-8	7,5.10-7	5.10-8	7,7.10-7	5.10-8		
09/05/2006	1,4.10-6	5.10-8	1,5.10-6	5.10-8	7,4.10-7	5.10-8	7.10-7	5.10-8		
07/07/2006					7,7.10-7	5.10-8	6,77.10-7	5.10-8		
31/08/2006	1,4.10-6	5.10-8	2,1.10-6	5.10-8	7,7.10-7	5.10-8	9.10-7	5.10-8		
12/09/2006					<i>8,0.10-7</i>		7,8.10-7	5.10-8		
02/10/2006	<i>1,3.10-6</i>				<i>8,7.10-7</i>		<i>8,00.10-7</i>			
11/10/2006	1,3.10-6	5.10-8	8,0.10-7	5.10-8	8,7.10-7	5.10-8	9,5.10-7	5.10-8	2,8.10-6	2.10-7
12/12/2006	1,6.10-6	5.10-8	2,0.10-6	5.10-8	8,0.10-7	5.10-8	8,01.10-7	5.10-8	2,9.10-6	2.10-7
16/01/2007	1,6.10-6	5.10-8	2,1.10-6	5.10-8	<i>8,0.10-7</i>		9.10-7	5.10-8	2,9.10-6	2.10-7
13/02/2007	1,5.10-6	5.10-8	1,9.10-6	5.10-8	8,7.10-7	5.10-8	8,7.10-7	5.10-8	2,9.10-6	2.10-7
14/03/2007	1,3.10-6	5.10-8	1,7.10-6	5.10-8						
04/04/2007	1,2.10-6	5.10-8	1,6.10-6	5.10-8	7,3.10-7	5.10-8	8,74.10-7	5.10-8	2,9.10-6	2.10-7
05/06/2007	1,4.10-6	5.10-8	1,8.10-6	5.10-8	9,5.10-7	5.10-8	8,74.10-7	5.10-8	6	2.10-7
13/07/2007	8,0.10-7	5.10-8	1,0.10-6	5.10-8	4,2.10-7	5.10-8	4,8.10-7	5.10-8	2,8.10-6	2.10-7

Les valeurs en italique sont estimées et utilisées pour les calculs de spéciation

Silicium dissous total**Tableau 39 : [Si]_{tot.diss.} au PZPK.**

PZPK					
Date	[Si] _{tot.diss.}	σ			
	(mol.L ⁻¹)				
25/04/2002	4,74.10-4	7.10-6	09/02/2006*	2,51.10-4	2.10-6
30/07/2002	4,99.10-4	7.10-6	10/02/2006	2,74.10-4	2.10-6
28/01/2003	2,23.10-4	6.10-6	10/02/2006	2,66.10-4	2.10-6
14/05/2003	2,99.10-4	6.10-6	10/02/2006	2,75.10-4	2.10-6
23/07/2003	4,28.10-4	6.10-6	10/02/2006	2,35.10-4	2.10-6
15/10/2003	3,65.10-4	6.10-6	12/03/2006*	1,83.10-4	2.10-6
10/02/2004	1,96.10-4	5.10-6	13/03/2006	1,96.10-4	2.10-6
07/04/2004	2,74.10-4	5.10-6	11/04/2006*	2,23.10-4	2.10-6
15/04/2004	3,54.10-4	6.10-6	12/04/2006	2,31.10-4	2.10-6
21/04/2004	3,50.10-4	6.10-6	09/05/2006	2,04.10-4	2.10-6
28/04/2004	4,07.10-4	1.10-5	07/07/2006	3,00.10-4	
05/05/2004	2,22.10-4	8.10-6	12/09/2006	4,80.10-4	2.10-6
12/05/2004	3,40.10-4	1.10-5	11/10/2006	6,35.10-4	2.10-6
25/05/2004	4,06.10-4	9.10-6	07/12/2006*	2,74.10-4	2.10-6
26/08/2004	5,70.10-4	2.10-5	07/12/2006	2,97.10-4	2.10-6
24/11/2004	2,31.10-4	1.10-6	07/12/2006 ^{x2}	2,82.10-4	2.10-6
16/02/2005	2,18.10-4	2.10-6	07/12/2006 ^{x3}	2,90.10-4	2.10-6
18/05/2005	2,21.10-4	2.10-6	16/01/2007	3,42.10-4	1.10-6
30/06/2005*	3,728.10-4	8.10-8	13/02/2007	2,40.10-4	1.10-6
01/07/2005	3,856.10-4	1.10-7	12/03/2007	2,40.10-4	
04/07/2005	2,646.10-4	7.10-8	05/06/2007	2,50.10-4	
30/08/2005*	4,110.10-4	8.10-8			
31/08/2005	4,551.10-4	1.10-7			
14/11/2005	4,294.10-4	8.10-8			
24/11/2005	4,810.10-4	9.10-8			
27/01/2006	2,57.10-4	2.10-6			
09/02/2006*	2,82.10-4	2.10-6			
09/02/2006*	2,56.10-4	2.10-6			
09/02/2006*	2,60.10-4	2.10-6			

Les valeurs en italique sont estimées et utilisées pour les calculs de spéciation

* Avant vidange

^a Filtration à

3 µm

^b Filtration à

0,1 µm

^c Filtration à 0,01 µm

^{x2} Après 2

vidanges

^{x3} Après 3

vidanges

Tableau 40 : $[Si]_{tot.diss.}$ dans les eaux porales et PZVP.

Date	EPX1-0.5m		EPX1-0.8m		EPX1-1.1m		EPX1-1.4m		PZVP	
	$[Si]_{tot.diss.}$ (mol.L ⁻¹)	σ								
14/11/2005	<i>2,02.10-4</i>		<i>4,00.10-4</i>							
27/01/2006	2,02.10-4	2.10-6					2,28.10-4	2.10-6		
13/03/2006	2,03.10-4	2.10-6	1,99.10-4	2.10-6	2,12.10-4	2.10-6	2,31.10-4	2.10-6		
12/04/2006	2,47.10-4	2.10-6	2,43.10-4	2.10-6	3,71.10-4	2.10-6	3,34.10-4	2.10-6		
09/05/2006	3,97.10-4	2.10-6	4,09.10-4	2.10-6	3,65.10-4	2.10-6	3,54.10-4	2.10-6		
							5,337.10-			
07/07/2006					5,701.10-4	2.10-7	4	1.10-7		
31/08/2006					<i>5,80.10-4</i>		<i>6,00.10-4</i>			
12/09/2006					5,98.10-4	2.10-6	7,07.10-4	2.10-6		
02/10/2006	<i>3,75.10-4</i>				<i>5,80.10-4</i>		5,36.10-4	2.10-6		
11/10/2006	3,75.10-4	1.10-6	4,56.10-4	1.10-6	5,38.10-4	2.10-6	5,50.10-4	2.10-6	5,87.10-4	2.10-6
12/12/2006	4,11.10-4	2.10-6	4,31.10-4	2.10-6	4,78.10-4	2.10-6			5,07.10-4	3.10-6
16/01/2007	3,90.10-4	2.10-6	3,81.10-4	2.10-6	<i>3,80.10-4</i>		3,87.10-4	2.10-6	4,36.10-4	2.10-6
13/02/2007	3,38.10-4	1.10-6	3,17.10-4	1.10-6	2,85.10-4	1.10-6	2,99.10-4	1.10-6	4,05.10-4	2.10-6
14/03/2007			<i>3,20.10-4</i>							
04/04/2007	<i>3,38.10-4</i>		<i>3,20.10-4</i>		<i>3,00.10-4</i>		<i>4,00.10-4</i>			
05/06/2007	<i>3,38.10-4</i>		<i>3,20.10-4</i>		<i>3,00.10-4</i>		<i>5,00.10-4</i>			
13/07/2007	<i>3,38.10-4</i>		<i>3,20.10-4</i>		<i>5,00.10-4</i>		<i>6,00.10-4</i>		<i>5,00.10-4</i>	

Les valeurs en italique sont estimées et utilisées pour les calculs de spéciation

Fluorure**Tableau 41 : [F⁻] au PZPK.**

PZPK			12/03/2006*	2,7.10-5	1.10-6
Date	[F ⁻]	σ (mol.L ⁻¹)	13/03/2006	3,1.10-5	3.10-6
25/04/2002	2,59.10-5	7.10-7	11/04/2006*	3,2.10-5	4.10-6
30/07/2002	3,25.10-5	8.10-7	12/04/2006	4,8.10-5	3.10-6
28/01/2003	3,16.10-5	3.10-7	09/05/2006	3,22.10-5	2.10-7
14/05/2003	2,30.10-5	3.10-7	07/07/2006	3,69.10-5	1.10-7
23/07/2003	1,95.10-5	3.10-7	31/08/2006	5,0.10-5	6.10-6
10/02/2004	7.10-5	2.10-5	12/09/2006	6,9.10-5	3.10-6
07/04/2004	6.10-5	2.10-5	11/10/2006	4,6.10-5	3.10-6
15/04/2004	3.10-5	1.10-5	07/12/2006*	3,2.10-5	3.10-6
21/04/2004	6.10-5	2.10-5	07/12/2006	2,9.10-5	2.10-6
28/04/2004	6.10-5	2.10-5	07/12/2006 ^{x2}	2,9.10-5	2.10-6
05/05/2004	6.10-5	2.10-5	07/12/2006 ^{x3}	2,9.10-5	2.10-6
12/05/2004	6.10-5	2.10-5	16/01/2007	4,6.10-5	5.10-6
25/05/2004	6.10-5	2.10-5	13/02/2007	4,7.10-5	2.10-6
26/08/2004	7.10-5	2.10-5	12/03/2007	4,3.10-5	3.10-6
24/11/2004	6.10-5	2.10-5	05/06/2007	3,93.10-5	8.10-8
16/02/2005	6.10-5	2.10-5	03/07/2007	3,31.10-5	7.10-7
18/05/2005	7.10-5	2.10-5	13/07/2007	3,87.10-5	7.10-7
30/06/2005*	7.10-5	2.10-5	<i>Les valeurs en italique sont estimées et utilisées pour les calculs de spéciation</i>		
01/07/2005	7.10-5	2.10-5	^a Avant vidange		
04/07/2005	6.10-5	2.10-5	^a Filtration à 3		
30/08/2005*	4.10-5	1.10-5	^b μm		
31/08/2005	3,1.10-5	1.10-6	^b Filtration à 0,1 μm		
14/11/2005	3,6.10-5	2.10-6	^c Après 2		
24/11/2005	3,8.10-5	2.10-6	^c Filtration à 0,01 μm		
27/01/2006	2,3.10-5	1.10-6	^{x2} Après 3		
09/02/2006*	2,3.10-5	1.10-6	^{x3} Vidanges		
10/02/2006	2,3.10-5	1.10-6	^{x3} Vidanges		

Tableau 42 : [F⁻] dans les eaux porales et PZVP.

Date	EPX1-0.5m		EPX1-0.8m		EPX1-1.1m		EPX1-1.4m		PZVP	
	[F ⁻] (mol.L ⁻¹)	σ								
14/11/2005	5,8.10-5	1.10-7	<i>5,14.10-5</i>							
27/01/2006	5,1.10-5	2.10-8					4,97.10-5	1.10-7		
13/03/2006	5,5.10-5	5.10-8	5,14.10-5	3.10-7	4,8.10-5	1.10-7	3,66.10-5	8.10-9		
12/04/2006	4,7.10-5	1.10-6	4,3.10-5	1.10-6	4,6.10-5	2.10-6	4,9.10-5	2.10-6		
09/05/2006	6,2.10-5	1.10-6	5,14.10-5	1.10-7	5,1.10-5	2.10-7	4,94.10-5	2.10-7		
07/07/2006					5,1.10-5	2.10-7	5,41.10-5	5.10-7		
31/08/2006					<i>6,0.10-5</i>		5,2.10-5	3.10-6		
12/09/2006					6,2.10-5	3.10-6	6,6.10-5	3.10-6		
02/10/2006	6,5.10-5	3.10-6			5,3.10-5	3.10-6	5,10.10-5	3.10-6		
11/10/2006	7,1.10-5	3.10-6	6,84.10-5	3.10-6	5,6.10-5	3.10-6	5,56.10-5	4.10-6	4,67.10-5	3.10-6
12/12/2006	6,6.10-5	3.10-6	6,77.10-5	2.10-6	5,7.10-5	2.10-6			4,09.10-5	2.10-6
16/01/2007	6,3.10-5	5.10-6	6,24.10-5	2.10-6	4,8.10-5	2.10-6	4,11.10-5	2.10-6	3,99.10-5	5.10-6
13/02/2007	6,6.10-5	3.10-6	6,37.10-5	2.10-6	4,9.10-5	7.10-6	5,50.10-5	2.10-6	4,36.10-5	2.10-6
14/03/2007	5,4.10-5	3.10-6	5,588.10-5	3.10-6						
04/04/2007	<i>5,4.10-5</i>		<i>5,60.10-5</i>		<i>4,2.10-5</i>		<i>5,00.10-5</i>			
05/06/2007	5,9.10-5	2.10-7	5,45.10-5	4.10-7	3,9.10-5	5.10-7	4,06.10-5	1.10-6	3,30.10-5	2.10-8
13/07/2007	6,3.10-5	8.10-7	5,966.10-5	2.10-6	4,1.10-5	5.10-7	4,95.10-5	1.10-5	3,22.10-5	7.10-7

Les valeurs en italique sont estimées et utilisées pour les calculs de spéciation

Fer**Tableau 43 : [Fe]_{tot.diss.} au PZPK.**

PZPK					
Date	[Fe] _{tot.diss.}	σ			
	(mol.L ⁻¹)				
22/08/2001	1,83.10-7	2.10-8	09/02/2006*	3,3.10-7	8.10-8
15/10/2001	2,33.10-7	2.10-8	10/02/2006	5,8.10-7	4.10-8
23/01/2002	3,26.10-6	2.10-8	10/02/2006	3,4.10-6	2.10-7
25/04/2002	9.10-8	2.10-8	10/02/2006	5,0.10-7	3.10-8
30/07/2002	1,63.10-7	2.10-8	10/02/2006	2,4.10-6	2.10-7
23/10/2002	1,15.10-6	1.10-7	12/03/2006*	5,2.10-7	3.10-8
28/01/2003	1,13.10-5	1.10-6	13/03/2006	4,8.10-7	3.10-8
14/05/2003	1,25.10-5	1.10-6	11/04/2006*	3,0.10-6	1.10-7
23/07/2003	3,26.10-5	3.10-6	12/04/2006	2,3.10-6	1.10-7
10/02/2004	9.10-7	4.10-8	09/05/2006	3,68.10-6	2.10-7
07/04/2004	2.10-5	8.10-7	07/07/2006	2,15.10-6	1.10-7
15/04/2004	2.10-6	9.10-8	31/08/2006	6,4.10-6	3.10-7
21/04/2004	2.10-5	1.10-6	12/09/2006	4,3.10-6	2.10-7
28/04/2004	3.10-5	2.10-6	07/12/2006*	7,7.10-6	4.10-7
05/05/2004	1.10-5	7.10-7	07/12/2006^{x2}	3,8.10-6	2.10-7
12/05/2004	2.10-5	1.10-6	07/12/2006^{x3}	3,0.10-6	2.10-7
25/05/2004	1.10-6	6.10-8	16/01/2007	3,0.10-6	2.10-7
26/08/2004	2.10-5	1.10-6	13/02/2007	2,0.10-6	1.10-7
24/11/2004	4.10-6	2.10-7	12/03/2007	4,3.10-6	2.10-7
16/02/2005	6.10-6	3.10-7	03/04/2007	6,1.10-6	3.10-7
18/05/2005	2.10-5	1.10-6	05/06/2007	6,80.10-5	3.10-6
30/06/2005*	1.10-5	6.10-7	03/07/2007	4,30.10-6	2.10-7
01/07/2005	8.10-6	4.10-7	13/07/2007	2,08.10-5	1.10-6
04/07/2005	9.10-7	4.10-8	<i>Les valeurs en italique sont estimées et utilisées pour les calculs de spéciation</i>		
30/08/2005*	4.10-5	2.10-6	* Avant vidange		
31/08/2005	3,1.10-5	2.10-6	^a Filtration à 3 µm		
14/11/2005	5,1.10-5	3.10-6	^b Filtration à 0,1 µm		
24/11/2005	2,9.10-5	1.10-6	^c Filtration à 0,01 µm		
27/01/2006	6,9.10-7	3.10-8	^{x2} Après 2 vidanges		
09/02/2006*	5,8.10-7	4.10-8	^{x3} Après 3 vidanges		
09/02/2006*	5,7.10-7	3.10-8			
09/02/2006*	6,9.10-7	4.10-8			

Tableau 44 : $[Fe]_{tot.diss.}$ dans les eaux porales et PZVP.

Date	EPX1-0.5m		EPX1-0.8m		EPX1-1.1m		EPX1-1.4m		PZVP	
	$[Fe]_{tot.diss.}$ (mol.L ⁻¹)	σ								
14/11/2005	9,0.10-7	4.10-8	2,0.10-6							
27/01/2006	2,9.10-6	1.10-7					1,0.10-6			
13/03/2006	1,4.10-6	7.10-8	2,0.10-6	1.10-7	9,0.10-7	4.10-8	9,0.10-7	4.10-8		
12/04/2006	2,7.10-6	1.10-7	1,8.10-6	9.10-8	9,8.10-6	5.10-7	4,7.10-6	2.10-7		
09/05/2006	5,4.10-6	3.10-7	5,4.10-6	3.10-7	9,0.10-6	4.10-7	5,9.10-6	3.10-7		
07/07/2006					4,5.10-6	2.10-7	1,1.10-6	5.10-8		
31/08/2006	9,0.10-7	4.10-8	9,7.10-7	5.10-8	9,0.10-7	4.10-8	9,0.10-7	4.10-8		
12/09/2006					1,0.10-6		9,0.10-7	4.10-8		
02/10/2006	9,0.10-7				3,3.10-5		9,0.10-6			
11/10/2006	9,0.10-7	4.10-8	9,0.10-7	4.10-8	3,3.10-5	2.10-6	9,5.10-6	5.10-7	4,4.10-5	1.10-6
12/12/2006	4,5.10-6	2.10-7	2,5.10-6	1.10-7	2,0.10-6	1.10-7	9,0.10-7	4.10-8	4,3.10-5	1.10-6
16/01/2007	4,1.10-6	2.10-7	3,9.10-6	2.10-7	1,0.10-6		1,3.10-6	6.10-8	7,8.10-5	1.10-6
13/02/2007	1,1.10-5	5.10-7	4,3.10-6	2.10-7	3,4.10-5	2.10-6	1,2.10-5	6.10-7	7,2.10-5	1.10-6
14/03/2007	7,5.10-6	4.10-7	4,5.10-6	2.10-7						
04/04/2007	1,0.10-5	5.10-7	4,8.10-6	2.10-7	9,0.10-7	4.10-8	2,1.10-5	1.10-6	8,2.10-5	1.10-6
05/06/2007	1,3.10-5	6.10-7	7,2.10-6	4.10-7	1,9.10-5	9.10-7	9,0.10-7	4.10-8	1,6.10-6	1.10-6
13/07/2007	1,8.10-5	9.10-7	1,1.10-5	5.10-7	9,5.10-6	5.10-7	1,1.10-6	5.10-8	7,5.10-5	1.10-6

Les valeurs en italique sont estimées et utilisées pour les calculs de spéciation

Manganèse**Tableau 45 : [Mn]_{tot.diss.} au PZPK.**

Date	[Mn] _{tot.diss.} (mol.L ⁻¹)	σ	07/07/2006	1,00.10-6	5.10-8	
22/08/2001	1,09.10-6	2.10-8	31/08/2006	4,5.10-6	2.10-7	
15/10/2001	5.10-8	2.10-8	12/09/2006	4,6.10-6	2.10-7	
23/01/2002	7,94.10-6	2.10-8	07/12/2006*	7,8.10-6	4.10-7	
25/04/2002	4.10-8	2.10-8	07/12/2006^{x2}	4,9.10-6	2.10-7	
30/07/2002	5,1.10-7	5.10-8	07/12/2006^{x3}	4,2.10-6	2.10-7	
23/10/2002	9,4.10-7	9.10-8	16/01/2007	8,9.10-6	4.10-7	
28/01/2003	7,1.10-6	7.10-7	13/02/2007	3,3.10-6	2.10-7	
14/05/2003	6,7.10-6	7.10-7	12/03/2007	6,2.10-6	3.10-7	
23/07/2003	1,1.10-5	1.10-6	03/04/2007	6,6.10-6	3.10-7	
10/02/2004	2.10-7	1.10-8	05/06/2007	5,28.10-6	3.10-7	
07/04/2004	1.10-5	5.10-7	03/07/2007	2,55.10-6	1.10-7	
15/04/2004	1.10-5	6.10-7	13/07/2007	9,10.10-6	5.10-7	
21/04/2004	1.10-5	5.10-7	<i>Les valeurs en italique sont estimées et utilisées pour les calculs de spéciation</i>			
28/04/2004	1.10-5	6.10-7	<i>* Avant vidange</i>			
05/05/2004	6.10-6	3.10-7	<i>^a Filtration à 3</i>			
12/05/2004	9.10-6	4.10-7	<i>^b Filtration à 0,1</i>			
25/05/2004	8.10-6	4.10-7	<i>^c Filtration à 0,01 μm</i>			
26/08/2004	7.10-6	3.10-7	<i>^{x2} Après 2</i>			
24/11/2004	2.10-6	1.10-7	<i>vidanges</i>			
16/02/2005	8.10-6	4.10-7	<i>^{x3} Après 3</i>			
18/05/2005	8.10-6	4.10-7	<i>vidanges</i>			
30/06/2005*	8.10-6	4.10-7				
01/07/2005	5.10-6	3.10-7				
04/07/2005	1.10-7	5.10-9				
30/08/2005*	7.10-6	4.10-7				
31/08/2005	7,7.10-6	4.10-7				
14/11/2005	7,9.10-6	4.10-7				
24/11/2005	7,2.10-6	4.10-7				
27/01/2006	2,0.10-6	2.10-7				
09/02/2006*	3,7.10-6	3.10-7				
09/02/2006*	3,1.10-6	3.10-7				
09/02/2006*	3,8.10-6	3.10-7				
10/02/2006	2,7.10-6	3.10-7				
10/02/2006	2,8.10-6	3.10-7				
12/03/2006*	1,3.10-6	6.10-8				
13/03/2006	7,6.10-7	4.10-8				
11/04/2006*	9,0.10-6	9.10-7				
12/04/2006	8,8.10-6	9.10-7				
09/05/2006	7,04.10-6	8.10-7				

Tableau 46 : $[Mn]_{tot.diss.}$ dans les eaux porales et PZVP.

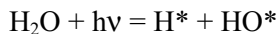
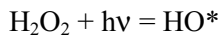
Date	EPX1-0.5m		EPX1-0.8m		EPX1-1.1m		EPX1-1.4m		PZVP	
	$[Mn]_{tot.diss.}$	σ								
	(mol.L ⁻¹)		(mol.L ⁻¹)		(mol.L ⁻¹)		(mol.L ⁻¹)		(mol.L ⁻¹)	
14/11/2005	3,6.10-8	2.10-9	1,2.10-5							
27/01/2006	1,0.10-5	5.10-7					5,8.10-6	3.10-7		
13/03/2006	1,1.10-5	5.10-7	1,2.10-5	6.10-7	6,7.10-6	3.10-7	6,2.10-6	3.10-7		
12/04/2006	1,1.10-5	6.10-7	1,1.10-5	6.10-7	7,0.10-6	3.10-7	6,0.10-6	3.10-7		
09/05/2006	1,0.10-5	5.10-7	1,0.10-5	5.10-7	6,8.10-6	3.10-7	5,6.10-6	3.10-7		
07/07/2006					6,8.10-6	3.10-7	5,2.10-6	3.10-7		
31/08/2006	7,3.10-8	4.10-9	1,1.10-7	5.10-9	6,4.10-6	3.10-7	6,2.10-6	3.10-7		
12/09/2006					7,0.10-6		5,4.10-6	3.10-7		
02/10/2006	5,5.10-7				7,5.10-6		6,0.10-6			
11/10/2006	5,5.10-7	3.10-8	9,1.10-7	5.10-8	7,5.10-6	4.10-7	6,6.10-6	3.10-7	5,6.10-6	5.10-7
12/12/2006	1,4.10-5	7.10-7	1,6.10-5	8.10-7	7,3.10-6	4.10-7	6,0.10-6	3.10-7	5,8.10-6	5.10-7
16/01/2007	1,4.10-5	7.10-7	1,8.10-5	9.10-7	7,5.10-6		6,9.10-6	3.10-7	5,6.10-6	5.10-7
13/02/2007	1,3.10-5	6.10-7	1,6.10-5	8.10-7	8,2.10-6	4.10-7	7,1.10-6	4.10-7	5,5.10-6	5.10-7
14/03/2007	1,1.10-5	6.10-7	1,5.10-5	7.10-7						
04/04/2007	1,1.10-5	5.10-7	1,3.10-5	7.10-7	7,6.10-6	4.10-7	7,3.10-6	4.10-7	5,5.10-6	5.10-7
05/06/2007	1,2.10-5	6.10-7	1,5.10-5	8.10-7	8,6.10-6	4.10-7	6,9.10-6	3.10-7	2,5.10-6	5.10-7
13/07/2007	6,2.10-6	3.10-7	8,6.10-6	4.10-7	3,8.10-6	2.10-7	3,8.10-6	2.10-7	5,1.10-6	5.10-7

Les valeurs en italique sont estimées et utilisées pour les calculs de spéciation

Annexe 2.6. Mode opératoire de la digestion de la matière organique dans les échantillons des eaux du site

Principe

Les échantillons sont mis en présence de peroxyde d'hydrogène et exposés à un rayonnement ultraviolet. Il s'ensuit une photolyse par rayons UV qui élimine la matière organique dissoute. L'irradiation UV entraîne la formation de radicaux OH* à partir du peroxyde d'hydrogène et de l'eau :



Ces radicaux permettent de décomposer des substances organiques. Plus ces radicaux sont nombreux, plus la photolyse à rayons UV est rapide. H₂O₂ est donc un initiateur de la réaction radicalaire. Si la température est assez élevée (70-90°C), une quantité suffisante de radicaux OH* se forme à partir de l'eau et l'ajout de H₂O₂ est inutile.

Les UV sont produits par une lampe à mercure, leur longueur d'onde est comprise entre 200 et 280 nm. Les tubes contenant les échantillons sont en quartz car le verre n'est pas totalement transparent aux UV. Ils sont munis de bouchons en téflon. Le chauffage s'effectue uniquement avec la lampe UV et le circuit de refroidissement comporte un indicateur de débit. Un thermomètre placé dans un tube de référence (eau) permet le contrôle de la température qui ne doit pas dépasser 90°C.

Mode opératoire

Matériel :

12 tubes en quartz : 11 échantillons + 1 témoin pour le thermomètre

Nettoyage des tubes par rinçages successifs :

HNO₃ 0,1 mol.L⁻¹ ;

Eau milliQ ;

Séchage à l'air.

La pesée des tubes vides permet de connaître le volume d'eau susceptible d'être évaporée lors de la digestion.

Par pesée, introduire 10 mL d'échantillon + 500 µL de H₂O₂ 30%.

IMPORTANT : utiliser des lunettes de protection adaptées aux rayons UV.

Placer les tubes sur le porte-échantillon.

IMPORTANT : Il faut remplir les tubes vides avec de l'eau distillée pour garantir une température inférieure à 90°C.

Enclever la **minuterie pour minimum 2h** : la lampe à mercure s'allume.

Ouvrir le robinet d'eau pour alimenter le circuit de refroidissement avec un débit de 110 à 115 mL.min⁻¹.

Pendant **30 minutes**, laisser monter la température jusqu'à 90°C en réajustant le débit d'eau si nécessaire. Surveiller constamment la température.

Pendant 1h30 de photolyse, surveiller le débit toutes les 15 minutes.

Si le voyant « Failure » s'allume, il y a surchauffe et la lampe s'éteint automatiquement.

Annexe 2.7. Estimating the stabilities of actinide aqueous species. Influence of sulfoxy-anions on uranium(IV) geochemistry and discussion of Pa(V) first hydrolysis



Available online at www.sciencedirect.com



C. R. Chimie 10 (2007) 978–993



<http://france.elsevier.com/direct/CRAS2C/>

Full paper / Mémoire

Estimating the stabilities of actinide aqueous species. Influence of sulfoxy-anions on uranium(IV) geochemistry and discussion of Pa(V) first hydrolysis[☆]

Pierre Vitorge ^{a,b,*}, Vannapha Phrommavanh ^c, Bertrand Siboulet ^d, Dominique You ^a, Thomas Vercouter ^a, Michael Descotes ^{b,c}, Colin J. Marsden ^e, Catherine Beaucaire ^c, Jean-Paul Gaudet ^f

^a Laboratoire de spéciation des radionucléides et des molécules (LSRM), CEA Saclay, DEN/DANS/DPC/SECR, 91191 Gif-sur-Yvette cedex, France

^b UMR 8587, CEA Saclay, DEN/DANS/DPC/SECR, 91191 Gif-sur-Yvette cedex, France

^c Laboratoire de mesures et modélisation de la migration des radionucléides (L3MR), CEA Saclay, DEN/DANS/DPC/SECR, 91191 Gif-sur-Yvette cedex, France

^d CEA Marcoule, DEN/DRCP/SCPS, 30207 Bagnols-sur-Cèze cedex, France

^e Laboratoire de physique quantique, CNRS–UMR 5626, Université Paul-Sabatier, 118, route de Narbonne, 31062 Toulouse cedex 4, France

^f Laboratoire d'étude des transferts en hydrologie et environnement (LTHE), UMR 5564, CNRS/INPG/IRD/UJF, BP 53, 38041 Grenoble cedex 9, France

Received 18 September 2006; accepted after revision 5 April 2007

Available online 29 June 2007

Abstract

Qualitative chemical information is used as a guideline for correlations between equilibrium constants or between equilibrium constants and atomic charges (deduced from quantum mechanics calculations). Pa(V) and Nb(V) hydrolysis constants are also recalculated from experimental data. $\log K_1^{\circ}(\text{An}^{\text{IV}}/\text{RO}_2^{2-}) = 6.59 \pm 0.55$ ($\text{S}_2\text{O}_3^{2-}$), 10.06 ± 0.88 (SO_3^{2-}), 11.97 ± 1.07 (CO_3^{2-}), and 10.05 ± 0.88 (HPO_4^{2-}) are estimated based on the trend of affinity for An cations in the series $\text{CO}_3^{2-} > \text{HPO}_4^{2-} \approx \text{SO}_3^{2-} > \text{SO}_4^{2-} \approx \text{S}_2\text{O}_3^{2-}$. These ideas and values are used to discuss U(IV) chemistry in S-containing ground-waters. *To cite this article:* P. Vitorge et al., C. R. Chimie 10 (2007).

© 2007 Académie des sciences. Published by Elsevier Masson SAS. All rights reserved.

Résumé

Des connaissances qualitatives ont été concrétisées sous la forme de corrélations empiriques entre constantes d'équilibres, voire avec les charges atomiques (issues de calculs quantiques) dans la série $\text{CO}_3^{2-} > \text{HPO}_4^{2-} \approx \text{SO}_3^{2-} > \text{SO}_4^{2-} \approx \text{S}_2\text{O}_3^{2-}$, pour, par exemple, estimer $\log K_1^{\circ}(\text{An}^{\text{IV}}/\text{RO}_2^{2-}) = 6.59 \pm 0.55$ ($\text{S}_2\text{O}_3^{2-}$), 10.06 ± 0.88 (SO_3^{2-}), 11.97 ± 1.07 (CO_3^{2-}), et 10.05 ± 0.88 (HPO_4^{2-}).

[☆] Partially presented at the Migration 05 conference [1], and part of the Ph.D. thesis of V. Phrommavanh.

* Corresponding author.

E-mail address: pierre.vitorge@cea.fr (P. Vitorge).

Ces valeurs sont utilisées pour prévoir l'influence éventuelle d'anions soufrés sur la chimie de U(IV) dans des eaux souterraines. **Pour citer cet article :** P. Vitorge et al., *C. R. Chimie* 10 (2007).

© 2007 Académie des sciences. Published by Elsevier Masson SAS. All rights reserved.

Keywords: Actinides; Hydrolysis; Sulphate; Sulfite; Thiosulphate; Carbonate; Groundwaters

Mots-clés : Actinides ; Hydrolyse ; Sulfate ; Sulfite ; Thiosulfate ; Carbonate ; Eaux souterraines

1. Introduction

The geochemical behaviour of actinides have been extensively studied for understanding uranium and thorium ore deposits, and more recently for assessing the environmental impact of the possible disposal of wastes that contain Pa, Np, Pu, Am or Cm. Starting with uranium [1], the Thermochemical Data Base project of the Nuclear Energy Agency (NEA-TDB) organised the reviewing of published experimental data relevant for modelling aqueous chemistries and solubilities of the most important radionuclides. The results of the NEA-TDB project are now well accepted as a reference critical review, essentially for aqueous chemistry and solubility at room temperature, but these reviews proposed data only when convincing experimental validations were published. There is therefore a gap between this restricted set of quantitative validated thermochemical data and qualitative chemical knowledge.

However, besides selected numerical values, the NEA-TDB reviews also provide qualitative information [2,3], which we used together with analogies for estimating the hydrolysis constants and standard potentials [4] needed for drawing Pourbaix' diagrams of actinides [5]. The present paper aims at testing such rough estimates for complexation.

Rules of thumb are currently used by chemists for checking the possible formation of hypothetical chemical species in specific chemical conditions, when these chemical species are not in databases. This might typically be the case for the environmental aqueous chemistry of An(IV), the actinide elements at the +4 oxidation state (An = Th, U, Np and Pu) in the presence of S-containing inorganic ligands; for this reason it is also an aim of the present paper to estimate the stabilities of An(IV) complexes with sulfoxo-anions.

For storing radioactive wastes, several projects are looking for geological sites that are well isolated from surface waters. These often correspond to anoxic conditions, where U, Np and Pu are expected to be stable in the +4 oxidation state [2,4]. Interestingly, chemical analogues are Ce(IV) and Th, and probably Zr and Hf.

Selected NEA-TDB equilibrium constants and redox potentials [2] are adequate for reliable modelling of uranium chemistry in most equilibrated groundwaters. Uranium is predicted to be stable in anoxic waters in the form of the $\text{U}(\text{OH})_4(\text{aq})$ aqueous species in equilibrium with uraninite, $\text{UO}_2(\text{s})$, a compound of low solubility [2,5,6]. Similar behaviour is expected for Np and Pu, even though Pu^{3+} might also be stable [4–7].

In natural under-ground-waters CO_3^{2-} , the carbonate anion is often the dominating ligand among the inorganic ligands (for actinide cations). However, carbonate complexes are predicted to be of little importance for An(IV) [2,4,7]. Nevertheless, many $\text{An}(\text{CO}_3)_i(\text{OH})_j^{4-2i-j}$ complexes have been proposed, but no reliable values could be validated for most of the corresponding formation constants [2,4], for which maximum possible values have been estimated from experimental observations, that also confirmed the similar behaviour of Th, U(IV), Np(IV) and Pu(IV) in carbonate/bicarbonate aqueous solutions [4,5,8]. Values have recently been proposed for the formation constants of several $\text{Th}(\text{CO}_3)_i(\text{OH})_j^{4-2i-j}$ complexes in an attempt to interpret a solubility study of $\text{ThO}_2(\text{s})$ [8,9], but the $\text{Th}(\text{CO}_3)_4^{4-}$ species were not included in the interpretation, even though we shall see it should not be completely negligible according to the NEA-TDB data [4]. For probing such competition between the HO^- and CO_3^{2-} ligands, the relative stabilities of the corresponding 1:1 complexes of An^{4+} will be compared. In this framework, the stability of AnCO_3^{2+} will be estimated: its existence has never been demonstrated, since it is always hidden by hydrolysed species. This over-stabilisation of hydrolysis is specific to the +4 oxidation state: the 1:1 carbonate complexes are well known, and their stabilities were well established for An(III), An(V) and An(VI) (it is not known for Pa(V), which is known to have a very different aqueous chemical behaviour from the other An(V)).

Several other inorganic hard anions are quite reactive toward actinide cations, specially those of high charge (PO_4^{3-}), of small size (F^-), or polydentate (HPO_4^{2-}): depending on their content in groundwaters they might form complexes with actinide cations. For example, it

was recently proposed that the pore-waters of Callovo–Oxfordian clay minerals, where an underground research laboratory is being built to study the feasibility of a deep geological repository for radioactive wastes in France [10], contain quite large amounts of SO_4^{2-} . The pore-water composition is approximately at the $\text{SO}_4^{2-}/\text{HS}^-/\text{H}_2\text{S}$ frontier point (Fig. 1). Although the most stable aqueous sulfur species – those bolded on Pourbaix’ diagrams – are sulfide (HS^-) and sulfate (SO_4^{2-}), some other sulfoxy-anions are often detected in natural environments, typically as thiosulfate ($\text{S}_2\text{O}_3^{2-}$) and sulfite (SO_3^{2-}) ions. For example, about 25% of the total S content has been reported to be $\text{S}_2\text{O}_3^{2-}$ in a reducing groundwater [11], and even in more oxidizing conditions [12]. Sulfoxy-anions are also suspected to form in the course of the oxidative dissolution of pyrite (FeS_2) [13], a mineral often associated with the redox regulation of ground-waters. For this reason, we focus on sulfoxy-anion ligands, specially on $\text{S}_2\text{O}_3^{2-}$.

Grenthe et al. have selected complexing constants for U(VI) complexes with these anions [2], but they wrote in their review that confirmation is needed: “*The only quantitative information about aqueous uranium thiosulfate complexes is the study by Melton and Amis [...] This review tentatively accepts [their] value, (although confirmation of the results from another study would be useful)*”. Furthermore: “*The solid formed seems to be a mixture indicating decomposition of thiosulfate into sulfite and elemental sulfur. This review finds no reliable evidence for the formation of solid uranium thiosulfate compounds.*” This decomposition might very well be the result of redox reactions (disproportionation), since both uranium and sulfur have a wide range of possible oxidation states, and their stability domains are not well established in mixtures of uranium and sulfur. This might in fact be a problem for other uranium compounds and complexes with sulfur-containing ligands. Unfortunately the NEA-TDB reviews could not validate such data for the Th and Zr analogues [14,15]. Since the NEA-TDB review has selected data for a thiosulfate complex of U(VI) [2], one might very well expect thiosulfate complexes of U(IV) in more reducing conditions – unless thiosulfate is strongly reduced, when U(IV) is formed – because the U^{4+} hard cation is usually more reactive (than UO_2^{2+}) toward oxygen-donor ligands. Based on the same hardness rule, thiosulfate should bind to hard cations *via* the O rather than the S atom of the sulfoxy-anion ligands. The same problem holds for the $\text{U}/\text{SO}_3^{2-}$ system: the NEA-TDB review has selected data for sulfite complexes of U(VI); but not for U(IV): “*Formation of*

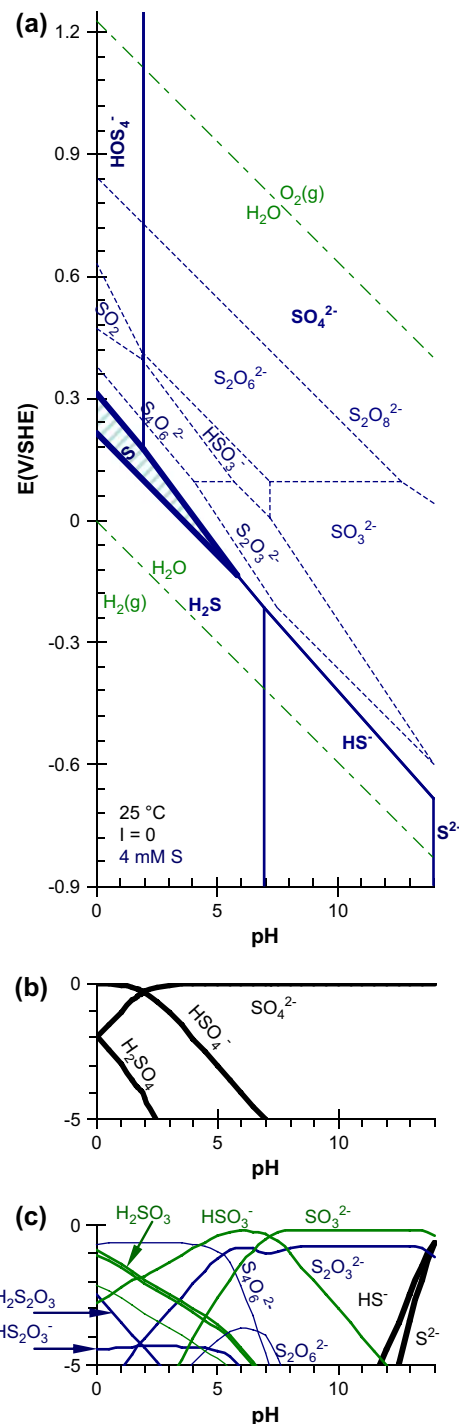


Fig. 1. Pourbaix diagram of sulfur. (a) The names of the major species (HS^- , H_2S , SO_4^{2-} , HSO_4^- and solid S) are in bold, and their predominance domains are drawn with thick lines. The domains (thin dashed lines) of the other (minor sulfur) species are obtained by suppressing SO_4^{2-} , HSO_4^- and H_2SO_4 . (b and c) The speciation (namely $\log[\text{H}_2\text{S}_j\text{O}_z]/[\text{S}]$) of each species ($\text{H}_2\text{S}_j\text{O}_z$) is represented for two kinetic assumptions (see text) in redox conditions corresponding to line B of Fig. 6.

aqueous uranium(IV) sulfite complexes was reported in a qualitative study by Rosenheim and Kelmy. However, no experimental chemical thermodynamic data on these species are available.” As a probe for ligand competition (between $S_2O_3^{2-}$ or SO_3^{2-} and typically OH^- or CO_3^{2-}), we shall estimate the formation constants of the corresponding 1:1 An(IV) complexes, namely $AnS_2O_3^{2+}$ and $AnSO_3^{2+}$.

Various methods are commonly used for estimating equilibrium constants, typically as empirical correlations with physical (or phenomenological) parameters (atomic radii and charges, solvent interactions...). They can also be obtained from molecular modelling methods. Indeed we recently estimated an uncertainty of 10 kJ mol^{-1} on Δ_rG for Pa(V) hydrolysis [16], which is about 20 times higher than the uncertainty of the experimental determinations of equilibrium constants and standard redox potentials in aqueous solutions. Furthermore, such methods need caution, when using calculated energies [17]. After others [18,19] (with a comment in Ref. [7]) we also tested empirical correlations, which appear to work surprisingly well for some of them: they actually help in putting numbers for quite encyclopedic qualitative knowledge. It is also a way to check such knowledge and corresponding chemical intuition. We use such correlations here, hoping this special issue will help such rules of thumb used by actinide chemistry specialists to become less mysterious. The rough estimates are only guidelines, which need experimental confirmation. They often originate in geometrical and electrostatics reasoning. Indeed, the chemical stabilities of hard cations are often correlated with the charge²/radius ratios of the reactants. Nevertheless, we shall see that the best correlations are not specially with the atomic charges; correlations between measured equilibrium constants will often appear to fit better: several physical contributions probably cancel out in those cases.

The present paper is organised as follows. First, definitions are given, together with features and explanations of methodologies from the NEA-TDB reviews. Results are first reported for correlations between U(VI) (or analogous An(VI)) 1:1 (1 cation with 1 ligand) complexes and protonation of the corresponding ligands, two types of reactions for which many published data are available. In a next step, such correlations are extended to An(III) and An(V). There are virtually no reliable published 1:1 complexing constants of An(IV), since An^{4+} hydrolysis usually overcomes complexation. Consequently we shall estimate An(IV) 1:1 complexing constants. We shall also consider the position of Pa(V) in our correlations, since its chemical behaviour is an exception as compared to that of the other An(V): this

comparison will be based only on hydrolysis data, since there are very few other published equilibrium constants for Pa(V) aqueous complexes. Prior to this comparison, we shall examine the impact of our estimated complexing constants on the geochemical behaviour of U(IV).

2. Methods

2.1. Equilibrium constants

For consistency, we used reaction data – i.e. Δ_rG° (equivalently standard equilibrium constants and potentials of redox couples) – they were preferred to formation data (Δ_fG°) [2].

$$K_1^\circ = \frac{|ML^{z_M+z_L}|}{|M^{z_M}||L^{z_L}|} \quad (1)$$

where $|A|$ is the activity of species A.

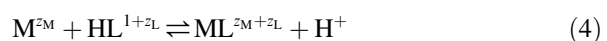
$$K_a^\circ = \frac{|H^+||L^{z_L}|}{|HL^{1+z_L}|} \quad (2)$$

$pK_a^\circ = -\log K_a^\circ$ is $pH_{1/2}$, the pH at the half-point reaction (where $|L^{z_L}| = |HL^{1+z_L}|$). pK_a° appears to be the ionic product of water, when $L^{z_L} = OH^-$ and when using $|H_2O| = 1$; but when comparing the complexing strengths of various ligands we used the concentration of liquid water: $|H_2O| = C_{H_2O}$ (55.34 mol kg^{-1}). Superscript \circ stands for infinite dilution (ionic strength, $I = 0$), the standard conditions (see Section 2.2).

$\log K_1^\circ$ values were plotted as a function of pK_a° , for example when K_1° is the formation constant of $AmCO_3^{2+}$, $1/K_a^\circ$ is the protonation constant of CO_3^{2-} . We observed

$$\log K_{1,x}^\circ = a_x + b_x pK_a^\circ \quad (3)$$

linear correlations, where we fitted the a_x and b_x parameters for a series of actinides (or analogues) of the same oxidation number X : $An(X) = M^{z_M} = An^{3+}$, An^{4+} , AnO_2^+ or AnO_2^{2+} . $10^a = K_1^\circ (K_a^\circ)^b = |ML^{z_M+z_L}| |H^+|^b / (|M^{z_M}| |L^{z_L}|^{1-b} |HL^{1+z_L}|^b)$ is obtained from Eqs. (1)–(3): it is actually an equilibrium constant. When $b = 1$, it simplifies into the $10^{a(l)} = K_1^\circ K_a^\circ = |ML^{z_M+z_L}| |H^+| / (|M^{z_M}| |HL^{1+z_L}|)$, the



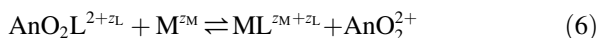
exchange equilibrium constant: $|L^{z_L}|$ cancels out in $K_1^\circ K_a^\circ (= 10^{a(l)})$, which is now the same for all the reactions; it also only depends on a , not on each K_a° (or equivalently K_1°). In that case, the half-point reaction definition is $[|H^+| / |M^{z_M}|]_{1/2} = K_1^\circ K_a^\circ$: a solution of

activity $|H^+|$ has the same reactivity (for the L^{z_L} ligand) as a solution of activity $|M^{z_M}|10^{a_{(1)}}$. Conversely, when the (b) slope is not 1, this simple equivalent solution definition is no longer relevant: the general half-point reaction definition is $10^a = K_1(K_a^\circ)^b = [(|H^+||L^{z_L}|)^b / (|M^{z_M}||L^{z_L}|)]_{1/2}$, whose interpretation is less intuitive. Furthermore the constant of the exchange equilibrium (Eq. (4)) is now specific for each reaction: $K_1^\circ K_a^\circ = 10^a (K_a^\circ)^{1-b} = 10^{a/b} (K_1^\circ)^{1-1/b}$ depends on each K_a° (or equivalently K_1°), not only on a and b .

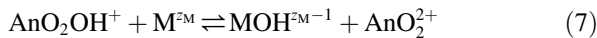
Since b_x did not seem to strongly depend on X, we finally used the same $b_x (=b)$ value for all the oxidation states; in that case, for comparing An(X) complexes with An(VI) ones, we used:

$$10^{a_X - a_{VI}} = \frac{K_{X,VII}^\circ}{K_{1,VI}^\circ} = K_{X,VI}^\circ = \frac{|ML^{z_M+z_L}| |AnO_2^{2+}|}{|AnO_2 L^{2+z_L}| |M^{z_M}|} \quad (5)$$

the constant of the



exchange equilibrium. This AnO_2^{2+}/M^{z_M} exchange equilibrium is similar to the H^+/M^{z_M} one (Eq. (4)), where now the half-point reaction definition is $[|AnO_2^{2+}| / |M^{z_M}|]_{1/2} = K_{X,VI}^\circ$: a solution of activity $|AnO_2^{2+}|$ has the same reactivity (for the L^{z_L} ligand) as a solution of activity $|M^{z_M}|K_{X,VI}^\circ$. Similarly, for comparing hydrolysis equilibria, we used the



hydrolysis competition equilibrium of constant

$$\frac{*K_{1,x}^\circ}{*K_{1,VI}^\circ} = *K_{X,VI}^\circ = \frac{|MOH^{z_M-1}| |AnO_2^{2+}|}{|AnO_2 OH^+| |M^{z_M}|} \quad (8)$$

where

$$*K_{i,X}^\circ = \frac{|M(OH)_i^{z_M-i}| |H^+|}{|M(OH)_{i-1}^{z_M-i+1}|} \quad (9)$$

is a classical stepwise standard equilibrium constant. $-\log *K_{i,X}^\circ$ is $pH_{1/2}$.

2.2. Activity coefficients

For ionic strength corrections, we used γ_i , the molal activity coefficient of ion i calculated with the “Specific Interaction Theory”, the SIT formula [2,4]. The corresponding ε_{ij} empirical (pair interaction) coefficients are taken from the NEA-TDB reviews [4]:

$$\log \gamma_i = -z_i^2 D + \sum_j \varepsilon_{ij} m_j \quad (10)$$

In most cases, the summation could here be restricted to the ClO_4^- and Na^+ (dominating) counter-ions ($= j$). m_j is j (molal) concentration (mol per kg of pure water). Molar ($M = \text{mol L}^{-1}$) to molal conversion coefficients are tabulated in Handbooks (including the cited NEA-TDB books):

$$D = \frac{A\sqrt{I_m}}{1 + B_r\sqrt{I_m}} \quad (11)$$

is a Debye–Hückel term, where I_m is molal I , $A = 0.509[298\varepsilon_{298}/T\varepsilon_{r,T}]^{1.5}[d_{298}/d_T]^{0.5} \text{ kg}^{1/2} \text{ mol}^{-1/2}$, and $B = 3.28 \times 10^9 [298\varepsilon_{298}d_T/(T\varepsilon_{r,T}d_{298})]^{0.5} \text{ kg}^{1/2} \text{ mol}^{-1/2} \text{ m}^{-1}$ are calculated from physical constants, and $\varepsilon_{r,T}$ the relative dielectric constant of the solvent (water) and d_T the density at absolute temperature T . r accounts for geometric exclusion about ion i . r is assumed to be constant, $B r = 1.5 \text{ kg}^{1/2} \text{ mol}^{-1/2}$ at 25 °C, an approximation that enables many measured mean activity coefficients of strong inorganic aqueous electrolytes to be fitted [2]; it corresponds to $r = 4.57 \times 10^{-10} \text{ m}$, which appears to be of the correct order of magnitude for most inorganic hydrated ions including their first hydration sphere (by definition if a counter-ion stays in the first hydration sphere, it is treated as complex formation, not non-ideality). Furthermore, $B\sqrt{I} = 1/l_D$, where l_D is the Debye distance, the distance between an ion and its counter-ion atmosphere: $3.05 \times 10^{-10} \text{ m}$ (at 25 °C and $I = 1 \text{ M}$) in the SIT approximation. The Debye–Hückel formula is valid for large l_D namely for $l_D >> r$: $B r = 1.5 \text{ kg}^{1/2} \text{ mol}^{-1/2}$ corresponds to $r/l_D = 1.5 \sqrt{I_m} << 1$. Indeed the Debye–Hückel formula (D term alone) is only valid at ionic strengths less than 10 or 1 mM, while the SIT formula is usually a good approximation for aqueous solutions with ionic strength up to 4 mol kg^{-1} [2]. The use of ε_{ij} empirical coefficients certainly partly compensates systematic errors (of D in the SIT formula), which might very well explain why the numerical values for ε_{ij} are correlated with the size and the charges of the ions (Fig. 2).

Unknown ε_{ij} numerical values can be estimated by analogy with ions of same charge and similar sizes [3,4]. In that case it was proposed to increase the ε_{ij} uncertainties by $\pm 0.05 \text{ kg mol}^{-1}$ [4]. Moreover, we observed a reasonable linear correlation between interaction coefficients and the charge/radius ratios (Fig. 2(a)). For this correlation we used the formal charge of the cation (or the complex), which is indeed the charge seen by the (ClO_4^-) counter-anion at large distance. Unfortunately this assumption does not hold for high ionic strengths, the only conditions where the ε_{ij} m_j term cannot be neglected. Indeed some data for

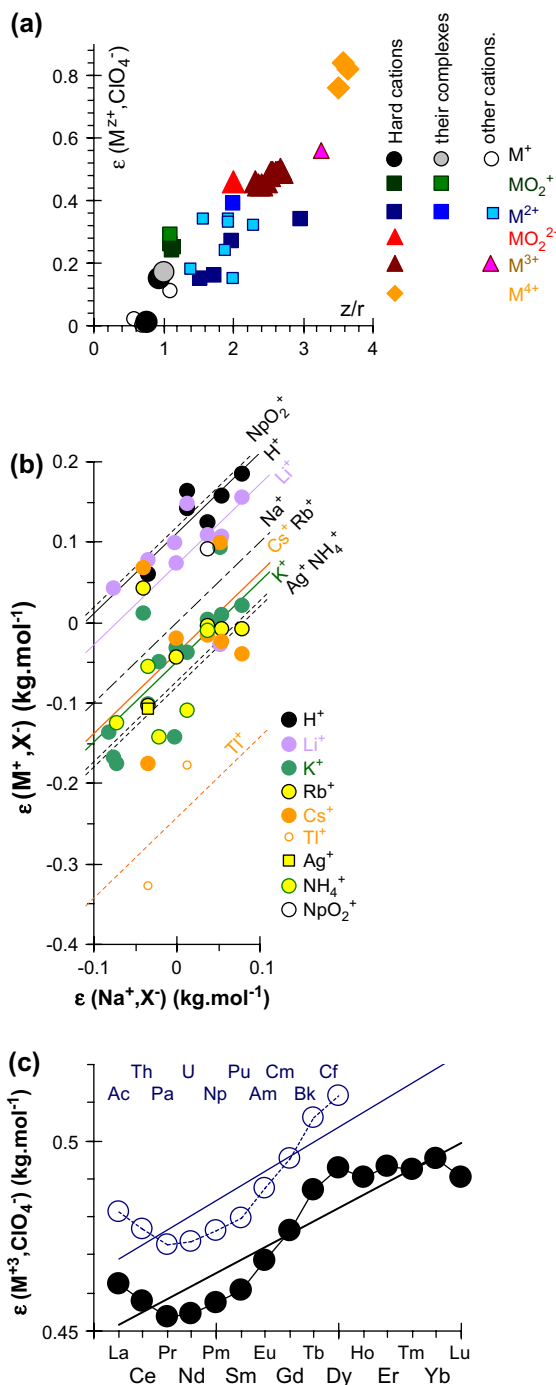


Fig. 2. Empirical correlations for estimating SIT ion pair coefficients.

AnO_2^{X-4} cations are not in the middle of the correlation cloud, indicating that the relevant phenomenological charge might be higher (than the formal one). Conversely, the corresponding points are moved to the other side of this correlation plot (not represented on the

figure), when using the atomic charge (Section 2.3) of An (in AnO_2^{X-4} , for this reason, we also plotted other correlations without using the charges (Fig. 2(b) and (c))).

2.3. Quantum calculations

In our hydrolysis correlation study, we used the formal charges of An^{3+} (3) and An^{4+} (4), while we used the atomic charge of $\text{An}(X)$ in AnO_2^{X-4} ($X = 5$ or 6). This latter was deduced from quantum (DFT) calculations performed at the same calculation levels (ECP and basis sets) as in our recent previous works [17,20], from which we extracted NPA atomic charges [21,22]. Note that in Gaussian98 and 03, these NPA charges are calculated with the NBO software, which is known to consider the UO_2^{2+} 6d orbitals as Rydberg orbitals, despite the final result gives the 7s5f6d electronic configuration. This overestimates the U atomic charge by 0.50 electron. For this reason we recalculated the NPA charge assuming the 6d to be valence orbitals for all the oxy actinide cations.

For the ligands (alone) closed-shell ab initio calculations were performed at the MP2/6-311+g(2df,2p) level; open-shell calculations are not needed, as checked at the B3LYP/6-31+g(d,p) level. All the quantum calculations were done with the Gaussian98 and 03 suites of programs [23,24].

$\Delta_r E$, the ab initio energy, was calculated for the protonation reaction corresponding to the pK_a equilibrium (Fig. 3). pK_a represents $\text{pH}_{1/2}$; similarly, when adding

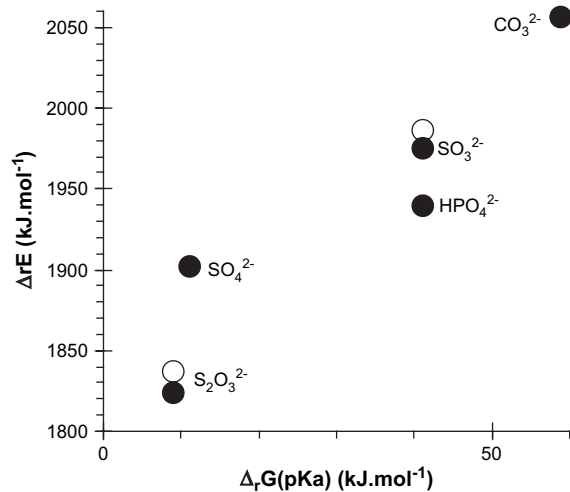
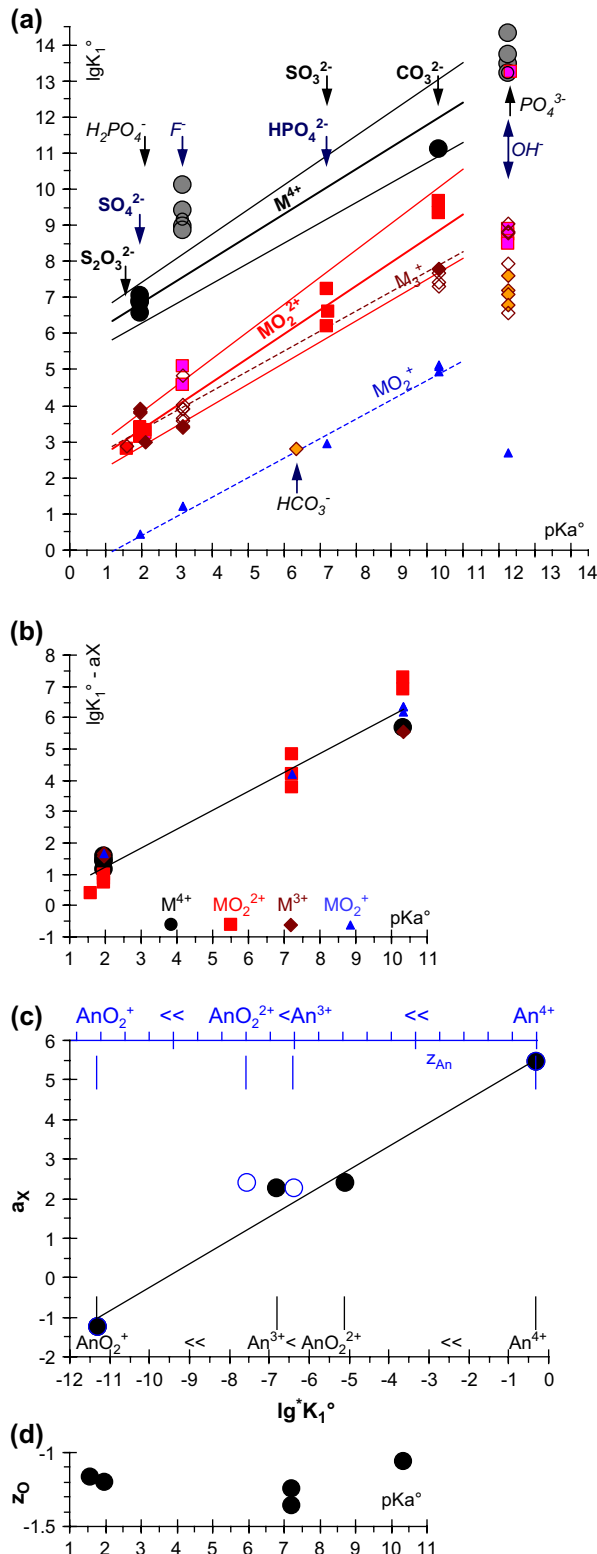


Fig. 3. Protonation reactions of RO_2^{2-} ligands in the gas phase and in aqueous solutions. The pK_a (in pure liquid water at 25 °C) are converted to kJ mol^{-1} ($\Delta_r G = -RT pK_a$) and compared to the energy of the corresponding reaction ab initio calculated (with neither matrix nor temperature correction), where the protonation is on an O (black points) or S (white points) atom.



the entropic contribution to $\Delta_r E$, it represents $P_{H^+}^{1/2}$, the H^+ partial pressure: the hydration energy of H^+ is related to the slope in the $\Delta_r E$ plot as a function of pK_a (Fig. 3), while the intercept rather reflects the hydration energy change between the reactants and products. Since the slope is much greater than 1, the E scale had to be contracted, which means that the final correlation is quite poor. Slope $\neq 1$ also means it is not equivalent to use pK_a or $\Delta_r E$ for our estimates of complexing constants: pK_a appeared to be better correlated with measured complexing constants. Furthermore pK_a represents a marginal value of $\Delta_r E$, which already is a marginal part of the DFT calculated electronic energy: the experimental pK_a values are more reliable for our purpose and more accurate than the $\Delta_r E$ ones obtained from quantum calculations in the gas phase.

3. Results and discussions

3.1. Comparing the affinities of hard anions for H^+ and AnO_2^{2+}

We first examined U(VI) aqueous complexation and hydrolysis data, since a sufficiently large set of complexing constants is available. Positive $\log K_1^\circ$ vs pK_a° correlations are observed, and even linear correlations appear to fit the data reasonably well. The plot appeared to be less scattered when restricted to the consistent set of data selected by the NEA-TDB reviews (Fig. 4): we finally used these (NEA-TDB) consistent sets of data for the figures and numerical correlations given in the present paper with the following exceptions. For An(VI) we did not use the NEA-TDB $PuO_2CO_3(aq)$ formation constant based on only ($\log K_1^\circ = 13.8^{+0.8}_{-0.6}$ [26] and 9.3 ± 0.5 [27]) two experimental determinations that are not consistent (within uncertainties). The latter

Fig. 4. Proton and other cation affinities for ligands. K_1° is the standard formation constant of the $ML^{z_M+z_L}$ complex, and K_a° is the protonation constant of the L^{z_L} ligand written on the figure (Table 1). Since all the $(\log K_{1,X}^\circ = a_X + b_X pK_a^\circ)$ lines are virtually parallel for all the (X) oxidation states (a). We also used the same ($b_X = 0.62 \pm 0.16$) slope in $\log K_{1,X-a_X}^\circ = ((0.62 \pm 0.16)pK_a^\circ)$ regressions for the RO_2^{2-} ligands, and shifted the curves by a_X (b): $a_X - a_{VI} = (\log K_{1,X}^\circ - \log K_{1,VI}^\circ) = \log K_{X/VI}^\circ$ (Eq. (5)), where $K_{X/VI}^\circ$ is the constant for the $AnO_2RO_2/MRO_2^{z_M-2}$ exchange equilibrium (Eq. (6a)) for $M^{z_M} = An^{3+}$, An^{4+} or AnO_2^+ . For An at the oxidation state X , $a_X = (\log K_{1,X}^\circ - 0.62 pK_a^\circ)$ can be used as a definition of a quantitative scale for the (up to now qualitative) $An^{4+} > AnO_2^{2+} \approx An^{3+} > AnO_2^+$ series (y axis of (c)). It is compared (black filled symbols) with the hydrolysis constant ($*K_1$) scale on the x axis (of (c)), and z_{An} , the An atomic charge (blue open symbols corresponding to the top scale). z_O , the atomic charge of O in RO_2^{2-} is not specially correlated with its pK_a (d). The x-axes are the same for (a), (b) and (d): the names of the ligands are only written on (a).

value (that we published ourselves) is closer to the U(VI) and Np(VI) ones (Table 1) [2,4], but it is rather a maximum possible value corresponding to the detection limit of our solubility measurements. For this reason, we also do not rely on the 9.5 ± 0.5 similar value more recently updated by the NEA-TDB review [16].

The PO_4^{3-} tri-anion is out of the correlation, while the F^- mono anion could probably be included into the correlation, but HO^- cannot (Fig. 4). When restricting the correlations to $\text{L}^{\text{zL}} = \text{RO}_2^{2-}$ potentially bidentate oxygen-donor ligands, virtually the same $\log K_1^\circ$ value is observed for a given ligand with AnO_2^{2+} for $\text{An} = \text{U}, \text{Np}, \text{Pu}$ or Am : the variations along this series are only slightly higher than experimental uncertainties. $\log K_{1,\text{VI}}^\circ = ((2.0 \pm 0.3) + (0.66_5 \pm 0.08_5) \text{ p}K_a)$ is obtained for these (AnO_2^{2+}) cations. Adding not critically reviewed ($\log K_{1,\text{VI}}^\circ$) values gives similar regression coefficients with increased uncertainties, namely (2.6 ± 0.8) instead of (2.0 ± 0.3) , and (0.58 ± 0.08) instead of $(0.66_5 \pm 0.08_5)$.

3.2. $\text{AnO}_2\text{RO}_2/\text{MRO}_2^{\text{zM}-2}$ exchanges for $\text{M}^{\text{zM}} = \text{An}^{3+}, \text{An}^{4+}$ or AnO_2^+

Similar $\log K_1^\circ$ vs $\text{p}K_a^\circ$ correlations and observations (as for AnO_2^{2+} , Section 3.1) are made for the An^{3+} and AnO_2^+ cations, while there are too few data for M^{4+} .

For the $\text{M}^{3+}/\text{CO}_3^{2-}$ systems, we used our own complexing constants (Table 1) [28], AmHCO_3^+ is an outlier, in part due to the stabilisation of H_2CO_3 as $\text{CO}_2(\text{aq})$: the measured $\text{p}K_a$ (of the $\text{HCO}_3^-/\text{CO}_2(\text{aq})$ couple) is not the relevant parameter for our correlations. For $\text{L}^{\text{zL}} = \text{RO}_2^{2-}$ we found K_1° values in the order $\text{An}^{4+} > \text{AnO}_2^{2+} \approx \text{An}^{3+} > \text{AnO}_2^+$, a classical order for the reactivity of actinide cations toward hard anions. However, $\text{AnO}_2^{2+} \geq \text{An}^{3+}$ is often written (instead of $\text{AnO}_2^{2+} \approx \text{An}^{3+}$). Here the available data for An^{3+} appear to be within the correlation lines of AnO_2^{2+} . The atomic charge of U in UO_2^{2+} is 2.8 electron, which compares with the charge of Am^{3+} . Nevertheless, using atomic charges in the correlations gave poorer results (see below and Fig. 4(c)). We obtained $\log K_{1,\text{III}}^\circ \approx 2.2 + 0.55 \text{ p}K_a^\circ$ for An^{3+} and $\log K_{1,\text{V}}^\circ \approx -0.7 + 0.54 \text{ p}K_a^\circ$ for AnO_2^+ .

There are too few data for a statistical evaluation of all the uncertainties. Nevertheless, it seems that b_x , the slopes (of every $\log K_1^\circ$ vs $\text{p}K_a^\circ$ correlations) are the same within uncertainties. Indeed a reasonable fit is obtained when fixing $b_x = b_{\text{VI}}$ ($= 0.66_5$), namely $\log K_{1,\text{X}}^\circ = (a_x + 0.66_5 \text{ p}K_a^\circ)$ for all the oxidation states. We finally fitted the slope (and a_x) on all the data, and obtained $\log K_{1,\text{X}}^\circ = (a_x + (0.61_6 \pm 0.05_5) \text{ p}K_a^\circ)$ with $a_{\text{III}} = 2.25_3 \pm 0.07_5$, $a_{\text{IV}} = 5.44_4 \pm 0.24_9$, $a_{\text{V}} = -1.23_6 \pm 0.48_9$ and $a_{\text{VI}} = 2.40_8 \pm 0.45_3$ fitted

Table 1

Formation constants used to draw Fig. 4: $\text{p}K_a^\circ$ of RO_2^{2-} ligands and corresponding $K_{1,\text{X}}^\circ$ formation constants^c with cations of f-block elements [2–4,16]

RO_2^{2-}	$\text{p}K_a^{\text{b}}$	$\log K_{1,\text{III}}^\circ$ ^c	$\log K_{1,\text{IV}}^\circ$ ^c	$\log K_{1,\text{V}}^\circ$ ^c	$\log K_{1,\text{VI}}^\circ$ ^c
$\text{S}_2\text{O}_3^{2-}$	1.59		$6.6 \pm 0.3^{\text{a}}$		$2.8(\text{U})$
SO_4^{2-}	1.98	$3.85(\text{Am})$	$6.58(\text{U})$	$0.44(\text{Np})$	$3.15(\text{U})$
		$3.91(\text{Pu})$	$6.85(\text{Np})$		$3.28(\text{Np})$
HPO_4^{2-}	7.21_2		$6.89(\text{Pu})$		$3.38(\text{Pu})$
			$9.5 \pm 2.3^{\text{a}}$	$2.95(\text{Np})$	$7.24(\text{U})$
SO_3^{2-}	7.22				$6.2(\text{Np})$
CO_3^{2-}	10.32_9	$7.7 \pm 0.3(\text{Am})$	$9.5 \pm 2.3^{\text{a}}$		$6.6(\text{U})$
		$7.8 \pm 0.2(\text{Eu})$	$11.1 \pm 3.2^{\text{a}}$	$4.96_2(\text{Np})$	$9.67(\text{U})$
				$5.12(\text{Pu})$	$9.32(\text{Np})$
				$5.1(\text{Am})$	
a_x^{d}		2.2	5.8 ± 0.4	-0.7	2.0 ± 0.3
b_x^{d}		0.55	$0.51 \pm 0.2_7$	0.54	$0.66_5 \pm 0.08_5$
a_x^{e}		$2.25_3 \pm 0.07_5$	$5.44_4 \pm 0.24_9$	$-1.23_6 \pm 0.48_9$	$2.40_8 \pm 0.45_3$
$\log K_{x/\text{VI}}^\circ$		-0.16 ± 0.5	3.04 ± 0.5	-3.64 ± 0.5	0
$\log *K_{x/\text{VI}}^\circ$		-1.7	4.81	-6.2	0

^a Value estimated in the present work.

^b $\text{p}K_a$ of the RO_2^{2-} ligand.

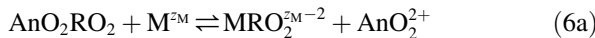
^c $K_{1,\text{X}}^\circ$ is the standard constant of equilibrium $\text{M}^{z+} + \text{RO}_2^{2-} \rightleftharpoons \text{MRO}_2^{(z-2)+}$ for $\text{M}^{z+} = \text{An}^{x+}$ ($X = 3$ or 4) or $\text{AnO}_2^{(X-4)+}$ ($X = 5$ or 6) from published data (see text) [2–4,7].

^d a and b , the coefficients of the $\log K_{1,\text{X}}^\circ = (a + b \text{ p}K_a^\circ)$ linear regression are fitted for a given oxidation state, X .

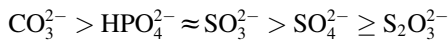
^e while a_x is the (fitted) intercept of a similar regression, but with the same (0.62 ± 0.16) slope for all the oxidation states: $\log K_{1,\text{X}}^\circ - a_x = ((0.62 \pm 0.16) \text{ p}K_a^\circ)$.

values, where uncertainties are 1.96σ (the maximum errors on $\log K_{1,X}^\circ$ was +0.9 for UO_2CO_3 and -0.8 for AnCO_3^+). Since there are not enough data for a meaningful statistical analysis, we finally increased the uncertainties: $\log K_{1,X}^\circ - a_X = (0.62 \pm 0.16)\text{p}K_a^\circ$ (Fig. 4(b)). The standard deviation of the fit is 0.5 (it represents less than 3 kJ mol^{-1}), a value only a little higher than that of many direct experimental determinations in aqueous solutions, and of the order of magnitude of the variations of the $\log K_1^\circ$ values among the series of the analogous cations considered here. However, when a slope is fitted for each oxidation state, a small systematic deviation can be inferred, namely the slopes seem slightly different for each type of central cation (AnO_2^{2+} , An^{3+} and AnO_2^+). On the other hand, this difference is small as compared to the scatter in the available data, and it is not specially correlated with the charge of the cation.

Since the (0.62 ± 0.16) slope does not depend on X , $(a_X - a_{\text{VI}}) = \log K_{X,\text{VI}}^\circ$ (Eq. (5)), the shift between the lines in Fig. 4(a) is related to the following equation:



$\text{AnO}_2\text{RO}_2/\text{MRO}_2^{\text{ZM}-2}$ exchange equilibrium (Eq. (5)) whose equilibrium constant is $K_{X,\text{VI}}^\circ$. For such anions the order of their reactivity toward H^+ and actinide ions is found to be



also corresponding to their $\text{p}K_a^\circ$ values, but not specially to z_O , the atomic charge of O (Fig. 4(d)).

We also attempted to force $b = 1$ in the fits, but without success: the correlations cannot simply be interpreted with Eq. (4).

Similarly, hydrolysis equilibria were compared using $*K_{X,\text{VI}}^\circ$ (Eq. (8)), the constant of a hydrolysis competition equilibrium (Eq. (7)) between actinide ions at oxidation states X and +6: $\log *K_{\text{III},\text{VI}}^\circ = -1.7$, $\log *K_{\text{IV},\text{VI}}^\circ = 4.81$ and $\log *K_{\text{V},\text{VI}}^\circ = -6.2$ for Np [4]. These results give nearly the same $\text{An}^{4+} >> \text{AnO}_2^{2+} > \text{An}^{3+} >> \text{AnO}_2^+$ qualitative scale (Fig. 4(c)), and the $\log *K_{X,\text{VI}}^\circ = (0.36 + 0.60)\log *K_{X,\text{VI}}^\circ$ linear correlation.

3.3. Estimating the stabilities of $\text{An}^{(\text{IV})}\text{RO}_2^{2+}$ complexes

We now want to estimate missing complexing constants for U(IV), namely with the SO_3^{2-} and $\text{S}_2\text{O}_3^{2-}$ anions. For this we could not use the same type of correlations as those observed for UO_2^{2+} and the other cations (Section 3.2), because reliable formation

constant has been published for only one type of 1:1 An(IV) complexes, namely for the MSO_4^{2+} complexes: $\log K_{1,\text{IV}}^\circ = 6.58$ (USO_4^{2+}) [2], 6.85 (NpSO_4^{2+}) [4], 6.89 (PuSO_4^{2+}) [4] and 7.04 (ZrSO_4^{2+}) [15]. When using this single datum and the (0.62 ± 0.16) slope value estimated above, the $(\log K_{1,\text{IV}}^\circ = ((5.6 \pm 0.2) + (0.62 \pm 0.16) \text{p}K_a^\circ)$ line is drawn, from which $\log K_{1,\text{IV}}^\circ = (12.0 \pm 1.9)$, (10.1 ± 1.4) , (6.8 ± 0.5) and (6.6 ± 0.5) are calculated for the An(IV) complexes of CO_3^{2-} , SO_3^{2-} , SO_4^{2-} and $\text{S}_2\text{O}_3^{2-}$, respectively. The value of $a_{\text{IV}} = 5.6 \pm 0.2$ was chosen to fit the 6.58 (USO_4^{2+}), 6.85 (NpSO_4^{2+}) and 6.89 (PuSO_4^{2+}) data by giving less weight to USO_4^{2+} , because the +4 oxidation state is more difficult to stabilise for uranium, even if more experimental studies of U(IV) are available. However, the $\log K_{1,\text{IV}}^\circ = (6.6 \pm 0.5)$ $\text{MS}_2\text{O}_3^{2+}$ value is close to the MSO_4^{2+} fixed point (of the correlation). Therefore it does not depend sensitively on the value estimated for the slope (of the $\log K_{1,\text{IV}}^\circ$ vs $\text{p}K_a^\circ$ linear correlation). Consequently the uncertainties are relatively small for (the $\log K_{1,\text{IV}}^\circ$ estimate of) $\text{MS}_2\text{O}_3^{2+}$. Conversely the biggest uncertainty is for MCO_3^{2+} the most stable complex, since CO_3^{2-} appeared to be the most reactive RO_2^{2-} ligand we studied: it is one of the endpoints of the correlation lines. For this reason, we estimated an upper bound for the value of $\log K_{1,\text{IV}}^\circ$ from experimental data: we re-interpreted available published experimental solubilities of actinides(IV) by using the same methodology as in Refs. [4,5,29]. We obtained formation constants consistent with the original interpretation (by the authors of Ref. [9]). However, for consistency we added the known stabilities of $\text{An}(\text{CO}_3)_i^{4-2i}$ ($i = 4$ and 5), and we tested many possible complexes for which we also estimated maximum possible stabilities (Table 2) for sensibility analysis; our purpose was essentially to estimate a value for AnCO_3^{2+} . As expected from pH vs $\log [\text{CO}_3^{2-}]$ predominance diagrams [7,26,28], the most restrictive conditions were found for published solubilities of An(IV) measured at low pH and high CO_2 partial pressure, namely in Refs. [9,30]. In both cases we obtained virtually the same values: $\log K_{1,\text{IV}}^\circ \leq 11.1$ or 11.5 for the ThCO_3^{2+} complex. Using this value (and the sulfate data), $\log K_{1,\text{IV}}^\circ = (5.8 + 0.51\text{p}K_a^\circ)$ is calculated, from which $\log K_{1,\text{IV}}^\circ = 11.1$, 9.5, 6.8 and 6.6 are calculated for the An(IV) complexes CO_3^{2-} , SO_3^{2-} , SO_4^{2-} and $\text{S}_2\text{O}_3^{2-}$, respectively. These values are within the uncertainties of the previous estimates above. The AnCO_3^{2+} value of 11.1 is identical as, or slightly smaller (by 0.9 ± 1.9) than the central value (12.0 ± 1.9) of the above estimate, and the same trend was observed for AmCO_3^+ : it was overestimated by 0.8 \log_{10} unit when using the

Table 2
Stabilities of An(IV) carbonato complexes

An(CO ₃) _i (OH) _j ^{4-2i-j}	log K _{i,j} [°] (Pu) ^a [5]	log K _{i,j} [°] (Th) ^a [9]	log K _{i,j} [°] (Th) ^{a,b}
AnOH ³⁺	13.2		
AnCO ₃ ²⁺			≤11.1
AnCO ₃ OH ⁺			<21.1
An(CO ₃) ₂			<20.8
AnCO ₃ (OH) ₂	<<42	27.0	<30.1
An(OH) ₄	<<47.9		38.5
An(CO ₃) ₂ OH ⁻	<<40.5		<29.4
AnCO ₃ (OH) ₃ ⁻	<<47.7	34.8	≤38.5
An(CO ₃) ₃ ²⁻	<<37.6		<27.5
An(CO ₃) ₂ (OH) ₂ ²⁻	<<46.2	33.3	≤36.8
AnCO ₃ (OH) ₄ ²⁻	<<51.8	37.4	≤39.9
An(CO ₃) ₃ OH ³⁻	<<42		≤34
An(CO ₃) ₂ (OH) ₃ ³⁻	<<50.5		<39.2
An(CO ₃) ₄ ⁴⁻	37		29.9
An(CO ₃) ₃ (OH) ₂ ⁴⁻	<41		<37.6
An(CO ₃) ₃ (OH) ₅ ⁵⁻	<40.5		<37.9
An(CO ₃) ₄ OH ⁵⁻	<39	34.4	35.4
An(CO ₃) ₅ ⁶⁻	35.6		28.4
An(CO ₃) ₄ (OH) ₂ ⁶⁻	<37		<36.4
An(CO ₃) ₃ (OH) ₄ ⁶⁻	<38.5		<39.3
An(CO ₃) ₆ ⁸⁻			<36

^a $K_{i,j}^{\circ}$ is the standard constant of equilibrium $\text{An}^{4+} + i\text{CO}_3^{2-} + j\text{HO}^- \rightleftharpoons \text{An}(\text{CO}_3)_i(\text{OH})_j^{4-2i-j}$.

^b Maximum possible values from the experimental data of Ref. [9]; these estimations are consistent with the original interpretation (by the authors of Ref. [9]), but the known stabilities of $\text{An}(\text{CO}_3)_i^{4-2i}$ are here added in the fits for $i = 4$ and 5; our purpose was essentially to estimate a value for AnCO_3^{2+} (see text) and to outline sensitivity analysis.

same slope (0.62) for all oxidation states. This correlation predicts under-stabilisation of the AnCO_3^{X-2} complexes ($X = 3$ or 4) as compared to the $\text{AnO}_2\text{CO}_3^{X-6}$ systems ($X = 5$ or 6); it might be attributed to the planar structure of CO_3^{2-} , which offers a better fit to the geometry of the coordinating equatorial plane of the AnO_2^{X-4} actinyl cations. Unfortunately, such an explanation would also hold

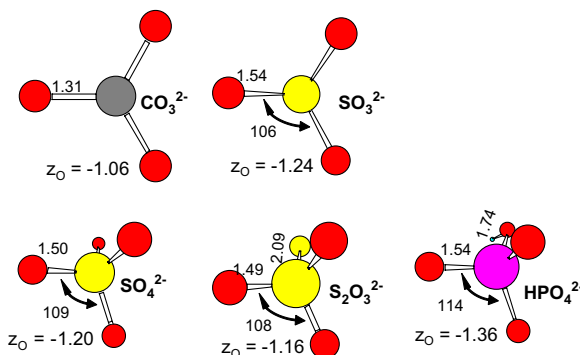


Fig. 5. Geometry of RO_2^{2-} ligands optimized in the gas phase. R–O bond distances (Å), angles (°) and z_{O} , the atomic charge of O are written on the figure.

for the SO_3^{2-} (quasi-) planar ligand (Fig. 5), which is not specially confirmed (Fig. 4). For consistency with our estimate, $\log K_{1,\text{IV}}^{\circ} \leq 11.1$, we prefer the last correlation $\log K_{1,\text{IV}}^{\circ} = (5.8 + 0.51 \text{ p}K_{\text{a}}^{\circ})$, where we increased the uncertainties to encompass the previous $\log K_{1,\text{IV}}^{\circ} = ((5.6 \pm 0.2) + (0.62 \pm 0.16) \text{ p}K_{\text{a}}^{\circ})$ correlation: $\log K_{1,\text{IV}}^{\circ} = ((5.8 \pm 0.4) + (0.51 \pm 0.27) \text{ p}K_{\text{a}}^{\circ})$ from which we obtain $\log K_{1,\text{IV}}^{\circ} \leq 11.1 \pm 3.2$ for AnCO_3^{2+} , 9.5 ± 2.3 for AnSO_3^{2+} , 9.5 ± 2.3 for AnHPO_4^{2+} and 6.6 ± 0.8 for $\text{AnS}_2\text{O}_3^{2+}$, where uncertainties are increased take into account the lack of experimental data.

$\log K_{1,\text{IV}}^{\circ} = 6.6 \pm 0.8$, the value estimated for $\text{AnS}_2\text{O}_3^{2+}$ is quite similar to those for the AnSO_4^{2+} complexes: 6.58 (USO_4^{2+}), 6.85 (NpSO_4^{2+}) and 6.89 (PuSO_4^{2+}). This is consistent with the molecular structures of these ligands: SO_4^{2-} and $\text{S}_2\text{O}_3^{2-}$ both have a tetrahedral structure (Fig. 5) – an O atom (of SO_4^{2-}) being replaced by an S atom (in $\text{S}_2\text{O}_3^{2-}$) and similar $\text{p}K_{\text{a}}$ values. SO_3^{2-} has a different structure, a higher $\text{p}K_{\text{a}}$, and a higher estimated value of the complexation constant. Unfortunately, it does not seem easy to draw any simple explanation just from z_{O} , the atomic charge of the free ligand in vacuum (Fig. 4(d)).

3.4. Uranium geochemistry

In non-complexing aqueous solutions, the solubility of uranium is controlled by uraninite ($\text{UO}_2(\text{s})$) in reducing conditions, and by schoepite ($\text{UO}_3(\text{s})$) in oxidizing and neutral conditions, as illustrated in Fig. 6(a) for 1 μM [U]_t. Besides those minerals, aqueous U(VI) species are predominant in a large $E-\text{pH}$ domain, while aqueous U(IV) is stable only in reducing conditions, and is mostly hydrolysed.

On adding carbonate ions at a typical concentration of underground waters, aqueous U(VI) carbonate complexes prevail between pH 4 and 12 (Fig. 6(b)), $\text{UO}_3(\text{s})$ is totally dissolved, and the $\text{UO}_2(\text{s})$ stability domain is reduced. We have ignored the reduction of the carbonate ions, since this reaction is usually very slow. Nevertheless, no carbonate complex of U(IV) appears on the Pourbaix diagrams. These complexes would predominate only at higher carbonate concentrations than those studied here. Rai and Ryan have already proposed that carbonate complexation of actinide(IV) ions in environmental conditions can be neglected [8].

Among the main sulfur species, SO_4^{2-} prevails over a large ($E-\text{pH}$) domain in oxidizing to slightly reducing equilibrium conditions. For high pH values, this domain even extends to reducing conditions (Fig. 1). H_2S^- and S^{2-} prevail in reducing conditions, but their

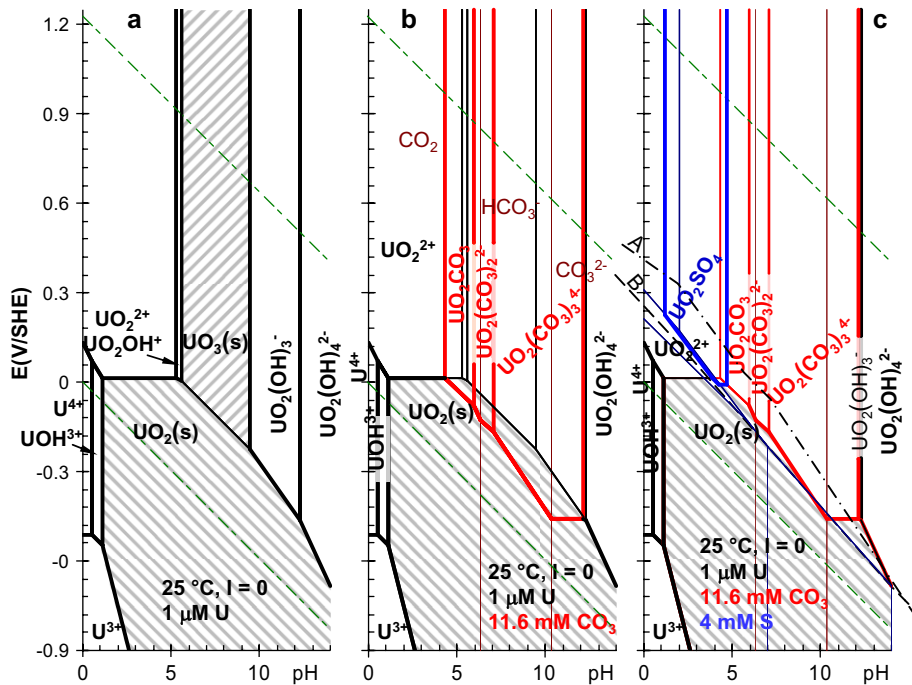
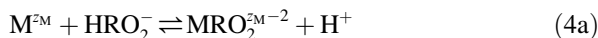


Fig. 6. Pourbaix' diagrams of uranium. The predominance domains of the major soluble species are shown as a function of pH and E , the redox potential of the solution in (a) non-complexing media, (b) adding the influences of carbonate ions and (c) sulfur species for a typical ($[CO_3]_t = 11.6 \text{ mM}$ and $[S]_t = 4 \text{ mM}$) composition of underground waters [11]. pH is taken into account for carbonate speciation ($CO_3^{2-}/HCO_3^-/CO_2(aq)$), but its reduction -typically into $CH_4(g)$ - is not. The mixed dashed line (A) represents redox conditions in Fig. 7. The long dashed line (B) represents redox conditions for Fig. 1(c).

complexing properties are not significant for the (hard) cations of the f-block elements. $UO_2SO_4(aq)$ is the only predominating sulfur species in our typical underground water conditions (Fig. 6(c)), even when introducing the 1:1 complexing constants estimated above (Section 3.3, Table 1) for $US_2O_3^{2+}$ and USO_3^{2+} . The RO_2^{2-} ligands are protonated in acidic conditions, which decreases their concentrations: the corresponding 1:1 complexing equilibria are actually the



exchange equilibria. Despite this concurrency between protonation and complexation, several complexes with the 1:1 stoichiometry are stable. Conversely, the existence of $AnCO_3^{2+}$ complexes has never been demonstrated, since the competition (between carbonate complexation and hydrolysis) is less favourable for An(IV) as compared to the actinides in the other oxidation states (Fig. 4(a)). The RO_2^{2-} concentration can also dramatically decrease as a result of redox reactions: CO_3^{2-} and SO_4^{2-} ($= RO_2^{2-}$) are reduced in equilibrium chemical conditions, where U(IV) is stable. However, these reduction reactions are very slow: we have

neglected them for the carbonate ions (Fig. 6). Similarly, the coexistence of S(VI) and S(-II) species is often observed, indicating that equilibrium conditions are not always achieved for S natural aqueous systems. The achievement of the U(IV)/U(VI) equilibrium can also last for a few weeks. Note that all these slow reduction reactions can be explained by the need to break strong (covalent) bonds of O(-II) with C, S(VI) or U(VI). Such kinetics is often handled by assuming that slow reactions are blocked, while equilibrium conditions are achieved for other equilibria. Therefore U(IV) might be complexed by sulfate and by reduced intermediary S species as well: we plotted two simulation diagrams corresponding to different kinetic assumptions that would stabilise sulfoxy-anion complexes (Fig. 7). In both cases, E , the redox potential, is at the limit of the $H_2S_2O_3^{i-2}$ and $H_2SO_3^{i-2}$ domains as plotted in Fig. 1(a) and line A in Fig. 6(c). In such redox conditions uranium aqueous species are stable at the +6 oxidation state. For this reason, the sulfate complexes of U(IV) are not seen on the Pourbaix' diagram (Fig. 6(c)): the sulfate ions are reduced in equilibrium conditions, where U(IV) aqueous species are dominating – i.e. the S(VI)/S(-II) frontier (line B in Fig. 6(c)) is at higher

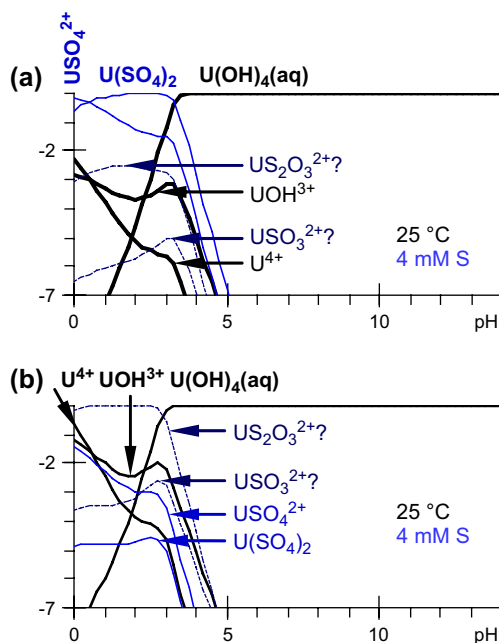


Fig. 7. Distribution of aqueous U(IV) species. $\lg(|A|/|U(\text{IV})|)$ is plotted as a function of pH, where $|A|$ is the activity of an aqueous U(IV) species. The conditions are the same as in Fig. 6(c) except for E, the redox potential of the solution: $\text{H}_2\text{SO}_4^{i-2}$ (a) or $\text{H}_2\text{S}_2\text{O}_3^{i-2}$ (b) are assumed to be the major S species. $[\text{H}_2\text{S}_2\text{O}_3^{i-2}]/[\text{H}_2\text{SO}_4^{i-2}] \approx 10$ (mixed dashed line A in Fig. 6(c)). $[\text{H}_2\text{SO}_4^{i-2}]/[\text{H}_2\text{S}_2\text{O}_3^{i-2}] \approx 20$ (a) or ≈ 1 (b) corresponding to different kinetic assumptions.

potentials than the U(VI)/U(IV) frontier in most pH conditions. Nevertheless we only focus on U(IV) aqueous species; therefore they would be minor uranium species, when the U(VI)/U(IV) equilibria are achieved.

In a first simulation we assumed that the major S species are in the +6 oxidation state (namely $\text{H}_2\text{SO}_4^{i-2}$), and that $[\text{H}_2\text{SO}_4^{i-2}]/[\text{H}_2\text{S}_2\text{O}_3^{i-2}] \approx 20$, which corresponds to much higher $\text{H}_2\text{S}_2\text{O}_3^{i-2}$ concentrations than in equilibrium conditions (for kinetic reasons). The USO_4^{2+} and $\text{U}(\text{SO}_4)_2$ sulfate complexes still appear to be U(IV) major species in acidic conditions ($\text{pH} < 3.2$), while nearly 1% of $\text{US}_2\text{O}_3^{2+}$ can be formed (Fig. 7(a)). Yet $\text{US}_2\text{O}_3^{2+}$ might be a kinetic intermediate, since uraninite is often associated with pyrite (FeS_2); indeed $\text{S}_2\text{O}_3^{2-}$ is an intermediary product of its oxidative dissolution [14]. $\text{S}_2\text{O}_3^{2-}$ and SO_4^{2-} have similar reactivities (Fig. 4), but (in our hypothesis) the SO_4^{2-} concentration is higher (than the $\text{S}_2\text{O}_3^{2-}$ one), which explains why the sulfate complexes dominate. Although the SO_4^{2-} ions are more reactive, the USO_3^{2-} complex is negligible in that simulation, since the reduction of SO_3^{2-} (Fig. 1) decreases its concentration and consequently its complexing ability.

In a second simulation we assumed that SO_4^{2-} is not formed at all (still for kinetic reasons). Therefore $\text{S}_2\text{O}_3^{2-}$

is now the dominating S aqueous species (Fig. 1). $\text{US}_2\text{O}_3^{2+}$ is the major U(IV) species, and up to a few percent of USO_3^{2+} is formed at pH less than 3.0 (Fig. 7(b)).

Even if sulfoxo-anions complexes of U(IV) are certainly not stable in equilibrium conditions, these simulations indicate that they might be formed as kinetic intermediates typically in the course of uraninite and pyrite oxidative dissolutions, or the interaction of aqueous uranium (including U(VI)) with pyrite surfaces [31,32]. Of course, this statement needs experimental confirmation, specially in less acidic to basic conditions, where higher and mixed $\text{An}(\text{RO}_2)_i(\text{OH})^{4-2i-j}$ complexes may form. Furthermore, at $\text{pH} > 3$, $\text{U}(\text{OH})_4(\text{aq})$ is the dominant species in equilibrium reducing conditions, and the formation of S-containing complexes is less favourable, specially in the usual pH conditions of equilibrated natural under-ground-waters.

3.5. Hydrolysis of actinide ions

We now consider where protactinium should be placed in the above correlations. There is little experimental published information on Pa aqueous chemistry. We first used the available information on its aqueous species in non-complexing (acidic) solutions and its hydrolysis. Although Pa is known to be an f-block element [17], Pa(V) aqueous chemistry is closer to that of d elements (in the same – the 5th- column of the periodic table) than to the chemistry of AnO_2^+ trans-protactinian actinide cations. Here is a strong indication that PaO_2^+ is not the dominating aqueous Pa species.

Jaussaud et al. recently reviewed previous measurements of the Pa(V) hydrolysis constants [33–35]. They are essentially based on liquid–liquid extraction measurements, for which they pointed out many experimental difficulties: side reactions of the organic chemicals, sorption of Pa(V) on vessels and unwanted side reactions. Surprisingly most of the published studies are only based on measurements at trace concentrations of Pa(V), while sorption reactions are classically made negligible by using (non-radioactive) chemical analogues at macro-concentrations. The hydrolysis behaviour of Nb(V) seems similar to that proposed for Pa(V): we calculated the hydrolysis constants of Nb(V) by interpreting the aqueous solubility of Nb_2O_5 (Table 3) [25]. We re-interpreted the (Pa) experimental measurements at 25 °C by giving more weight to the data for which systematic errors seemed the lowest according to Jaussaud's observations and comments: the measurements at high ionic strength and low (TTA = thenoyltrifluoroacetone) extractant concentrations. This essentially confirmed the original interpretation

Table 3
Pa(V) hydrolysis constants

I (M)	$\log^* K_{1,m}^e$	$\log^* K_{2,m}^e$	$\log^* K_{3,m}^e$	
3		-2.0 ± 0.15	-5.8 ± 0.3^b	[33–35]
3	-0.35 ± 0.29	-1.75 ± 0.91	<-3.5	[33] ^a
1		-1.7 ± 0.2	-6.9 ± 0.6^b	[33–35]
1	$\geq -0.38^c$	-1.50 ± 0.56	$<-0.98^b$	[33] ^a
0.5		-1.6 ± 0.2	-6.9 ± 0.6^b	[33,35]
0.5		-1.49^c		[33] ^a
0.1		-1.5 ± 0.2	-7.0 ± 0.6^b	[33–35]
0.1		-1.80 ± 0.34		[33] ^a
0.1	$\geq -0.75^c$	-1.65 ± 0.2	-4.95 ± 0.2	$Nb(V)^d$ [36] ^a
0		-1.24 ± 0.02	-7.03 ± 0.15^b	[33,35]
0		-1.26 ± 0.15	-7.15 ± 0.4^b	[34]
0	-0.04 ± 0.36^c	-1.44 ± 0.71	$<-3.6^c$	[33] ^a

One value is also tabulated for $Nb(V)$.

^a Graphically interpreted in the present work, and (last line) extrapolated to $I = 0$. See Fig. 8.

^b Inconsistent value: since the measurements were performed at $pH < 4$, it is not possible to fit (from them) a $\log K_i$ value less than about -4 .

^c There is no clear experimental evidence of the corresponding reaction.

^d $Nb(V)$ value fitted from solubility data [36], and here tabulated for comparison.

^e $K_{i,m}$ is the constant of equilibrium PaO .

given by the authors, but increased uncertainties and suppressed an inconsistency (Table 3). Namely, classical slope analyses of the raw experimental data imply a Pa species of charge +1 in 0.1 M NaClO_4 aqueous solutions, and +2 at higher I (3 M), consistent with the PaOOH(OH)^+ and PaOOH^{2+} stoichiometries [17] in nearly the whole pH range studied ($0 < \text{pH} < 4$). Indeed, high I usually stabilizes the species of higher charges. There is no clear evidence for neutral and tricationic species, due to the scattering of the data (Fig. 8). A neutral Pa species is certainly formed, but it is clearly stabilized by increasing $[\text{TTA}]_t$, the total TTA concentration (results not reproduced in Fig. 8 for clarity), which suggests the corresponding aqueous Pa(V) species might include ionised deprotonated TTA ligands, which would hide the formation of PaOOH(OH)_2 (equivalently written PaO(OH)_3 or Pa(OH)_5). The formation of PaO^{3+} is not proposed in the original interpretation of the authors, and indeed needs confirmation. Finally, the most reliable published Pa(V) standard hydrolysis constant is certainly $\log^* K_2^\circ = -(1.26 \pm 0.15)$ [34], a value consistent with our re-interpretation (-1.44 ± 0.71) (Fig. 8 and Table 3), and with the $Nb(V)$ value of $-(1.65 \pm 0.2)$. We also propose $\log^* K_1^\circ = -(0.04 \pm 0.36)$ and $\log^* K_3^\circ \ll -3.6$, giving no credit to the $(-(7.15 \pm 0.4)$ [34] and $-(7.03 \pm 0.15)$ [33,35]) published interpretations from

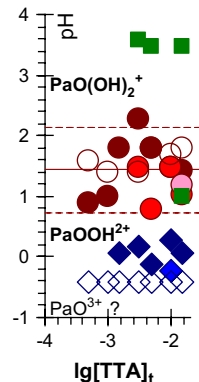


Fig. 8. Predominance diagram of Pa(V) hydrolysis species. The hydrolysis constants ($-\log^* K_i^\circ = \text{pH}_{1/2,i}$ correspond to the pH value at the half-point reaction) have been re-interpreted (Table 3) from the experimental data (and extrapolated to $I = 0$ with the SIT formula) of Ref. [30] in 0.1 (open symbols) to 3 (filled symbols of the same colour) mol L^{-1} NaClO_4 aqueous solutions for the successive formations of species of charges 2 (dark blue diamonds), 1 (brown circles) and 0 (green squares). The intermediate colours are for 1 and 0.5 mol L^{-1} . For higher $[\text{TTA}]$ values (not represented), a systematic deviation is observed. (For interpretation of the references to colour in this figure legend, the reader is referred to the web version of this article.)

the same experimental data, because the corresponding hydrolysis species could not be detected in the experimental conditions used in this work ($\text{pH} \leq 4$ corresponding to a maximum value of about $10^{-7+4} = 0.1\%$ for the concentration of the hydrolysis species to be compared with the $10^{0.71}$ uncertainty in the measurements of $\log^* K_2^\circ$), even though they might provide a reasonable value: the $Nb(V)$ value of $-(4.95 \pm 0.2)$ might also be used as a rough estimate. These $\log^* K_i^\circ$ constants are actually the hydrolysis constant of PaO^{3+} , but the existence of this species has not clearly been demonstrated, and for this reason only the second stepwise experimental determination ($\log^* K_2^\circ$) seems reliable, while the first one ($\log^* K_1^\circ$) needs confirmation. The $-\log^* K_2^\circ$ value is only a little larger than that of $-\log^* K_1^\circ$: the two first hydrolyses of Pa(V) would be nearly simultaneous. This is also observed for the other actinide aqueous species.

A linear regression correlates reasonably well $\log^* K_1^\circ$, the logarithm of the hydrolysis constant and z , the charge of the M^{z+} cation for $M^{z+} = \text{Ra}^{2+}$, Am^{3+} , Pu^{4+} (brown dotted line in Fig. 9(a)): $-\log^* K_i^\circ \approx (25.2_4 - 6.1_6 z)$. Adding other An^{3+} and An^{4+} cations gives virtually the same correlation (brown dotted line in Fig. 9(b)): $-\log^* K_i^\circ \approx (25.6_7 - 6.2_8 z)$. The actinyl ions such as UO_2^{2+} , and NpO_2^+ are below this correlation line. This stabilisation of their hydrolysed species might be originated in an $\text{An}-\text{O}_{\text{yl}}$ (intramolecular) charge transfer induced on approaching equatorial water

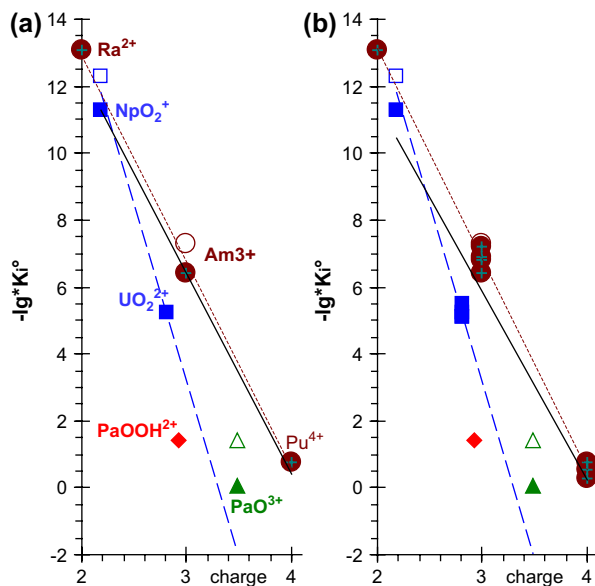


Fig. 9. Hydrolysis constants of actinide aqueous ions: $-\log^* K_1^\circ$ (filled symbols) and $-\log^* K_2^\circ$ (open symbols). The lines represent the linear regressions for (black line) all the points plotted on the figures excepted Pa(V) ones, only for the (Ra^{2+} , Am^{3+} , Pu^{4+}) set (brown dotted line), or only for the (NpO_2^+ and UO_2^{2+}) set (blue dashed line). The (atomic NPA) charges of the bare An cations (written in Fig. 9(a)) were obtained from DFT quantum calculations in gas phase. Data and corresponding lines are plotted by adding similar cations in Fig. 9(b). Two possible stoichiometries of “the” Pa(V) aqueous species are represented. (For interpretation of the references to colour in this figure legend, the reader is referred to the web version of this article.)

molecules to UO_2^{2+} [21], an inductive effects of O_{water} , which is expected to be more important for HO^- equatorial ligands (where O_{yl} is an O atom of an $\text{AnO}_2^{(X-4)+}$ actinyl cation, while O_{water} is an O atom of a water equatorial ligand of the actinyl). Nevertheless, the actinyl cations are not far from the correlation lines: including UO_2^{2+} and NpO_2^+ but excluding Ra^{2+} (black lines in Fig. 9); $-\log^* K_i^\circ \approx (24.4_3 - 6.0_1 z)$, and adding other AnO_2^{2+} and AnO_2^+ : $-\log^* K_i^\circ \approx (22.7_3 - 5.6_2 z)$, while extrapolating (blue dashed lines in Fig. 9) the AnO_2^{2+} and AnO_2^+ data give (blue dashed lines in Fig. 9) that are between the PaO^{3+} and PaOOH^{2+} data. Namely, PaO^{3+} (aq) would be intermediate between the bare actinide hard cations (An^{x+} , $X = 3$ or 4), and the usual actinyl cations ($\text{AnO}_2^{(X-4)+}$, $X = 5$ or 6, $\text{An} = \text{U}$, Np , Pu or Am), whose polarization by equatorial ligands essentially results in the intramolecular charge transfer between An and O_{yl} . Note that despite this polarization $\text{AnO}_2^{(X-4)+}$ is still a hard cation for the equatorial ligands – i.e. negligible charge transfer from the equatorial ligands – we may wonder whether assuming this concept of

(equatorial) hardness/(intra-actinyl) softness is still relevant for such a behaviour. However, the AnO_2^+ / AnO_2^{2+} / PaO^{3+} set can as well be considered as a series of actinide oxo-cations on their own line (approximately the blue dashed one in Fig. 9). As a result of their polarizability, these oxo-cations are below the (brown dotted) line of the bare M^{z+} cations. This polarizability probably decreases z_{An} , the An atomic charge (in the oxo-cation) by inductive effect. This inductive effect would increase with z_{An} : this can explain the quite surprisingly low calculated atomic charges of U (in UO_2^+) and Pa (in PaO^{3+}), which would therefore be at the origin of the more negative slope for the actinide oxo-cation line (as compared to that of the bare cations). However, this proposition needs confirmation, since the Pa(V) experimental results are neither very accurate, nor validated, and since physical explanations cannot be proven by only such empirical correlations: it is a limit of such correlations, rather than problems in the (very few) experimental data. According to this interpretation, two correlation lines are expected, one for the bare An^{x+} cations, and the other one for the $\text{AnO}_2^{(X-4)+}$ di-oxo-cations, while the PaO^{3+} mono-oxo-cation would fall between these lines, as we actually observed.

The experimental hydrolysis data already indicated that PaOOH^{2+} should be only a little less reactive than Pu^{4+} . Finally, it can still be under debate whether it is better to consider PaO^{3+} or PaOOH^{2+} , or both, as the Pa(V) aqueous species. Using atomic charges here gave unexpected correlations, as compared to the other chemical studies reviewed in the present paper. Nevertheless, it is not a convincing proof that PaO^{3+} can be an important aqueous species (i.e. it is not a confirmation of the above estimate of its $-\log^* K_1^\circ$ value).

Our DFT calculations give pictures confirming that PaOOH^{2+} (aq) is a logical species, similar to UO_2^{2+} (aq), while PaO_2^+ (aq) is easily protonated. PaOOH^{2+} is merely protonated PaO_2^+ [17]. However, our continuing DFT calculations for interpreting published EXAFS measurements clearly indicate that the PaO^{3+} geometry exists in the Pa(V) species formed in concentrated H_2SO_4 aqueous solutions, since none of the other tested model geometries reproduced the shortest experimental distance, including PaOOH^{2+} : it thus dissociates in complexing media, to give aqueous sulfate complexes of PaO^{3+} .

4. Concluding remarks on analogies

$(\log K_1^\circ \text{ vs } \text{p}K_a^\circ)$ correlations fit experimental data surprisingly well (Fig. 4(a)) for An(III to VI) complexes, with the exception of Pa(V), with 5 anionic

potentially bidentate and oxygen-donor RO_2^{2-} ligands: $\text{CO}_3^{2-} > \text{HPO}_4^{2-} \approx \text{SO}_3^{2-} > \text{SO}_4^{2-} \geq \text{S}_2\text{O}_3^{2-}$ in the order of their reactivities for the actinide cations. Furthermore, the correlations were found to be linear for each oxidation state, and the (0.62) slope of these $\text{H}^+/\text{An}(X)$ correlations are approximately the same for all the oxidation states (X). This, of course, means that the $\text{An}(X)/\text{An(VI)}$ correlations deduced are linear with slope 1: a_x , the intercept, is interpreted in terms of the half-reaction point, namely $10^{a_{\text{X}} - a_{\text{VI}}} = K_{1,\text{X}}^\circ / K_{1,\text{VI}}^\circ = K_{\text{X}/\text{VI}}^\circ$ (Eq. (5)) is the constant of the exchange equilibrium (Eq. (6a)), which takes (approximately) the same value (Table 1) for all the RO_2^{2-} ligands and for a given oxidation state. This provides a_x -based numerical values for the (up to now qualitative) scale $\text{An}^{4+} > \text{AnO}_2^{2+} \approx \text{An}^{3+} > \text{AnO}_2^+$ (Fig. 4(c)). The a_x values are also qualitatively correlated with z , the atomic charges of the An cations; but using z instead of a_x gives a poorer correlation (Fig. 4(c)). Note that measured energies of reactions, namely the hydrolysis constants of Pa(V) , show clearly that it is not an analogue of the other An(V) ; quantum calculations give a chemical explanation of the destabilization of PaO_2^+ by hydration, typically resulting in clear apical H-bonded water molecules [17]. The two approaches are complementary: the experimental energies of reactions are more accurate, while quantum calculations provide geometries and other physical data that can be interpreted in terms of usual chemical concepts (atomic charges, bounds and their covalency...) for explaining the observed chemical reactivity.

All the correlations we used are totally empirical. They are probably the result of various effects, some of them more or less cancel out in the correlations, and they are probably all linked to z , the atomic charge of the cation. However, using z gave poorer linear correlations than comparing only experimental equilibrium constants. For this reason it is certainly better to interpret the correlations with chemical concepts than with any unproven physical explanation. Nevertheless, intramolecular charge transfers are deduced from quantum calculations for (possibly protonated) actinyl cations. These charge transfers can be related to the slightly different trends observed between the hydrolysis behaviours for these three types of cations (An^{z+} , PaO^{3+} and AnO_2^{X-4}). This effect would be a little less important for PaO^{3+} than for the AnO_2^{X-4} cations where there are more covalent bounds (which promote intramolecular charge transfer). Charge transfers might as well be at the origin of the over-stabilisation of the aqueous An(IV) hydroxides as compared to complexation. These predictions are restricted to similar complexes: the linear

regression numbers cannot be extended to all types of complexes without validations. Indeed such approaches exist in literature, overestimating the stabilities of several hypothetical chemical species, whose existences have never been confirmed; such numbers are not considered in the NEA-TDB reviews [2–4].

We have in fact used several levels of analogy giving different rules of thumb (although some have similar mathematical equations), which might indicate that it is hopeless to develop more general empirical formulae. The strongest analogy is typically for $\text{M}(X)$, the series of An and other cations with the same charge, geometry and oxidation state, X : they form soluble complexes and hydroxides with the same stoichiometries, and with stability constant values that hardly differ by more than the experimental uncertainties. For different (X) oxidation states, linear correlations were found with slope 1, which defines a second type of analogy: considering the $\text{AnO}_2^{2+}/\text{M}^{z\text{M}}$ exchange, a solution of activity $|\text{AnO}_2^{2+}|$ has the same reactivity (for the $\text{L}^{z\text{L}}$ ligand) as a solution of activity of $|\text{M}^{z\text{M}}| K_{\text{X}/\text{VI}}^\circ$.

In a third type of analogy, the (b) slope of the linear correlation is no longer 1 ($b \neq 1$), as found here for $\text{H}^+/\text{M}^{z\text{M}}$ exchanges (b is not correlated with z_M , so it is better not to consider the $(z_M \text{ H}^+)/\text{M}^{z\text{M}}$ exchange); $K_1^\circ K_a^\circ$, as its equilibrium constant is no longer a relevant parameter for the analogy: analogue solutions should instead be based on the parameter $10^a = K_1^\circ (K_a^\circ)^b = [(|\text{H}^+||\text{L}^{z\text{L}}|)^b / (|\text{M}^{z\text{M}}||\text{L}^{z\text{L}}|)]_{1/2}$, whose interpretation is less intuitive.

Similarly when comparing protonation energies in aqueous and gas phases, the slope of the energy correlation is determined by the ratio of the H^+ activity scales in both phases. It is far from 1 (Fig. 3), corresponding to differences in the orders of magnitude (of the energies of reactions) in each phase. The intercept is related to the balance of the hydration energies (it can be shifted by changing the reference state).

Finally the rules of thumb are often characterized by the value of the (fitted) slopes in linear correlations of equilibrium constants, or equivalently by the value of the corresponding exponent in ratios of activities, the ideal concentrations.

References

- [1] V. Phrommavanh, M. Descotes, P. Vitorge, C. Beaucaire, J.-P. Gaudet, Estimating the Stabilities of Aqueous Actinide Complexes with Sulfoxyanions. Poster PA3-9 at the 10th International Conference on Chemistry and Migration Behaviour of Actinides and Fission Products in the Geosphere, MIGRATION'05, September 18–23, 2005. Avignon, France.

- [2] I. Grenthe, J. Fuger, R.J.M. Konings, R. Lemire, A.B. Muller, C. Nguyen-Trung, H. Wanner, Chemical Thermodynamics of Uranium download:, Paris OECD/NEA and Elsevier, 1992, <http://www.nea.fr/html/dbtdb/pubs/uranium.pdf>.
- [3] R. Silva, G. Bidoglio, M. Rand, P. Robouch, H. Wanner, I. Puigdomenech, Chemical Thermodynamics of Americium download:, Paris OECD/NEA and Elsevier, 1995, <http://www.nea.fr/html/dbtdb/pubs/americium.pdf>.
- [4] R. Lemire, J. Fuger, H. Nitsche, M. Rand, K. Spahiu, J. Sullivan, W. Ullman, P. Vitorge, Chemical Thermodynamics of Neptunium and Plutonium, Paris OECD/NEA and Elsevier, 2001.
- [5] P. Vitorge, H. Capdevila, Radiochim. Acta 91 (2003) 623.
- [6] P. Vitorge, H. Capdevila, S. Maillard, M.-H. Fauré, T. Vercouter, J. Nuclear Sci. Technol. 3 (2002) 713.
- [7] P. Vitorge, Chimie des actinides. Article and Formulaire form B, Techniques de l'Ingénieur, vol. 3520, 1999.
- [8] D. Rai, J.L. Ryan, Inorg. Chem. 24 (1985) 247.
- [9] M. Altmaier, V. Neck, T. Fanghänel, Solubility and Ternary Hydroxo-Carbonate Complexes of Thorium, NRC6 2004-03, Sixth International Conference on Nuclear and Radiochemistry, August 29th to September 3rd 2004, Aachen, Germany. <http://www.fz-juelich.de/NRC6/>.
- [10] M. Altmaier, V. Neck, R. Muller, T. Fanghanel, Radiochim. Acta 93 (2) (2005) 83.
- [11] E. Gaucher, C. Robelin, J.-M. Matray, G. Negral, Y. Gros, J.-F. Heitz, A. Vinsot, H. Rebours, A. Cassagnabère, A. Bouchet, Phys. Chem. Earth 29 (1) (2004) 55.
- [12] C. Beaucaire, P. Toulhoat, Appl. Geochem. 2 (1987) 417.
- [13] M. Descostes, C. Beaucaire, F. Mercier, S. Savoye, J. Sow, P. Zuddas, Bull. Soc. Géol. Fr. 173 (2002) 265.
- [14] M. Descostes, P. Vitorge, C. Beaucaire, Geochim. Cosmochim. Acta 68 (22) (2004) 4559.
- [15] P.L. Brown, E. Curti, B. Grambow, Chemical Thermodynamics of Zirconium, Paris OECD/NEA and Elsevier, 2005.
- [16] R. Guillaumont, T. Fanghänel, J. Fuger, I. Grenthe, V. Neck, D.A. Palmer, M.H. Rand, Update on the Chemical Thermodynamics of Uranium, Neptunium, Plutonium, Americium and Technetium, Paris OECD/NEA and Elsevier, 2003.
- [17] B. Siboulet, C.J. Marsden, P. Vitorge, Submitted for publication.
- [18] R.L. Martin, P.J. Hay, L.R. Pratt, J. Phys. Chem. A 102 (20) (1998) 3565.
- [19] G. Choppin, in: J. Rydberg, C. Musikas, G. Choppin (Eds.), Principles and Practices of Solvent Extraction, Marcel Dekker, New York, USA, 1992, p. 71.
- [20] B. Allard, J. Rydberg, C. Musikas, G. Choppin, in: J. Rydberg, C. Musikas, G.R. Choppin (Eds.), Principles and Practices of Solvent Extraction, Marcel Dekker, New York, USA, 1992, p. 209.
- [21] B. Siboulet, C.J. Marsden, P. Vitorge, Chem. Phys., in press.
- [22] A.E. Reed, L.A. Curtiss, F. Weinhold, W. Aas, Chem. Rev. 88 (1988) 899.
- [23] E.D. Glendening, A.E. Reed, J.E. Carpenter, F. Weinhold, Natural Population Analysis in Gaussian. NBO Version 3.1, 1998.
- [24] M.J. Frisch, G.W. Trucks, H.B. Schlegel, G.E. Scuseria, M.A. Robb, J.R. Cheeseman, V.G. Zakrzewski, J.A. Montgomery Jr., R.E. Stratmann, J.C. Burant, S. Dapprich, J.M. Millam, A.D. Daniels, K.N. Kudin, M.C. Strain, O. Farkas, J. Tomasi, V. Barone, B. Mennucci, M. Cossi, G. Scalmani, N. Rega, G.A. Petersson, H. Nakatsuji, M. Hada, M. Ehara, K. Toyota, R. Fukuda, J. Hasegawa, M. Ishida, T. Nakajima, Y. Honda, O. Kitao, H. Nakai, M. Klene, X. Li, J.E. Knox, H.P. Hratchian, J.B. Cross, V. Bakken, C. Adamo, J. Jaramillo, R. Gomperts, R.E. Stratmann, O. Yazyev, A.J. Austin, R. Cammi, C. Pomelli, J.W. Ochterski, P.Y. Ayala, K. Morokuma, G.A. Voth, P. Salvador, J.J. Dannenberg, V.G. Zakrzewski, S. Dapprich, A.D. Daniels, M.C. Strain, O. Farkas, D.K. Malick, A.D. Rabuck, K. Raghavachari, J.B. Foresman, J.V. Ortiz, Q. Cui, A.G. Baboul, S. Clifford, J. Cioslowski, B.B. Stefanov, G. Liu, A. Liashenko, P. Piskorz, I. Komaromi, R.L. Martin, D.J. Fox, T. Keith, M.A. Al-Laham, C.Y. Peng, A. Nanayakkara, M. Challacombe, P.M.W. Gill, B. Johnson, W. Chen, M.W. Wong, C. Gonzalez, J.A. Pople, Gaussian 03, Revision C.02, Gaussian, Inc., Wallingford CT, 2004.
- [25] M.J. Frisch, G.W. Trucks, H.B. Schlegel, G.E. Scuseria, M.A. Robb, J.R. Cheeseman, J.A. Montgomery Jr., T. Vreven, K.N. Kudin, J.C. Burant, J.M. Millam, S.S. Iyengar, J. Tomasi, V. Barone, B. Mennucci, M. Cossi, G. Scalmani, N. Rega, G.A. Petersson, H. Nakatsuji, M. Hada, M. Ehara, K. Toyota, R. Fukuda, J. Hasegawa, M. Ishida, T. Nakajima, Y. Honda, O. Kitao, H. Nakai, M. Klene, X. Li, J.E. Knox, H.P. Hratchian, J.B. Cross, V. Bakken, C. Adamo, J. Jaramillo, R. Gomperts, R.E. Stratmann, O. Yazyev, A.J. Austin, R. Cammi, C. Pomelli, J.W. Ochterski, P.Y. Ayala, K. Morokuma, G.A. Voth, P. Salvador, J.J. Dannenberg, V.G. Zakrzewski, S. Dapprich, A.D. Daniels, M.C. Strain, O. Farkas, D.K. Malick, A.D. Rabuck, K. Raghavachari, J.B. Foresman, J.V. Ortiz, Q. Cui, A.G. Baboul, S. Clifford, J. Cioslowski, B.B. Stefanov, G. Liu, A. Liashenko, P. Piskorz, I. Komaromi, R.L. Martin, D.J. Fox, T. Keith, M.A. Al-Laham, C.Y. Peng, A. Nanayakkara, M. Challacombe, P.M.W. Gill, B. Johnson, W. Chen, M.W. Wong, C. Gonzalez, J.A. Pople, Gaussian 03, Revision C.02, Gaussian, Inc., Wallingford CT, 2004.
- [26] P. Robouch, Contribution à la prévision du comportement de l'américium, du plutonium et du neptunium dans la géosphère ; données géochimiques, Thèse n°1987STR13230-SUDOC n° 043589863, Université Louis-Pasteur, Strasbourg, France, 13/11/1987. CEA-R-5473, 1989.
- [27] P. Robouch, P. Vitorge, Inorg. Chim. Acta 140 (1/2) (1987) 239.
- [28] T. Vercouter, Complexes aqueux de lanthanides (III) et actinides (III) avec les ions carbonate et sulfate. Étude thermodynamique par spectrofluorimétrie laser résolue en temps et spectrométrie de masse à ionisation électrospray. Thèse n°2005EVRY0003-SUDOC n° 09483699X, Université d'Évry, France, 2005.
- [29] P. Vitorge, H. Capdevila, CEA-R-5793, 1998.
- [30] E. Osthols, J. Bruno, I. Grenthe, Geochim. Cosmochim. Acta 58 (2) (1994) 613.
- [31] N. Eglizaud, M. Descostes, M. Schlegel, E. Simoni, 10^{es} Journées nationales de radiochimie et de chimie nucléaire, Avignon, France, 7–8/09/2006.
- [32] N. Eglizaud, F. Miserque, E. Simoni, M. Schlegel, M. Descostes, MIGRATION'05, Avignon, France, 18–23/09/2005.
- [33] C. Jaussaud, Contribution à l'étude thermodynamique de l'hydrolyse de Pa(V) à l'échelle des traces par la technique d'extraction liquide–liquide avec la TTA, Thèse, Université Paris-Sud, Orsay, 2003.
- [34] D. Trubert, C. Le Naour, C. Jaussaud, J. Solution Chem. 31 (4) (2002) 261.
- [35] D. Trubert, C. Le Naour, C. Jaussaud, O. Mrad, J. Solution Chem. 32 (6) (2003) 505.
- [36] C. Peiffert, Solubilité et hydrolyse du niobium en solution aqueuse à 25 °C et 0.1 Mpa, Poster, Journées scientifiques ANDRA, Nancy (France), 7–9 décembre 1999.

Annexe 2.8. Calcul de la solubilité de O₂ en fonction de la température et la salinité par l'algorithme de Benson et Krause (1984)

$$\begin{aligned} \ln C = & -135,29996 + \left(1,572288 \times \frac{10^5}{T} \right) - \left(6,637149 \times \frac{10^7}{T^2} \right) + \left(1,243678 \times \frac{10^{10}}{T^3} \right) - \left(8,621061 \times \frac{10^{11}}{T^4} \right) \\ & - (0,020573 \times S) + \left(12,142 \times \frac{S}{T} \right) - \left(2,3631 \times \frac{10^3 \times S}{T^2} \right) \end{aligned}$$

avec

C : concentration de O₂ en μmol.kg⁻¹ ;

T : température en degrés kelvin ;

S : salinité.

Annexe 2.9. Indices de saturation vis-à-vis des phases solides d'uranium

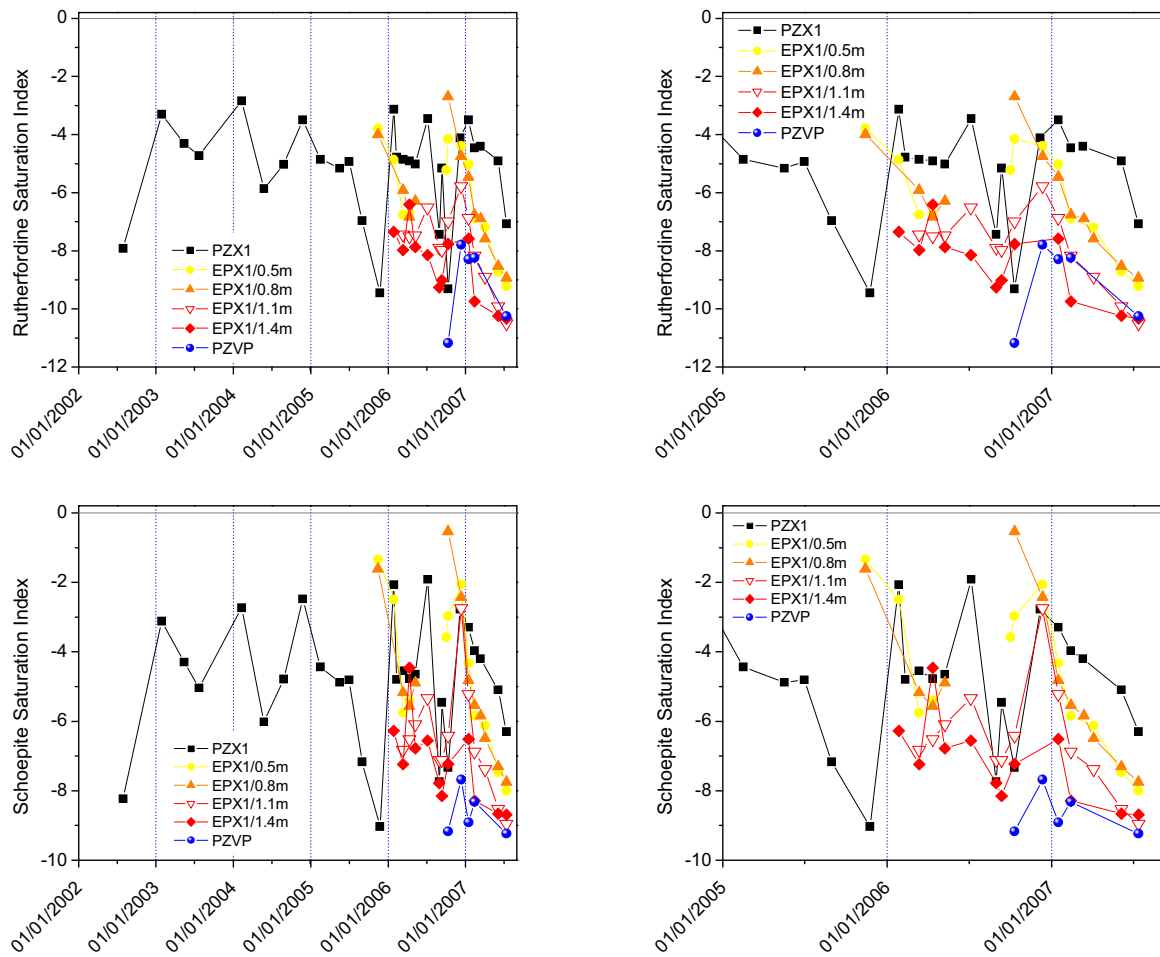


Figure 1 : Indices de saturation de la rutherfordine $\text{UO}_2\text{CO}_{3(s)}$ et schoepite $\text{UO}_2(\text{OH})_{2(s)}$ en fonction du temps dans les eaux de tourbe (notées EPX1), au PZPK et PZVP.

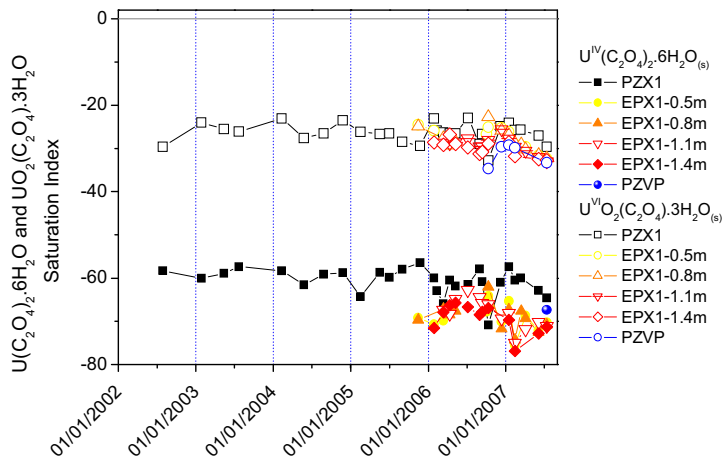


Figure 2 : Indices de saturation de $\text{U}^{\text{IV}}(\text{C}_2\text{O}_4)_2 \cdot 6\text{H}_2\text{O}_{(\text{s})}$ et $\text{U}^{\text{VI}}(\text{C}_2\text{O}_4)_2 \cdot 3\text{H}_2\text{O}_{(\text{s})}$ en fonction du temps dans les eaux de tourbe (notées EPX1), au PZPK et PZVP.

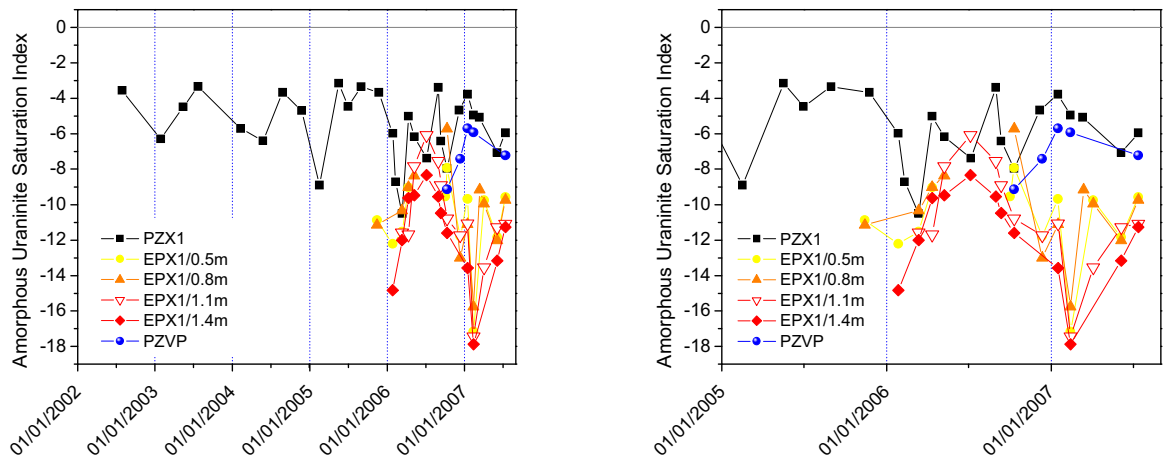


Figure 3 : Indices de saturation de l'uraninite amorphe $\text{UO}_{2(\text{am})}$ en fonction du temps dans les eaux de tourbe (notées EPX1), au PZPK et PZVP.